EFFECT OF MIXED MICELLES ON RELATIVE COUNTERION BINDING CONSTANTS AND COUNTERION-INDUCED MICELLAR GROWTH

FAGGE IBRAHIM ISAH

FACULTY OF SCIENCE
UNIVERSITY OF MALAYA
KUALA LUMPUR

2017

EFFECT OF MIXED MICELLES ON RELATIVE COUNTERION BINDING CONSTANTS AND COUNTERION-INDUCED MICELLAR GROWTH

FAGGE IBRAHIM ISAH

THESIS SUBMITTED IN FULFILMENT OF THE REQUIREMENTS FOR THE DEGREE OF DOCTOR OF PHILOSOPHY

DEPARTMENT OF CHEMISTRY
FACULTY OF SCIENCE
UNIVERSITY OF MALAYA
KUALA LUMPUR

2017

UNIVERSITY OF MALAYA

ORIGINAL LITERARY WORK DECLARATION

Name of Candidate: Fagge Ibrahim Isah

Matric No: SHC130097

Name of Degree: Doctor of Philosophy

Title of Thesis: Effect of Mixed Micelles on Relative Counterion Binding Constants and Counterion-induced Micellar Growth

Field of Study: Physical Organic Chemistry

I do solemnly and sincerely declare that:

(1) I am the sole author/writer of this Work;
(2) This Work is original;
(3) Any use of any work in which copyright exists was done by way of fair dealing and for permitted purposes and any excerpt or extract from, or reference to or reproduction of any copyright work has been disclosed expressly and sufficiently and the title of the Work and its authorship have been acknowledged in this Work;
(4) I do not have any actual knowledge nor do I ought reasonably to know that the making of this work constitutes an infringement of any copyright work;
(5) I hereby assign all and every rights in the copyright to this Work to the University of Malaya ("UM"), who henceforth shall be owner of the copyright in this Work and that any reproduction or use in any form or by any means whatsoever is prohibited without the written consent of UM having been first had and obtained;
(6) I am fully aware that if in the course of making this Work I have infringed any copyright whether intentionally or otherwise, I may be subject to legal action or any other action as may be determined by UM.

Candidate's Signature Date:

Subscribed and solemnly declared before,

Witness's Signature Date:

Name:

Designation:

ABSTRACT

Semi empirical kinetic technique has been used to determine the values of both cationic CTABr (hexadecyltrimethylammonium bromide) and mixed cationic-nonionic CTABr-$C_{16}E_{20}$ (hexadecyltrimethylammonium bromide-polyethoxy hexadecyl ether) micellar relative binding constants (K_X/K_{Br} and ${}^{m}K_X/{}^{m}K_{Br}$) of counterions, X^- and Br^-, (= K_X^{Br} or R_X^{Br} and ${}^{m}K_X^{Br}$ or ${}^{m}R_X^{Br}$), where superscript "m" signifies mixed micellar system, for X^- = 2-$NaOC_6H_4CO_2^-$, 3,5-$Cl_2C_6H_3CO_2^-$ and 4-$ClC_6H_4CO_2^-$ and correlate them to their specific rheological observations. The kinetic investigations on the influence of CTABr-$C_{16}E_{20}$ on the values of K_X^{Br} or R_X^{Br} in aqueous solutions of 2-$NaOC_6H_4CO_2Na$ and NaBr has been carried out. The presence of 0.006 M $C_{16}E_{20}$ decreases the mean values of K_X^{Br} or R_X^{Br} from 42 to 16 (2.6-fold lower). Rheological measurements of 0.015 M CTABr/2-$NaOC_6H_4CO_2Na/H_2O$ solutions at 25 and 35 °C revealed a single maximum for [2-$NaOC_6H_4CO_2Na$] = 0.02 M as the zero shear viscosity (η_o) was plotted against [2-$NaOC_6H_4CO_2Na$]. This shows, indirectly, that the is a possibility of the presence of wormlike micelles whereas the possible existence of spherical micelles was revealed at [$C_{16}E_{20}$] ≥ 0.006 M. A similar study, with a different counterion, 3,5-$Cl_2C_6H_3CO_2^-$ has also been reported. The average value of K_X^{Br} or R_X^{Br}, for CTABr/3,5-$Cl_2C_6H_3CO_2Na/H_2O$ solution (K_X^{Br} or R_X^{Br} = 198) appeared to be almost 2½-fold larger than that of CTABr/3,5-$Cl_2C_6H_3CO_2Na/C_{16}E_{20}/H_2O$ (${}^{m}K_X^{Br}$ or ${}^{m}R_X^{Br}$ = 78). Rheometric results of 0.015 M CTABr/3,5-$Cl_2C_6H_3CO_2Na/H_2O$ solution at 25 and 35 °C indicate that the plot of zero shear viscosity (η_o) against [3,5-$Cl_2C_6H_3CO_2Na$] has two maxima at two different concentrations of 3,5-$Cl_2C_6H_3CO_2Na$ (0.015 and 0.04 M) and this also shows the possible existence of wormlike micelles. Contrarily, a possible formation of spherical micelles for CTABr/3,5-$Cl_2C_6H_3CO_2Na/C_{16}E_{20}/H_2O$ solution ($[CTABr]_T$ = 0.015 M and $[C_{16}E_{20}]_T$ = 0.006 M) was observed at the same temperatures. The effects of CTABr-$C_{16}E_{20}$ on 4-

$ClC_6H_4CO_2^-$ has also been investigated. The respective mean values of K_X^{Br} or R_X^{Br} obtained for CTABr/4-$ClC_6H_4CO_2Na$/H_2O solution (K_X^{Br} or R_X^{Br} = 50) is 2.3-fold larger than that of CTABr/4-$ClC_6H_4CO_2Na$/$C_{16}E_{20}$/H_2O ($^mK_X^{Br}$ or $^mR_X^{Br}$ = 22). The possible existence of wormlike micelles was also observed from the rheometric data of 0.015 M CTABr/4-$ClC_6H_4CO_2Na$/H_2O solution based on the plot of η_o against [4-$ClC_6H_4CO_2Na$]. The observation also revealed the presence of a single maximum at [4-$ClC_6H_4CO_2Na$] = 0.03 M where it was thought that spherical micelles were formed in CTABr/4-$ClC_6H_4CO_2Na$/$C_{16}E_{20}H_2O$ with 0.015 M CTABr and 0.006 M $C_{16}E_{20}$. The quantitative correlation between the magnitudes of relative counterion (X^-) binding constant (K_X^{Br}or R_X^{Br} and $^mK_X^{Br}$ or $^mR_X^{Br}$) and X^--induced cationic micellar structural growth have been reported for the first time in this thesis. The highlight on the possible cause was that adding nonionic surfactant to an aqueous solution of cationic micelle-forming surfactant could be a technique to achieving changes in the structural, as well as the viscoelastic behavior of cationic micelles in the presence of certain inert organic salts.

ABSTRAK

Teknik kinetik separa empirik telah digunakan untuk menentukan nilai relatif pemalar ikatan misel untuk kedua-dua bahan kation CTABr (*heksadecyltrimethylammonium bromida*) dan campuran bahan kation-bukan kation CTABr-$C_{16}E_{20}$ (*hexadecyltrimethylammonium bromide-polietoksi heksadecil ether*) (K_X/K_{Br} and ${}^mK_X/{}^mK_{Br}$) dengan ion-lawan X^- dan Br^- (= K_X^{Br} or R_X^{Br} and ${}^mK_X^{Br}$ or ${}^mR_X^{Br}$), di mana superskrip "m" menandakan sistem campuran misel, untuk X^- = 2-$NaOC_6H_4CO_2^-$, 3,5-$Cl_2C_6H_3CO_2^-$ dan 4-$ClC_6H_4CO_2^-$ dan mengaitkannya dengan pemerhatian rheologinya secara khusus. Penyiasatan kinetik mengenai pengaruh CTABr-$C_{16}E_{20}$ terhadap nilai-nilai K_X^{Br} atau R_X^{Br} dalam larutan akueus 2-$NaOC_6H_4CO_2Na$ dan NaBr telah dilaksanakan . Kehadiran 0.006 M M $C_{16}E_{20}$ menurunkan nilai min K_X^{Br} atau R_X^{Br} dari 42 ke 16 (2.6-kali lebih rendah). Pengukuran rheologi 0.015 M CTABr/2-$NaOC_6H_4CO_2Na/H_2O$ pada 25 ^oC dan 35 ^oC menunjukkan satu maksimum tunggal untuk [2-$NaOC_6H_4CO_2Na$] = 0.02 M apabila kelikatan ricih (η_o) telah diplotkan terhadap [2-$NaOC_6H_4CO_2Na$]. Ini menunjukkan, secara tidak langsung, kemungkinan wujudnya misel cecacing sedangkan kemungkinan wujudnya misel sfera diungkapkan pada [$C_{16}E_{20}$] ≥ 0.006 M. Sebuah kajian yang sama, dengan ion-lawan yang berbeza, 3,5-$Cl_2C_6H_3CO_2^-$ juga dilaporkan. Nilai purata K_X^{Br} or R_X^{Br}, untuk larutan CTABr/3,5-$Cl_2C_6H_3CO_2Na/H_2O$ (${}^mK_X^{Br}$ or ${}^mR_X^{Br}$ = 198) adalah hampir 2½ kali lebih besar daripada CTABr/3,5-$Cl_2C_6H_3CO_2Na/C_{16}E_{20}/H_2O$ (${}^mK_X^{Br}$ or ${}^mR_X^{Br}$ = 78). Keputusan rheometrik untuk larutan 0.015 M CTABr/3,5-$Cl_2C_6H_3CO_2Na/H_2O$ pada 35 ° C menunjukkan bahawa plot kelikatan ricih (η_o) terhadap [3,5-$Cl_2C_6H_3CO_2Na$] mempunyai dua maksima pada dua kepekatan yang berbeza untuk 3,5-$Cl_2C_6H_3CO_2Na$ (0.015 dan 0.04 M) dan ini juga menunjukkan kemungkinan wujudnya misel cecacing. Sebaliknya, kemungkinan pembentukan misel sfera untuk larutan CTABr/3,5-$Cl_2C_6H_3CO_2Na/C_{16}E_{20}/H_2O$ ([CTABr]$_T$ = 0.015 M dan [$C_{16}E_{20}$]$_T$ = 0.006 M) diperhatikan pada suhu yang sama. Kesan CTABr-$C_{16}E_{20}$ terhadap 4-$ClC_6H_4CO_2^-$ juga telah disiasat. Nilai min K_X^{Br} or R_X^{Br} masing-masing diperolehi untuk larutan CTABr/4-$ClC_6H_4CO_2Na/H_2O$ solution (K_X^{Br} or R_X^{Br} = 50) adalah 2.3 kali lebih

besar daripada CTABr/4-$ClC_6H_4CO_2Na/C_{16}E_{20}/H_2O$ ($^mK_X^{Br}$ or $^mR_X^{Br}$ = 22). Kemungkinan wujudnya misel cecacing juga dapat dilihat dari data rheometrik larutan 0.015 M CTABr/4-$ClC_6H_4CO_2Na/H_2O$ berdasarkan plot η_o terhadap [4-$ClC_6H_4CO_2Na$]. Pemerhatian juga menunjukkan kehadiran maksimum tunggal pada [4-$ClC_6H_4CO_2Na$] = 0.03 M di mana ada kemungkinan wujudnya misel sfera yang terbentuk dalam larutan CTABr/4-$ClC_6H_4CO_2Na/C_{16}E_{20}H_2O$ dengan 0.015 M CTABr dan 0.006 M $C_{16}E_{20}$. Kaitan kuantitatif di antara magnitud ikatan relatif ion-lawan X^- (K_X^{Br}or R_X^{Br} and $^mK_X^{Br}$ or $^mR_X^{Br}$) dengan misel kationik dan pertumbuhan struktur misel kation yang disebabkan oleh X^- telah dilaporkan buat kali pertama dalam tesis ini. Apa yang boleh dikatakan dari fenomena ini adalah penambahan surfaktan tidak berion kepada larutan akueus surfaktan yang membentuk misel kation dengan kehadiran garam organik lengai tertentu boleh dijadikan sebagai teknik untuk mencapai perubahan struktural, serta kelakuan elastik-kelikatan untuk misel kation.

ACKNOWLEDGEMENTS

All praises are due to Allah, the All-Known. I thank him, ask him for His help, and seek for His forgiveness. I thank Him, *subhanaHu wa ta'ala,* for His favours and blessings to me in completing this PhD thesis. I pray to Him to accept and make this research work as a beneficial to mankind.

Secondly, I want to express my gratitude to my beloved parent for their tireless care throughout my life. May Allah forgive and grant His mercy upon them. I equally extend my thanks to my brothers and sisters for their supports and prayers. I know they are always there for me. Words are not enough to thank my beloved wife for her continuous supports, care, and encouragement during this struggle.

Thirdly, I extend my profound regards to my supervisor, Prof. Dr. Mohammad Niyaz Khan, for his advices, supports, motivations, helps and encouragement. His kindness supervision and numerous inputs in the area of my research, during my MSc. study, was the reason for me to nominate him again as PhD supervisor. Similar regards go to Prof. Dr. Sharifuddin Md Zain, whom his kindness and vast knowledge in chemistry prompted me to nominate him as my co-supervisor. Both have done their best throughout my candidature and towards the completion of this thesis. Their contribution would never be in vain. I cannot end without showing my appreciation to my laboratory mates: Wan Hamdah, Mohd Azri, Khalisanni and Norazizah were all helpful to me.

The last but not the least is to express my acknowledgement to Kano University of Science and Technology, Wudil, Nigeria, for my fellowship nomination to Tertiary Education Trust Fund, TETFund Nigeria.

Finally, I dedicated this thesis to my three important persons who answered Allah's calls before me;

(i) My biological father (Alhaji Isah Abubakar)
(ii) My father in-law (Alhaji Ya'u Ahmad)
(iii) My daughter (Hafsa Ibrahim Isah)

May their departed souls rest in eternal peace, Ameen.

TABLE OF CONTENTS

Abstract iii

Abstrak v

Acknowledgements vii

Table of Contents viii

List of Figures xiv

List of Tables xvii

List of Symbols and Abbreviations xix

List of Appendices xxiii

CHAPTER 1: GENERAL INTRODUCTION

1.1 Background of the research 1

1.1.1 Surfactants in water 1

1.1.2 Different types of surfactants 2

1.2 Aims and objectives 3

1.3 Likely benefits of the research 4

1.4 Thesis outline and structure 5

CHAPTER 2: LITERATURE REVIEW

2.1 History of micelles (Nanoparticles) and CMC 7

2.2 Micelles of mixed cationic-nonionic surfactants system 10

2.3 Micellar growth 11

2.4 Applications 13

2.5 Amminolysis/piperidinolysis of ester 14

2.6 Proposed micellar mechanisms 14

2.7 Micellar models and their conditions/assumptions 15

2.7.1 Pre-equilibrium micellar kinetic model 16
2.7.2 Pseudophase micellar model 18
2.7.3 Pseudophase ion exchange micellar model 18
2.8 Viscoelastic properties of micelles 19

CHAPTER 3: INFLUENCE OF MIXED CTABr–$C_{16}E_{20}$ MICELLES/NANOPARTICLES ON RELATIVE COUNTERION BINDING CONSTANTS IN AQUEOUS SOLUTIONS OF INERT SALTS (2-$NaOC_6H_4CO_2Na$ AND NaBr): KINETIC AND RHEOMETRIC STUDY

3.1 Introduction 21
3.2 Methodology 23
3.2.1 Materials 23
3.2.2 Kinetic method 23
3.2.2.1 Product characterization of piperidinolysis of PS^- 24
3.2.3 Determination of relative counterion binding constants (K_X^{Br} or R_X^{Br}) for X = $^-OC_6H_4CO_2Na$ using the semi empirical kinetics technique 26
3.2.4 Rheological measurements 27
3.3 Results. 28
3.3.1 Effect of [NaBr] on k_{obs} for the piperidinolysis of PS^- at constant concentration of pure $C_{16}E_{20}$ and 35 °C 28
3.3.2 Effect of mixed CTABr-$C_{16}E_{20}$ on k_{obs} for the piperidinolysis of PS^- at various [NaBr] and 35 °C 28
3.3.3 Effect of [2-$NaOC_6H_4CO_2Na$] on k_{obs} for the piperidinolysis of PS^- at constant concentration of pure CTABr and 35 °C 28
3.3.4 Effect of [2-$NaOC_6H_4CO_2Na$] on k_{obs} for piperdinolysis of PS^- at constant concentration of pure $C_{16}E_{20}$ and 35 °C 29

3.3.5 Effect of mixed CTABr-$C_{16}E_{20}$ on k_{obs} for piperidinolysis of PS^- at various [2-$NaOC_6H_4CO_2Na$] and 35 °C.....29

3.3.6 Rheological behavior of aqueous pure CTABr and mixed CTABr-$C_{16}E_{20}$ micelles in the presence of various [2-$NaOC_6H_4CO_2Na$] at 25 and 35 °C..... 29

3.4 Discussion.....38

3.4.1 Explanation of kinetic observations for the piperidinolysis of PS^- in the presence of pure $C_{16}E_{20}$ micelles at various [MX] or [M_2X] and 35 °C...38

3.4.2 Explanation of kinetic observations for the piperidinolysis of PS^- in the presence of pure CTABr and mixed CTABr-$C_{16}E_{20}$ micelles at various [MX] or [M_2X] and 35 °C 39

3.4.3 Explanation of rheological measurements for the piperidinolysis of PS^- in the presence of pure CTABr and mixed CTABr-$C_{16}E_{20}$ micelles at various [M_2X].....48

3.5 Conclusion 50

CHAPTER 4: STUDY OF CATIONIC AND NONIONIC MIXED MICELLES WITH NaBr AND 3,5-$CL_2C_6H_3CO_2Na$ BY THE USE OF PROBE NUCLEOPHILIC REACTION OF PIPERIDINE WITH IONIZED PHENYL SALICYLATE

4.1 Introduction 52

4.2 Methodology.....54

4.2.1 Reagents and chemicals.....54

4.2.2 Kinetic method 55

4.2.3 Use of semi empirical kinetic, SEK, method to find the values of relative counterion binding constants (K_X^{Br} or R_X^{Br}) for X = 3,5-$Cl_2C_6H_3CO_2^-$ ..55

4.2.4 Rheological study 55

4.3 Results 55

4.3.1 Effect of [NaBr] on k_{obs} for the piperidinolysis of PhS^- at lower concentrations of $C_{16}E_{20}$ in mixed CTABr-$C_{16}E_{20}$ and 35 °C 55

4.3.2 Effect of [3,5-$Cl_2C_6H_3CO_2Na$] on k_{obs} for the piperidinolysis of PS^- at a constant concentration of pure CTABr and 35 °C 55

4.3.3 Effect of [3,5-$Cl_2C_6H_3CO_2Na$] on k_{obs} for the piperidinolysis of PS^- at a constant concentration of $C_{16}E_{20}$ and 35 °C 56

4.3.4 Effect of [3,5-$Cl_2C_6H_3CO_2Na$] on k_{obs} for the piperidinolysis of PS^- at various concentrations of mixed CTABr-$C_{16}E_{20}$ and 35 °C 56

4.3.5 Rheological characteristics of aqueous pure CTABr micellar solutions at various [3,5-$Cl_2C_6H_3CO_2Na$], 25 and 35 °C 57

4.3.6 Rheological characteristics of aqueous mixed CTABr-$C_{16}E_{20}$ micellar solutions at various [3,5-$Cl_2C_6H_3CO_2Na$], 25 and 35 °C 57

4.4 Discussion 64

4.4.1 Explanation of kinetic observations for the piperidinolysis of PS^- in the presence of pure $C_{16}E_{20}$ micelles at various [MX] and 35 °C 64

4.4.2 Explanation of kinetic results at constant concentration of pure CTABr micelles, various values of [3,5-$Cl_2C_6H_3CO_2Na$] and 35 °C 64

4.4.3 Ion exchange catalysis 65

4.4.4 Explanation of kinetic results at constant mixed CTABr-$C_{16}E_{20}$ micelles, various [3,5-$Cl_2C_6H_3CO_2Na$] and 35 °C 67

4.4.5 Explanation of rheometric data in the presence of pure CTABr and mixed CTABr-$C_{16}E_{20}$ micelles at various [3,5-$Cl_2C_6H_3CO_2Na$] 69

4.5 Conclusion 74

CHAPTER 5: KINETICS AND MECHANISM OF COUNTERIONIC SALT (4-$CLC_6H_4CO_2NA$)-CATALYZED PIPERIDINOLYSIS OF ANIONIC PHENYL SALICYLATE IN THE PRESENCE OF CATIONIC-NONIONIC MIXED MICELLES

5.1 Introduction 76

5.2 Methodology 78

5.2.1 Reagents 78

5.2.2 Kinetic and rheometric studies 78

5.2.3 Use of semi empirical kinetic, SEK, method for the determination of K_X^{Br} or R_X^{Br} for X = 4-$ClC_6H_4CO_2^-$ 78

5.3 Results 78

5.3.1 5.3.1 Effect of [4-$ClC_6H_4CO_2Na$] on k_{obs} for the reaction of Pip with PS^- at constant concentration of pure CTABr and 35 °C 78

5.3.2 Effect of [4-$ClC_6H_4CO_2Na$] on k_{obs} for the reaction of Pip with PS^- at constant concentration of pure $C_{16}E_{20}$ and 35 °C 79

5.3.3 Effect of [4-$ClC_6H_4CO_2Na$] on k_{obs} for the reaction of Pip with PS^- in the presence of mixed CTABr-$C_{16}E_{20}$ at 35 °C 79

5.3.4 Rheological behavior of aqueous pure CTABr and mixed CTABr-$C_{16}E_{20}$ micelles in the presence of various [4-$ClC_6H_4CO_2Na$] at 25 and 35 °C .. 79

5.4 Discussion 86

5.4.1 Explanation of kinetic observations for the reaction of pip with PS^- in the presence of pure $C_{16}E_{20}$ at various [4-$ClC_6H_4CO_2Na$] and 35 °C 86

5.4.2 Explanation of the effect of [4-$ClC_6H_4CO_2Na$] on k_{obs} for piperidinolysis of PS^- in the presence of pure CTABr and mixed CTABr-$C_{16}E_{20}$ micelles 86

5.4.3 5.4.3 Explanation of rheological behaviours for the reaction of Pip with PS^- in the presence of pure CTABr and mixed CTABr-$C_{16}E_{20}$ micelles at various [4-$ClC_6H_4CO_2Na$] 88

5.5 Conclusion 92

CHAPTER 6: CONCLUSIONS AND FUTURE DIRECTIONS

6.1 Conclusion 94

6.2 Future Directions 95

References 96

List of Publications and Papers Presented 111

Appendices 116

LIST OF FIGURES

Figure 2.1: Physical properties of the aqueous solutions of micelles against the total amount of surfactant, $[Surf]_T$. The intersection in each pair of linear plots represents the CMC. 8

Figure 2.2: Micellar growth as a result of additives**.** 12

Figure 2.3: Graphs of k_{obs} vs. $[D_n]$ showing a monotonic increase (a) and decrease (b) in k_{obs} with the increase in $[D_n]$**.** 16

Figure 3.1: Plot of k_{obs} against [2-$NaOC_6H_4CO_2Na$] for the piperidinolysis of PS^- at 35 °C in the presence of $[CTABr]_T$/M = 0.006 (●), 0.010 (♦) and 0.015 (▲). The solid curves are sketched via the calculated values of the rate constant (k_{calcd}). Insert: The plots at magnified scale for the data points at lower values of $[M_2X]$ 34

Figure 3.2: Plots of $^mk_{obs}$ (where superscript "m" represents mixed micelles) against [2-$NaOC_6H_4CO_2Na$] for the piperidinolysis of PS^- at $[CTABr]_T$ + $[C_{16}E_{20}]_T$/M = 0.006 + 0.006 (●), 0.006 + 0.010 (♦) and 0.006 + 0.015 (▲) and 35 °C. The solid curves represent the calculated values of rate constant (k_{calcd}). Insert: The enlarged plots for the concentrations of M_2X at lower values. 34

Figure 3.3: Plots of $^mk_{obs}$ (where superscript "m" represents mixed micelles) against [2-$NaOC_6H_4CO_2Na$] for the piperidinolysis of PS^- at $[CTABr]_T$ + $[C_{16}E_{20}]_T$/M = 0.010 + 0.006 (●), 0.010 + 0.010 (♦) and 0.010 + 0.015 (▲) and 35 °C. The solid curves are sketched via the calculated values of rate constant (k_{calcd}). Insert: The enlarged plots for the concentrations of M_2X at lower values. 35

Figure 3.4: Plots of $^mk_{obs}$ (where superscript "m" represents mixed micelles) against [2-$NaOC_6H_4CO_2Na$] for the piperidinolysis of PS^- at $[CTABr]_T$ + $[C_{16}E_{20}]_T$/M = 0.015 + 0.006 (●), 0.015 + 0.010 (♦) and 0.015 + 0.015 (▲) and 35 °C. The solid curves are sketched via the calculated values of rate constant (k_{calcd}). Insert: The enlarged plots for the concentrations of M_2X at lower values. 35

Figure 3.5: Graphs of shear viscosity (η) against shear rates (γ̇) for the piperidinolysis of PS^- containing 0.015 M CTABr and [2-$NaOC_6H_4CO_2Na$]/M = (a) 0.006 (•) 0.008 (□) 0.012 (▲) 0.020 (♦) 0.040 (○) 0.08 (◊) and 0.120 (■) at 25 °C and (b) 0.006 (•) 0.008 (□) 0.0120 (▲) 0.020 (♦) 0.040(○) 0.080 (◊) and 0.120 (■)at 35 °C. 36

Figure 3.6: Plots of shear viscosity (η) against shear rate (γ̇) for the piperidinolysis of PS^- containing 0.015 M CTABr, 0.006 M $C_{16}E_{20}$ and [2-$NaOC_6H_4CO_2Na$]/M = (a) 0.006 (•) 0.008 (□) 0.0120 (▲) 0.020 (♦) 0.040 (○) and 0.120 (◊) at 25 °C and (b) 0.006 (•) 0.008 (□) 0.0120 (▲) 0.020 (♦) 0.040 (○) and 0.120 (◊) at 35 °C. 37

Figure 3.7: Graphs of zero shear viscosity (η_o) at a constant shear rate ($\dot{\gamma}$) against [2-$HOC_6H_4CO_2Na$] with 0.015 M CTABr in absence of $C_{16}E_{20}$ at 25°C (□) and 35 °C (◊), and presence of 0.006 M $C_{16}E_{20}$ at 25 °C (Δ) and 35 °C (○). 50

Figure 4.1: Plots showing the relationship between $^{m}k_{obs}$ (where superscript "m" represents mixed micelles) and [NaBr] for the reaction of Pip and PS^- at three different constant $[CTABr]_T + [C_{16}E_{20}]_T$ = 0.006 M + 0.00 M (●), 0.006 M + 0.6 μM (♦) and 0.006 M + 0.060 mM (▲), and 35 °C. The solid lines are drawn via the calculated values of the rate constant (k_{calcd}). Insert: The plots for magnified scale for the data points at lower values of [NaBr]. 58

Figure 4.2: Plots showing the relationship between $^{m}k_{obs}$ (where superscript "m" represents mixed micelles) and [3,5-$Cl_2C_6H_3CO_2Na$] for the reaction of Pip and PS^- at three different constant $[CTABr]_T + [C_{16}E_{20}]_T$/M = 0.006 + 0.006 (●), 0.006 + 0.010 (♦) and 0.006 + 0.015 (▲), and 35 °C. The solid lines are drawn via the calculated values of the rate constant (k_{calcd}). Insert: The plots for magnified scale for the data points at lower values of [3,5-$Cl_2C_6H_3CO_2Na$]. 58

Figure 4.3: Plots showing the relationship between $^{m}k_{obs}$ (where superscript "m" represents mixed micelles) and [3,5-$Cl_2C_6H_3CO_2Na$] for the reaction of Pip and PS^- at three different constant $[CTABr]_T + [C_{16}E_{20}]_T$/M = 0.010 + 0.006 (●), 0.010 + 0.010 (♦) and 0.010 + 0.015 (▲), and 35 °C. The solid lines are drawn via the calculated values of the rate constant (k_{calcd}). Insert: The plots for magnified scale for the data points at lower values of [3,5-$Cl_2C_6H_3CO_2Na$]. 61

Figure 4.4: Plots showing the relationship between $^{m}k_{obs}$ (where superscript "m" represents mixed micelles) and [3,5-$Cl_2C_6H_3CO_2Na$] for the reaction of Pip and PS^- at of three different constant $[CTABr]_T + [C_{16}E_{20}]_T$/M = 0.015 + 0.006 (●), 0.015 + 0.010 (♦) and 0.015 + 0.015 (▲), and 35°C. The solid lines are drawn via the calculated values of the rate constant (k_{calcd}). Insert: The plots for magnified scale for the data points at lower values of [3,5-$Cl_2C_6H_3CO_2Na$]. 61

Figure 4.5: Plots representing shear viscosity (η) against shear rate ($\dot{\gamma}$) for the piperidinolysis of PS^- containing 0.015 M CTABr and [3,5-$Cl_2C_6H_3CO_2Na$]/M = (a) 0.004 (•) 0.007 (□) 0.015 (▲) 0.025 (♦) 0.040 (○) and 0.070 (◊) at 25 °C and (b) 0.004 (•) 0.007 (□) 0.015 (▲) 0.025 (♦) 0.040 (○) and 0.070 (◊) at 35 °C.....62

Figure 4.6: Plots representing shear viscosity (η) against shear rate ($\dot{\gamma}$) for the piperidinolysis of PS^- containing 0.015 M CTABr, 0.006 M $C_{16}E_{20}$ and [3,5-$Cl_2C_6H_3CO_2Na$]/M = (a) 0.004 (•) 0.007 (□) 0.015 (▲) 0.025 (♦) 0.040 (○) and 0.070 (◊) at 25 °C and (b) 0.004 (•) 0.007 (□) 0.015 (▲) 0.025 (♦) 0.040 (○) and 0.070 (◊) at 35 °C. 63

Figure 4.7: Plots representing zero shear viscosity (η_o at constant shear rate ($\dot{\gamma}$) against [3,5-$Cl_2C_6H_3CO_2Na$] with 0.015 M CTABr in the absence of $C_{16}E_{20}$ at 25 °C (□) and 35 °C (◊), and the presence of 0.006 M $C_{16}E_{20}$ at 25 °C (Δ) and 35 °C (○). 74

Figure 5.1: Plots showing the relationship between $^{m}k_{obs}$ (where superscript "m" represents mixed micelles) and [MX], MX = 4-$ClC_6H_4CO_2Na$, for the reaction of Pip and PS^- at three different constant $[CTABr]_T$ + $[C_{16}E_{20}]_T$/M = 0.006 + 0.006 (●), 0.006 + 0.010 (♦) and 0.006 + 0.015 (▲), and 35 °C. The solid lines are drawn via the calculated values of the rate constant (k_{calcd}). Insert: The plots for magnified scale for the data points at lower values of [MX]. 82

Figure 5.2: Plots showing the relationship between $^{m}k_{obs}$ (where superscript "m" represents mixed micelles) and [MX], MX = 4-$ClC_6H_4CO_2Na$, for the reaction of Pip and PS^- at three different constant $[CTABr]_T$ + $[C_{16}E_{20}]_T$/M = 0.010 + 0.006 (●), 0.010 + 0.010 (♦) and 0.010 + 0.015 (▲), and 35 °C. The solid lines are drawn via the calculated values of the rate constant (k_{calcd}). Insert: The plots for magnified scale for the data points at lower values of [MX]. 82

Figure 5.3: Plots showing the relationship between $^{m}k_{obs}$ (where superscript "m" represents mixed micelles) and [MX], MX = 4-$ClC_6H_4CO_2Na$, for the reaction of Pip and PS^- at three different constant $[CTABr]_T$ + $[C_{16}E_{20}]_T$/M = 0.015 + 0.006 (●), 0.015 + 0.010 (♦) and 0.015 + 0.015 (▲), and 35 °C. The solid lines are drawn via the calculated values of the rate constant (k_{calcd}). Insert: The plots for magnified scale for the data points at lower values of [MX]. 83

Figure 5.4: Graphs of shear viscosity (η) against shear rate ($\dot{\gamma}$) for the piperidinolysis of PS^- containing 0.015 M CTABr and [4-$ClC_6H_4CO_2Na$]/M = **(a)** 0.008 (•) 0.015 (□) 0.030 (▲) 0.050 (♦) 0.080 (○) and 0.150 (◊) at 25 °C and **(b)** 0.008 (•) 0.015 (□) 0.030 (▲) 0.050 (♦) 0.080 (○) and 0.150 (◊) at 35 °C. 84

Figure 5.5: Graphs of shear viscosity (η) against shear rate ($\dot{\gamma}$) for the piperidinolysis of PS^- containing 0.015 M CTABr, 0.006 M $C_{16}E_{20}$ and [4-$ClC_6H_4CO_2Na$]/M = **(a)** 0.008 (•) 0.015 (□) 0.030 (▲) 0.050 (♦) 0.080 (○) and 0.150 (◊) at 25 °C and **(b)** 0.008 (•) 0.015 (□) 0.030 (▲) 0.050 (♦) 0.080 (○) and 0.150 (◊) at 35 °C..... 85

Figure 5.6: Plots of zero shear viscosity (η_o) against [4-$ClC_6H_4CO_2Na$] at a constant shear rate ($\dot{\gamma}$) with 0.015 M CTABr in the absence of $C_{16}E_{20}$ at 25 °C (□) and 35 °C (◊), and the presence of 0.006 M $C_{16}E_{20}$ at 25 °C (Δ) and 35 °C (○). 92

LIST OF TABLES

Table 1.1: Examples of various types of surfactant and their two different components……. 3

Table 3.1: Pseudo-first-order rate constants (k_{obs}) for the reaction of piperidine with anionic phenyl salicylate (PS^-) at 0.006 M CTABr in the presence of 0.006, 0.010, and 0.015 M $C_{16}E_{20}$ and different [MX] (= NaBr).[a] 31

Table 3.2: Pseudo-first-order rate constants (k_{obs}) for the reaction of piperidine with anionic phenyl salicylate (PS^-) at 0.010 M CTABr in the presence of 0.006, 0.010 and 0.015 M $C_{16}E_{20}$ and different [MX] (= NaBr).[a] 32

Table 3.3: Pseudo-first-order rate constants (k_{obs}) for the reaction of piperidine with anionic phenyl salicylate (PS^-) at 0.015 M CTABr in the presence of 0.006, 0.010 and 0.015 M $C_{16}E_{20}$ and different [MX] (= NaBr).[a] 33

Table 3.4: Values of kinetic parameters for the reaction of Pip and PS^- in the presence of inert salts MX or M_2X at different $[C_{16}E_{20}]_T$ and 35 °C.[a].....40

Table 3.5: Values of empirical constants, ${}^m\theta$, ${}^mF_{X/S}$ and ${}^mK^{X/S}$ calculated from **Eqs. 3.13** and **3.14** for MX = NaBr at different concentrations of mixed CTABr-$C_{16}E_{20}$.[a] 45

Table 3.6: Values of empirical constants, θ, $F_{X/S}$ and $K^{X/S}$ obtained using **Eqs. 3.13** and **3.14** with the $[M_2X]_0^{op}$ values for M_2X = 2-$NaOC_6H_4CO_2Na$ at different $[CTABr]_T$.[a] ..46

Table 3.7: Values of empirical constants, ${}^m\theta$, ${}^mF_{X/S}$ and ${}^mK^{X/S}$ calculated from **Eqs. 3.13** and **3.14** with the $[M_2X]_0^{op}$ values for M_2X = $2NaOC_6H_4CO_2Na$ at different concentrations of mixed CTABr-$C_{16}E_{20}$[a] 47

Table 4.1: Pseudo first-order rate constants (k_{obs}) for the reaction of Pip with PS^- at 0.006, 0.010 and 0.015 M CTABr at different [3,5-$Cl_2C_6H_3CO_2Na$].[a] 59

Table 4.2: Pseudo-first-order rate constants (${}^mk_{obs}$) for the reaction of piperidine with anionic phenyl salicylate (PS^-) at 0.006 M CTABr in the presence of 0.600 μM, and 0.060 mM $C_{16}E_{20}$ and different [3,5-$Cl_2C_6H_3CO_2Na$].[a].....60

Table 4.3: Values of kinetic parameters for the reaction of Pip and PS^- in the presence of 3,5-$Cl_2C_6H_4CO_2Na$ at different $[C_{16}E_{20}]_T$ and 35 °C.[a] 64

Table 4.4: Values of empirical constants, θ, and $K^{X/S}$ obtained using **Eqs. 3.13 and 3.14** with the $[MX]_0^{op}$ values for MX = 3,5-$Cl_2C_6H_3CO_2Na$ at different $[CTABr]_T$.[a] 70

Table 4.5: Values of empirical constants, ${}^m\theta$, and ${}^mK^{X/S}$ obtained using **Eqs. 3.13 and 3.14** with the $[MX]_0^{op}$ values for MX = 3,5-$Cl_2C_6H_3CO_2Na$ at different concentrations of mixed CTABr-$C_{16}E_{20}$.[a].....71

Table 5.1: Values of observed pseudo-first-order rate constant, k_{obs}, obtained for the piperidinolysis of PS^- at 0.006, 0.010 and 0.015 M CTABr and different [4-$ClC_6H_4CO_2Na$].[a] 81

Table 5.2: Values of kinetic parameters for the reaction of Pip and PS^- in the presence of 4-$ClC_6H_4CO_2Na$ at different $[C_{16}E_{20}]_T$ and 35 °C.[a] 86

Table 5.3: Values of empirical constants, θ, and $K^{X/S}$ obtained using **Eqs. 3.13 and 3.14** with the $[MX]_0^{op}$ values for MX = 4-$ClC_6H_4CO_2Na$ at different $[CTABr]_T$.[a] 90

Table 5.4: Values of empirical constants, $^m\theta$ and $^mK^{X/S}$, obtained using **Eqs. 3.13 and 3.14** with the $[MX]_0^{op}$ values for MX = 4-$ClC_6H_4CO_2Na$ at different concentrations of mixed CTABr-$C_{16}E_{20}$.[a] 91

LIST OF SYMBOLS AND ABBREVIATIONS

°C	:	Degree celsius
μM	:	Micromole
$[\ ]_{sp}$	:	Specific concentration
$[\ ]_T$	:	Total concentration
$[MX]_0^{op}$	:	Optimum values of [MX] needed to expel both HO^- and Br^- from micellar psuedophase to aqueous phase
$[PhS^-]_0$	:	Initial concentration of ionized phenyl salicylate
A_∞	:	Observered absorbance at time = ∞
A_{obs}	:	Observed absorbance
$C_{16}E_{20}$	:	Polyethylene glycol hexadecyl ether
CM	:	Cationic micelles
CMC	:	Critical micellar concentration
C_nE_m	:	Nonionic micelles
C_nIM	:	Ionic surfactants
COO^-	:	Carboxylate ion
CTABr	:	Hexadecyl/Cetyltrimethylammonium bromide
DDMAO	:	Dodecyldimethylamine oxide
DHC	:	District heating and cooling
D_n	:	Detergent/micelles/nanoparticles
Eq.	:	Equation
$F_{X/S}$	:	Empirical constant whose magnitude should be (by definition) > 0 and ≤1
ISI	:	Institute for scientific information
k_0	:	Rate constant at [MX] = 0

k_n^2	:	nucleophilic second-order rate constant for the reaction of Pip with anionic PS^-
k_W^2	:	Nucleophilic second order rate constant for the reaction of Pip with PS^- in nonionic micellar phase
K_{Br}	:	Micellar binding constant of Br^-
$K_{Br/S}$	:	Empirical constant whose magnitude shows the tendency of Br^- to expel S^- from cationic micellar pseudophase to aqueous phase
$K_{Br/S}^n$	:	Normalized values of $K_{Br/S}$
k_{calcd}	:	Calculated pseudo first order rate constant
K_{eqS}	:	Equilibrium constant for the micellization of ester molecules (S)
k_M	:	Rate constants for the hydrolysis of the micellized ester (S)
k_{obs}	:	Observed pseudo first order rate constant
k_{obs}^0	:	average of higher values of k_{obs}
$k_{obs}^{M_2X\ (max)}$	:	k_{obs} at maximum value $[M_2X]$
$k_{obs}^{MX\ (max)}$	:	k_{obs} at maximum value [MX]
K_S	:	Micellar binding constant of PS^-
K_S^0	:	K_S in the absence of X^-
k_W	:	Rate constants for the hydrolysis of the aqueous ester
K_X	:	Micellar binding constant of X^-
$K^{X/S}$	:	Empirical constant
$K_{X/S}$	:	Empirical constant whose magnitude shows the tendency of X^- to expel S^- from cationic micellar pseudophase to aqueous phase
$K_{X/S}^n$	:	Normalized values of $K_{X/S}$
K_X^{Br}	:	Conventional ion exchange/counterion binding constants for ion-exchange process X^-/Y^-

L	:	Empirical constant
M	:	Molarity
m	:	Mixed micelles
M_2X	:	Disodium salicylate, 2-$NaOC_6H_4CO_2Na$
mL	:	Milliliter
mM	:	Milimole
MMPP	:	Multiple Micellar Pseudophase
MX	:	Inert aromatic salt
NaBz	:	Sodium benzoate
NaHx	:	Sodium hexanoate
nm	:	Nanometer
NMR	:	Nuclear Magnetic Resonance
NSE	:	Negative salt effect
nsp	:	Nonspherical
P	:	Product
Pa	:	Pascal
PEK	:	Preequilibrium kinetic
PFPE-Na	:	Sodium perfluoropolyether
pH	:	Potency of hydrogen ion
PIE	:	Pseudophase ion exchange
Pip	:	Piperidine
PP	:	Pseudophase
PS^-	:	Ionized phenyl salicylate
PSH	:	Phenyl salicylate
R_X^{Br}	:	Ion exchange/counterion binding constants determined in the presence of micelles with different structural features

S	:	Substrate/Ester
s	:	Second
SANS	:	Small angle neutron scattering
SAS	:	Surface active substances
SDS		Sodium dodecyl sulphate
SEK	:	Semi empirical kinetic
SER	:	Surfactant-enhanced remediation
S_M	:	Micellized substrate/ester molecules
sp	:	Spherical
Surf	:	Micelle-forming surfactant
S_W	:	Aqueous substrate/ester molecules
t	:	Time
TEM	:	Transmission electron microscopy
UV	:	Ultra violet
WM	:	Wormlike micelles
X^-	:	Counterion
$^{X}k_{cat}$	:	Apparent catalytic constant
β	:	Fraction of ionic surfactant coverage
$\dot{\gamma}$	:	Shear rates
γ_{cr}	:	Critical shear rate
δ_{app}	:	Apparent molar extinction coefficient/apparent molar absorptivity
η	:	Steady-shear viscosity
η_o	:	Zero shear viscosity
θ	:	Empirical parameter
λ	:	Wavelenght

LIST OF APPENDICES

APPENDIX A: Pseudo-first-order rate constants (k_{obs}) for the reaction of piperidine with anionic phenyl salicylate (PS^-) in the presence 0.001, 0.003 and 0.006 M $C_{16}E_{20}$ and different [MX] (MX = NaBr) at 35 °C.……..... 116

APPENDIX B: Pseudo-first-order rate constants (k_{obs}) for the reaction of piperidine with anionic phenyl salicylate (PS^-) in the presence 0.008, 0.010 and 0.015 M $C_{16}E_{20}$ and different [MX] (MX = NaBr) at 35 °C.……..... 117

APPENDIX C: Pseudo-first-order rate constants (k_{obs}) for the reaction of piperidine with anionic phenyl salicylate (PS^-) in the presence 0.001, 0.003 and 0.006 M $C_{16}E_{20}$ and different [MX] (MX = 2-$NaC_6H_4CO_2Na$) at 35 °C.……..... 118

APPENDIX D: Pseudo-first-order rate constants (k_{obs}) for the reaction of piperidine with anionic phenyl salicylate (PS^-) in the presence 0.008, 0.010 and 0.015 M $C_{16}E_{20}$ and different [MX] (MX = 2-$NaC_6H_4CO_2Na$) at 35 °C.……..... 119

APPENDIX E: Pseudo-first-order rate constants (k_{obs}) for the reaction of piperidine with anionic phenyl salicylate (PS^-) in the presence 0.001, 0.003 and 0.006 M $C_{16}E_{20}$ and different [MX] (MX = 3,5-$Cl_2C_6H_4CO_2Na$) at 35 °C.……..... 120

APPENDIX F: Pseudo-first-order rate constants (k_{obs}) for the reaction of piperidine with anionic phenyl salicylate (PS^-) in the presence 0.008, 0.010 and 0.015 M $C_{16}E_{20}$ and different [MX] (MX = 3,5-$Cl_2C_6H_4CO_2Na$) at 35 °C.……..... 121

APPENDIX G: Pseudo-first-order rate constants (k_{obs}) for the reaction of piperidine with anionic phenyl salicylate (PS^-) in the presence 0.001, 0.003 and 0.006 M $C_{16}E_{20}$ and different [MX] (MX = 4-$ClC_6H_4CO_2Na$) at 35 °C.……..... 122

APPENDIX H: Pseudo-first-order rate constants (k_{obs}) for the reaction of piperidine with anionic phenyl salicylate (PS^-) in the presence 0.008, 0.010 and 0.015 M $C_{16}E_{20}$ and different [MX] (MX = 4-$ClC_6H_4CO_2Na$) at 35 °C.……..... 123

CHAPTER 1: GENERAL INTRODUCTION

1.1 Background of the research

1.1.1 Surfactants in water

The word “SURFACTANTS” is a short form of “Surface Active Agents/Ingredients;” (Karsa, 2006). It represents any substance with the properties of absorption and wetting thereby lowering the surface tension of an aqueous solution. They allow easier spreading between two different phases (Holmberg *et al.*, 2002; Tripathy *et al.*, 2017). They can also be expressed as molecules or compounds that play a role in decreasing the tensions at the surface/interface of two different phases (Drew, 2006; Tripathy *et al.*, 2017). This reduction in tensions is directly proportional to the amount of the molecules at the boundary of the phases (Drew, 2006).

In the context of aqueous solutions, surfactants molecules are “*amphiphilic*” which is a Greek word meaning that the solutes have dual characteristics: *amphi* which means "dual or double", and then the *philos* which shows friendship or affinity. These dual characteristics emerge because a solute molecule contains both hydrophobic and hydrophilic parts. They have well differentiated polar and non-polar portions with measurable aqueous solubility as both aggregates and monomers (Salager, 2002).

There are abundant naturally occurring surfactant molecules (polar lipids) which are usually organic substances and exist in living matters (Doehlert *et al.*, 2010; Romantsov & Wood, 2016). The manufacture of affordable synthetic surfactants, used in petrochemical and oilfield industries, has been reported elsewhere (Foley *et al.*, 2012). In addition, Willcox reported that the naturally occurring surfactants (also called alkali soap) were used as domestic cleaning detergent for more than 20 decades ago (Willcox, 2000). These stages of development in the productions of surfactants prompted its scientific and industrial advancement (Drew, 2006; Holmberg *et al.*, 2002).

Surfactants are believed to have influence in quite some fields in chemical and technological processes of fundamental and applied sciences (Drew, 2006). Their molecules consist a polar (or a positively/negatively charged) hydrophilic head group (having a strong affinity to water interface) and a non-polar hydrophobic tail group (usually an alkyl chain which does possess the features of the later) (Cetin & Nasr-El-Din, 2017). This particular duality behavior of surfactants in an aqueous system results on their different types of complex self-aggregation/assembly in the bulk of aqueous solution (Chakraborty *et al.*, 2005; Drew, 2006; Farías, *et al.*, 2009; Islam & Kato, 2003a, 2003b). Their molecules also dissolve in the bulk of the aqueous solution to produce monolayers (when spontaneously adsorbed at the air-water interface) as a result of their preferential surface active characteristics (Islam & Kato, 2003a).

1.1.2 Different types of surfactants

Surfactants are of the various types, based upon the nature of their hydrophobic parts. Their tendency to influence certain biochemical processes has been reported to be associated with their composition (the hydrophilic headgroups being the polar parts and the non-polar segments as hydrophobic tail) (Roy *et al.*, 2014). Depending on a specific and intended application, their components differ when either the headgroups or the tails are modified. Aromatic rings (Sigoillot & Nguyen, 1992), Heteroatoms components, for instance; fluoro (Park *et al.*, 2007), siloxane (Sadegh & Naghash, 2015) and naphthalenes (Abdel-Raouf *et al.*, 2011) are also part of the nonpolar tails of some surfactants. This non-polar hydrophobic component may also be primary, secondary of tertiary saturated and/or unsaturated hydrocarbon chain with a different number of carbon atoms (eight to 16) (Clint, 2012; Khan, 2006). Drew as well as Foley and his coworkers have independently reported the presence of the hydrophobic tail of surfactants in the derivatives of both synthetic and natural polymers (Drew, 2006; Foley *et al.*, 2012).

The characteristics of a particular surfactant headgroups are the basis of their classification, and the four major types are classified as cationic, anionic, zwitterionic, and nonionic (Cetin & Nasr-El-Din, 2017; Cullum, 1994). Table 1.1 presents some examples of the various types of surfactants and their components. Quite some studies, nowadays, on different type surfactants have been industrially and academically paid serious attention in the field of nanoscience and nanotechnology due to their specific features (Deda & Araki, 2015; Otzen, 2015).

Table 1.1: Examples of various types of surfactant and their two different components.

Surfactant types	Molecules	Headgroups	Tails
Cationic (e.g. CTABr)[a]	$CH_3–(CH_2)_{15}–N^+(CH_3)_3Br^–$	$N^+(CH_3)_3Br^–$	$CH_3–(CH_2)_{15}–$
Anionic (e.g. SDS)[b]	$CH_3–(CH_2)_{11}–SO_2–O^–Na^+$	$SO_2–O^–Na^+$	$CH_3–(CH_2)_{11}–$
Zwitterionic (e.g. DDMAO)[c]	$CH_3–(CH_2)_{11}–N^+(CH_3)_2–O^–$	$N^+(CH_3)_2–O^–$	$CH_3–(CH_2)_{11}–$
Nonionic (e.g. $C_{16}E_{20}$)[d]	$CH_3–(CH_2)_{15}–(O–(CH_2)_{20}–OH$	$(O–(CH_2)_{20}–OH$	$CH_3–(CH_2)_{15}–$

[a]Hexadecyltrimethylammonium bromide. [b]Sodium dodecyl sulphate. [c]Dodecyldimethylamine oxide. [d]Polyoxyethylene glycol (20) hexadecyl ether (Brij 58).

1.2 Aims and objectives

As discussed in section 1.1, the vast importance of different types of surfactants nowadays prompted the study on relatively less number of the literature for mixed surfactants systems in the form of cationic-nonionic. It has been established that addition of nonionic surfactant in an aqueous solution of cationic ones not only reduces the value of relative counterion binding constant but also causes cationic micellar structural growth (Gao *et al.*, 2002). The nonionic surfactant acts as an additive which can be used to achieve the desired cationic micellar structure and viscoelastic behavior (Kamada *et al.*, 2014). The following are the aims and objectives of the research;

(i) To discover probable quantitative correlation between the relative counterion binding constants, K_X^{Br}or R_X^{Br}, and the structural growth of cationic CTABr (hexadecyltrimethylammonium bromide) micelles.

(ii) To study the changes in the values of K_X^{Br} or R_X^{Br} for CTABr/MX/H_2O or CTABr/M_2X/H_2O solution in the presence of different counterions, X (X = Br^-, 2-$NaOC_6H_4CO_2^-$, 3,5-$Cl_2C_6H_3CO_2^-$ and 4-$ClC_6H_4CO_2^-$).

(iii) To study the changes in the values of K_X^{Br} or R_X^{Br} in CTABr/MX/H_2O or CTABr/M_2X/H_2O solution in the presence of a nonionic surfactant, $C_{16}E_{20}$ (where MX and M_2X are inert organic salts and $C_{16}E_{20}$ = $C_{16}H_{33}(OCH_2$-$CH_2)_{20}OH$).

(iv) To use the rheometric measurements of both CTABr/MX/H_2O or CTABr/M_2X/H_2O and CTABr/MX/$C_{16}E_{20}$/H_2O or CTABr/M_2X/$C_{16}E_{20}$/H_2O (MX = NaBr, 3,5-$Cl_2C_6H_3CO_2Na$ and 4-$ClC_6H_4CO_2Na$ and M_2X = 2-$NaOC_6H_4CO_2Na$) solutions in ascertaining the cationic micellar structural changes with the variations in the values of K_X^{Br} or R_X^{Br}.

The introduction of the mixed micellar system has been skillfully achieved in changing the CTABr micellar structural transition. This method does not require a change in added salt, pH, temperature, and other factors, for the modification. Thus, the present method is providing more reliable and precise way to alter the cationic micellar structure.

1.3 Likely benefits of the research

Most of the commercially used surface active substances comprise of mixed surfactants systems is because of their relatively lower cost than that of pure surfactants (Khan, 2006). Furthermore, the performance of micelles of pure surfactants systems (due to their good response to concentrations and compositions optimisation for various purposes) is comparatively poor than that of the mixed surfactants system (Christian & Scamehorn, 1995; Holland & Rubingh, 1992). There are several potential benefits of mixed cationic-nonionic micellar systems in modern science and technology. Some of the likely advantages of the research are briefly discussed below;

(i) The district heating and cooling (DHC) systems are vital applications of drag reducers where recirculation of fluid is needed. Polymers that are vulnerable to shear stresses cannot operate effectively but the use of mixed surfactants reduces costs for pumping energy, capital investments, and operation (Ezrahi *et al.*, 2006).

(ii) As wormlike micelles come in contact with petroleum products from the fracture, they are transformed into less viscous spherical micelles, thereby facilitating the flow of residues out of the pack and fracture (Walker, 2001).

(iii) Adding a small quantity of anionic perfluoropolyether surfactants, PFPE-Na to CTABr solution enhances the surface properties and wetting of the mixed micellar system. Therefore, the application of cost could also be reduced. In addition, the mixed micellar systems can form vesicles which could extend the applications as drug delivery vehicles or as micro/nano templates for material synthesis (Hentze *et al.*, 2003; Lipowsky & Sackmann, 1995; Ojogun *et al.*, 2009; Wang *et al.*, 2017; Xiao, 2005).

1.4 Thesis outline and structure

The thesis comprises of six different chapters. Chapter one discusses the background of surfactants, where their amphiphilic nature due to a polar hydrophilic head and a nonpolar hydrophobic tail are discussed. Availability of natural and synthetic surfactants are also discussed. Their different types (cationic, anionic, zwitterionic and nonionic) are highlighted. The aims and objectives, and possible benefits of the research are also included in this chapter. Chapter two presents the survey on the relevant literature where different types of micelles are reviewed. Counterion binding constants, micellar models and viscoelastic nature of micelles are thoroughly discussed. Chapter three and four report, respectively, the findings on counterions, 2-$NaOC_6H_4CO_2^-$ and 3,5-$Cl_2C_6H_3CO_2^-$ while chapter five reports on 4-$ClC_6H_4CO_2^-$. These chapters (chapter three, four and five) are presented in such a way that each chapter provides a report on experimental details,

results, discussion, and conclusion based on a particular organic salt used. The last chapter (chapter six) concludes on the research outcome, from chapter three, four, and five, where the influence of $C_{16}E_{20}$ on the relative counterion binding constants, K_X^{Br} or R_X^{Br}, and counterion-induced CTABr micellar structural growth are highlighted. Recommendations on the directions of future work are also given in the conclusions chapter.

CHAPTER 2: LITERATURE REVIEW

2.1 History of micelles (Nanoparticles) and CMC

Challenges and looking forward to solutions for certain problems have no specific history since the beginning of the world; as one challenge is tackled with, or a problem is solved, a room for more and more to emerge would then be opened. However, in search for a way out of a particular challenge or problem, there should either be a positive or a negative outcome at the end. Both results are useful in the field of research as they can be used to build on the previous work, or to avoid in future. Strive for knowledge opens the sky for researchers to propose whatever type of idea they have as long as it does not violet the fundamentals of its subject. "Nonsense, McBain" were the words uttered by an eminent scientist, chairman of a meeting of the Royal Society in London, responding to the proposal submitted by McBain (McBain, 1944) that surfactants, might aggregate in aqueous solution. Subsequent events confirmed that the nub of McBain's model was correct (Vincent, 2014). The enormous industry based 'soaps' and detergents prompts intensive studies of these complicated systems, supported by monographs and detailed reviews (Menger, 1979).

In early 20th century (1913), McBain introduced (for the first time) the word "micelle" in his attempt to explain the process of molecular self-assembly in an aqueous solution of detergent or soap (Vincent, 2014). When small amounts of a given surfactant are gradually added to a given volume of water, the properties of the aqueous solutions are unexceptional until the surfactant exceeds a specific concentration called the critical micellar concentration, CMC. At this point, further added surfactant exists in solution as aggregates of generally 20 to 100 monomers, which are called micelles. This CMC is acting as a very narrow gateway of surfactants concentration which provides sudden variation in many physicochemical properties, e.g. reaction rates, turbidity, surface tension, magnetic resonance, and others (Drew, 2006). The formation of micelles is often

observed by a change in the pattern of the dependence of a given property of a solution on surfactant concentration (**Figure 2.1**). This property can be surface tension, the molar conductance of an ionic surfactant, UV-visible absorption spectra of water-soluble dyes (or an iron complex) (Clint, 1992).

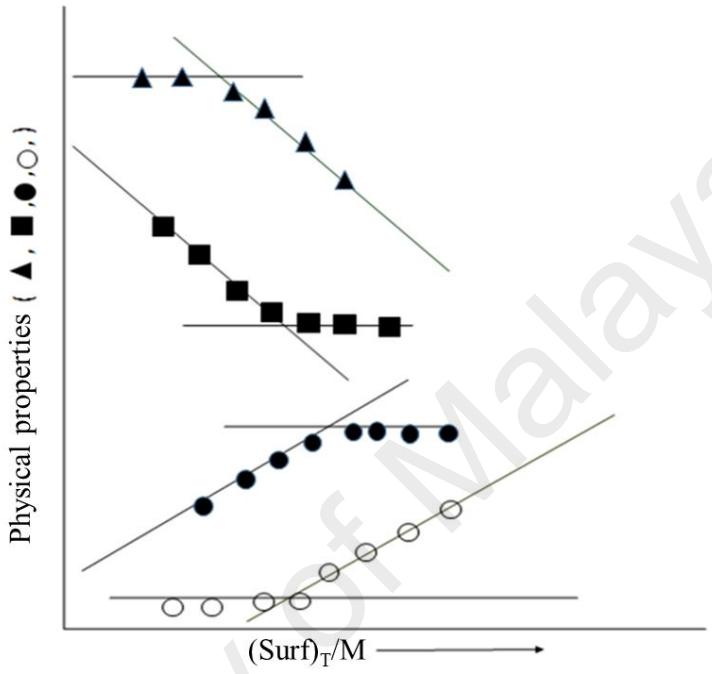

Figure 2.1: Physical properties of the aqueous solutions of micelles against the total amount of surfactant, $[Surf]_T$. The intersection in each pair of linear plots represents the CMC.

When more surfactant is added, the micelles cluster forms more complex aggregates. Micelles are not formed by the gradual association of monomers, forming dimers, trimer, and so on. Rather micelles are examples of organised structures spontaneously formed by simple molecules. A quoted aggregation number is not a stoichiometric number. As the hydrophilic ends of surfactants are attracted to the surface of the polar phase, they line up with it. Micelles of different shapes will begin to form (depending on their concentrations) when the phase is filled up (Evans & Wennerstrom, 1994).

The formation of micelles depends on various factors which include surfactant type, pH, temperature, additives, counterion binding (for ionic surfactants). Surfactant type is one of the major factors affecting the micellization process. The non-polar hydrophobic

tail groups (alkyl chain) of the molecules interact freely among themselves owing to the formation of micelles whereas the charged/polar hydrophilic head groups (for ionic surfactants) exhibit opposing repulsion (Crook *et al.*, 1964)**.** More charged heads have significant influence on micellization process and possess higher CMC value because it will be difficult to overcome the head to head repulsion of the groups as they come to aggregate (Anacker & Ghose, 1968). In general, cationic surfactants have a relatively higher value of CMC, followed by the anionic (Holmberg *et al.*, 2002). Nonionic surfactants have a lower value of CMC due to micellar stabilisation by the alkyl chain (Islam & Kato, 2003b). Also, different tail groups of various surfactants have an influence on micellization process by a change in some carbon atoms in the group. An increase in some carbon atoms in the chain brings about a decrease in the value CMC (Lin *et al.*, 1974). Ali and his co-workers (2014) reported that presence of amino acid additives; glycine, diglycine, and triglycine, favours the CTABr micelle formation by decreasing the value of the CMC (Ali *et al.*, 2014). The CMC exhibits a decreasing pattern as the length of the alkyl chain increases from glycine to triglycine. They concluded that it was the result of increased solvation of CTA^+ by water molecules and other factors. This solvation increases as the hydrophobicity increase from glycine to triglycine (Ali *et al.*, 2014).

Nature of counterions can also affect the micellization process. Polarizability of a particular counterion will tell whether the CMC value required is less or more. Counterions with higher polarizability results in less CMC value as well as more aggregation number (Ruckenstein & Beunen, 1988). It has been reported by Cheng (2015) that in aqueous solution, the presence of counterions decreases the CMC of mixed surfactant systems because the counterionic salts screen the ionic charge of the polar hydrophilic headgroups. Consequently, reduce the electrostatic repulsion between them in the micelles phase (Cheng *et al.*, 2015). They further concluded that the CMC decreases

with increase in the concentration of the counterion and the relatively stronger electrolyte, Br^-, decreases the CMC most compared to the weaker Cl^- (Cheng *et al.*, 2015).

2.2 Micelles of mixed cationic-nonionic surfactants system

Pure ionic or non-ionic surfactant molecules in aqueous solution produce what is considered as "micelles" or "normal micelles". In addition to this category, another type of micelles made up from a combination of monomers of two different/similar micelle-forming surfactants (such as ionic-ionic, nonionic-nonionic or ionic-nonionic surfactants with various features) in aqueous solutions are regarded as "mixed micelles" (Rathman & Scamehorn, 1984). Due to the availability of various surfactants, different types of the mixture are likely to provide different features and application fields (M. N. Khan, 2006). The mixed surfactants micellar system for the present research is strategically chosen to be cationic-nonionic because their intensive investigations in the last almost three decades were only on the physicochemical properties (Alargova *et al.*, 2001; Esumi *et al.*, 1998; Ghosh & Moulik, 1998; Griffiths *et al.*, 1999; Islam *et al.*, 2002; Palous *et al.*, 1998; Shiloach & Blankschtein, 1998; Yoshida & Dubin, 1999). The current research is different as it discusses quantitatively the effects of mixed micelles on the reaction rates together with some empirical approaches (Khan, 2015). This method requires the investigation of the structural behaviours of the mixed micelles. It is believed that the energy processes during formation of mixed micelles are almost the same as those during the formation of pure micelles. Therefore, the mixed micellar structural transitions are relatively similar to those of pure micelles. It has been understood that a solution of mixed micelles of two different surfactant *y* and *z*, *y* behaves as an additive for *z* and the vice versa (Khan, 2015).

2.3 Micellar growth

Due to their amphiphilic behavior, surfactant molecules can aggregate in solution to form different microstructures. At concentration similar to CMC, the micellar structure is spherical or rodlike (Menger, 1979; Schramm *et al.*, 2003; Wennerström & Lindman, 1979). However, several factors (such as temperature, pH, increase in concentration of micelle-forming surfactant, additives) affect the shape and size, causing the micellar structural transition/growth (Cates & Candau, 1990; Davies *et al.*, 2006; Kern *et al.*, 1991; Kumar *et al.*, 1996; Patel *et al.*, 2014; Yin, *et al.*, 2006). The morphology of spherical micelles can be skillfully altered to provide different micellar structures such as wormlike, rodlike, or vesicles by the use of specific additives **(Figure 2.2)**. Hence, by the proper choice of a specific factor, the micelles can be manipulated to obtain different micellar structures. These self-assemblies provided significant importance for applications in various industries as well as modern technology, for instance, drag reduction, enhanced oil recovery, drug delivery (Karayil *et al.*, 2016).

The addition of certain inorganic or organic salt, as counterions, to micellar aggregates of a spherical structure, also induces the formation of wormlike micelles (Hayashi & Ikeda, 1980; Ikeda *et al.*, 1980). Bijma and co-authors reported (Bijma *et al.*, 1998) that the nature of counterion among other factors influencing the growth of spherical micelles to wormlike micelles. Depending upon the type and molecular nature of the surfactant cationic headgroup and the position of the substituent in the aromatic counterion, wormlike micelles may be formed. They concluded that the growth is largely dependent upon the nature and structure of the counterion.

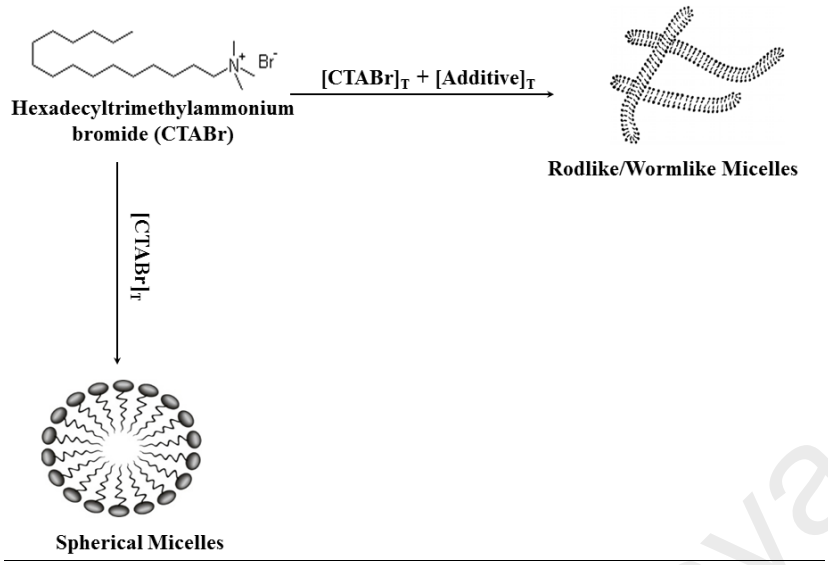

Figure 2.2: Micellar growth as a result of additives**.**

The CTABr micellar growth has been investigated by different methods such as small angle X-ray scattering (Hirata *et al.*, 1988), dynamic light scattering (Dorshow *et al.*, 1982; Kuperkar *et al.*, 2011; Nemoto & Kuwahara, 1993), viscosity measurement (Inoue *et al.*, 2005; Kim & Yang, 2000), small angle neutron scattering (Aswal *et al.*, 1998; Mata, Aswal *et al.*, 2006), and static light scattering (Brown *et al.*, 1989). Patel and coauthors (2014) have also examined the pH-induced CTABr micellar growth in the presence of p-toluic acid, p-toluidine, and p-cresol as weakly polar aromatic additives by different techniques (Patel *et al.*, 2014) and concluded that interaction between the aromatic additives and CTABr micelles brought about the micellar structural growth from spherical to extended ellipsoidal micelles (Patel *et al.*, 2014).

It is, therefore, a common perception that different factors including temperature, pH, increase in the concentration of micelle-forming surfactant, additives, could appropriately be used to change the morphology (shape and size) of surfactant micelles, which is the leading cause for the micellar structural transition/growth.

2.4 Applications

Because of their encounter in almost all domestic and industrial importance, micelles of mixed surfactants system have been the great area of research interest in the field of colloids and interfaces (Hoffmann & Pössnecker, 1994; Holland & Rubingh, 1992; Rosen, 1986; Shiloach & Blankschtein, 1998). There are quite some potential applications of the mixed cationic-nonionic micellar medium. They cover a broad range of industrial processes (from oil and gas, pharmaceutical, cosmetics, to mention but few). Some of the applications of mixed micelles include but not limited to the following;

a) Some studies reported that curcumin (with enol-keto tautomeric ability) could be soluble in the aqueous micellar solution of triblock copolymer of polyethylene oxide and polypropylene oxide, Pluronic P123 (PEG-PPG-PEG), by simply heating the solution. In drugs delivery to a specified target, less solubility of curcumin and its poor bioavailability becomes a great challenge (Anand *et al.*, & Aggarwal, 2007; Ganguly *et al.*, 2017; Hatcher *et al.*, 2008). However, the micellar system of ionic and nonionic surfactants mixture could be a method to the solubilization (Ganguly *et al.*, 2017). These micelles are very useful to enhance the movement of the drug into the blood brain and intestine barriers. They are also found to be good in mediating the drug effectiveness over multidrug-resistant cancer cells (Batrakova & Kabanov, 2008; Batrakova *et al.*, 2010).
b) Due to their increase in bioavailability and tendency to make the polyaromatic hydrocarbons soluble in aqueous solution, cationic-nonionic surfactant mixtures are extremely, nowadays, used in environmental remediation (for surfactant-enhanced remediation, SER) (Liang *et al.*, 2017; Mao *et al.*, 2015; Shah *et al.*, 2016). When the ionic surfactant concentration reaches CMC, the micelles behave as hydrocarbon-like phase and enhance the partition of polyaromatic hydrocarbons into aqueous solutions (Liang *et al.*, 2017). The relatively weaker

repulsion in nonionic surfactants influences the headgroups to form aggregate and larger micelles. These micelles have higher affinity to polyaromatic hydrocarbons in ionic surfactants (Dar *et al.*, 2007; Liang *et al.*, 2017).

2.5 Amminolysis/piperidinolysis of ester

The general reaction for the piperidinolysis of ester can represented as secondary aminolysis as shown in **Scheme 2.1.**

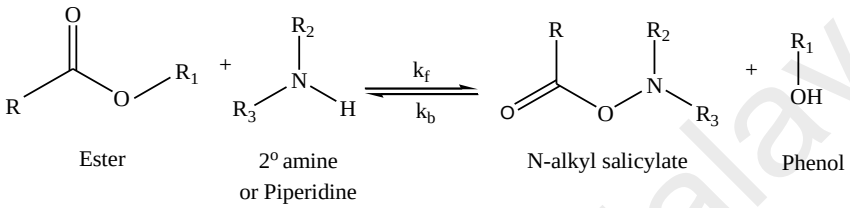

Scheme 2.1: General acid/base piperidinolysis of ester

The acid catalysed reaction of piperidine with ester increaeses the rate of both forward (k_f) and backward (k_b) reaction (i.e it favours the formation of N-alkyl salicylate and ester). In the other hand, if the rate of reaction is base catalysed, **Scheme 2.1** will no longer be reversible as the product, N-alkyl salicylate, is comparatively a stronger than the conjugate acid, 2° amine (in this case piperidine). Hence, R_1O^- undergoes irriversible reaction with N-alkyl salicylate to yield more stable ionized N-alkyl salicylate as product. Therefore, a base cannot catalyse the rate of revesible reaction between phenol and N-alkyl salicylate.

2.6 Proposed micellar mechanisms

The set-up of larger number of the reaction mechanism were best determined using kinetic studies. These were achieved by the use of data obtained (with respect to the reaction rates) under certain conditions. The proposed reaction mechanisms were considered for the use of the derived kinetic equations (Khan, 2006). **Scheme 2.2** illustrates a brief reaction mechanism in which a bimolecular system is involved with k_M^W

representing second-order rate constant for two reactions at both micellar and aqueous interfaces. Subscript M and W denote micellar and aqueous phases, respectively. The reactant, R, K_R and K_S are the respective equilibrium constants for the reactants and substrate (ester).

For the majority bimolecular reactions which are mediated by micelles, the parallel stepst for the reactions are reported to occur at the same time in the two different phases as demonstrated in **scheme 2.2.** However, comparatively small number of reports have presented different results. The drawback is related different factors, such as possible occurrence of cross-interface reaction (Bunton & Romsted, 1979; Vera & Rodenas, 1986; Bunton & Moffatt, 1986; Ortega & Rodenas, 1987).

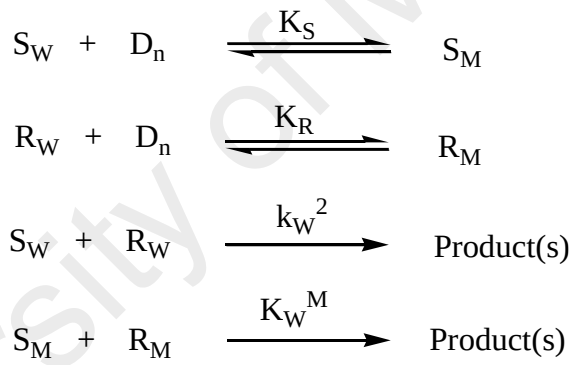

Scheme 2.2: Micellar-mediated bimolecular reaction mechanism.

2.7 Micellar models and their conditions/assumptions

Until mid-1960's, the qualitative explanations of the observed kinetic results on the rate of micellar-mediated reactions were the only available and reliable ways of data interpretation. This was due to the absence of acceptable kinetic model which could describe, logically and convincingly, the mechanisms of micellar-mediated reactions. Some years later (late 1960's), the quantitative explanations were possible due to the availability of kinetic micellar models which could be enough for the interpretations of kinetic data on micellar-mediated reactions. Despite the fact that all the models appeared to be imperfect (Khan, 2006), their emergence provided a merely perfect or comparatively

perfect model (Khan, 2006). Some of the micellar kinetic models, developed so far, were examine to understand the quantitatively the effects of micelles on the reaction rates. These models and their assumptions are discussed in the subsequent subsections.

2.7.1 Pre-equilibrium micellar kinetic model

This is also called Menger's phase separation model or enzyme-kinetic-type model. The different experimentally obtained values of micellar-mediated reaction rate constants were used to demonstrate their response over the change surfactant concentration. The increase in surfactant concentration shows either a monotonic decrease or increase in the values of the rate constant **(Figure 2.3)**. As reported by Menger and Portnoy (1967) (Menger & Portnoy, 1967), the anionic and cationic micellar-mediated hydrolysis of some esters follow the pattern in **Figure 2.3.**

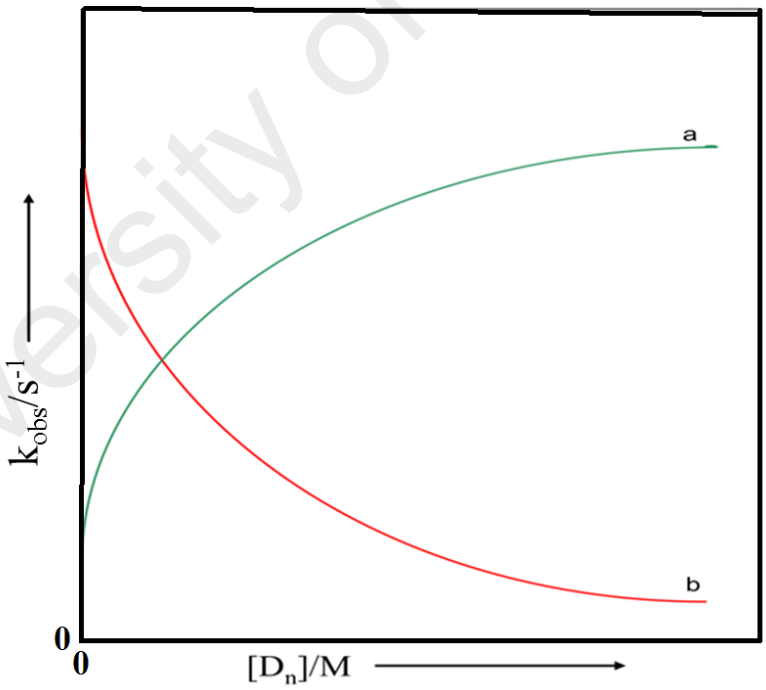

Figure 2.3: Graphs of k_{obs} vs. $[D_n]$ showing a monotonic increase (a) and decrease (b) in k_{obs} with the increase in $[D_n]$**.**

They suggested the reaction pathway illustrated in **Scheme 2.1** where K_{eqS} and P represent, respectively, the equilibrium constant for the micellization of ester molecules (S) and the product of the reaction. D_n, S_W, and S_M represent aqueous/free ester and

micellized ester molecules, respectively. Symbols k_W and k_M denote the respective rate constants for the hydrolysis of the aqueous and micellized ester.

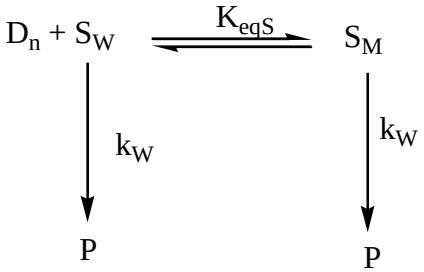

Scheme 2.1: Reaction pathways for the unimolecular reaction based on pre-equilibrium kinetic, PEK, micellar model.

The PEK micellar model has the following assumptions;

i. The unassociated surfactant concentration remains constant above the CMC. Therefore, the expression $[D_n] = \{[Surf]_T - CMC\}/n$ should hold with $[Surf]_T$ standing for total surfactant concentration and n representing the average number of surfactant micellar aggregate.
ii. The formation of micelles occurs at exactly the CMC (not within the certain small range of concentration).
iii. The formation of micelles is not disturbed/interrupted by the substrate.
iv. The stoichiometric ratio between the substrate and the micelles should be in the form of 1:1.
v. There will be no formation of complex molecules between the surfactant monomer and the substrate.

The relationship between the pseudo first order rate constant, k_{obs}, and the illustration in **Scheme 2.1** gives **Eq. 2.1** for several micellar models (Bunton & Savelli, 1986; Menger & Portnoy, 1967).

$$k_{obs} = \frac{k_W + k_M K_S[D_n]}{1 + K_S[D_n]} \qquad \textbf{(2.1)}$$

2.7.2 Pseudophase micellar model

At $[Surf]_T$ below and beyond the CMC, an aqueous solution of the surfactant is transparent to UV-visible radiation. This is regarded as a micellar single homogeneous phase and, in this case, the micelles are not being able to form a real phase (Khan, 2006). With this reason, some reports (Bunton *et al.*, 1991; Rathman, 1996) proposed the idea of pseudophase model to be considered, instead of a real micellar model. The pseudophase, PP, micellar model retains all the assumption in PEK (Menger & Portnoy, 1967) with the addition of other assumptions as explained thoroughly elsewhere (Khan, 2006). The details of this model could be found in several reports (Bunton, 1991, 1997; Bunton *et al.*, 1993).

2.7.3 Pseudophase ion exchange micellar model

The concept of pseudophase ion exchange, PIE, model was developed based upon the competition (exchange) between counterions (X) and (Y), of similar charge, in an ionic micellar surface. It was independently reported by Romsted and other researchers (Quina & Chaimovich, 1979; Romsted, 1977) and it provides the quantitative or semi-quantitative explanations of ion exchange. The PIE micellar model is an extension of PP model and, hence, it retains all the assumptions involved in PEK and PP models with the addition of some more assumptions as highlighted in various excellent literature reports (Bunton, 1979, 1991, 1997; Bunton *et al.*, 1991; Bunton & Savelli, 1986; Romsted, 1977). The assumptions and the theories and concepts are discussed in detail elsewhere (Khan, 2006).

The PIE model of micelles was initially provided to explain, quantitatively, the data obtained from several bimolecular kinetic reactions related to a monovalent ion exchange process involving reverse micelles (Quina & Chaimovich, 1979), aqueous ionic micelles (Bunton *et al.*, 1991), and cosurfactant modified micelles (El Seoud & Chinelatto, 1983;

Pal *et al.*, 2005). Based on this model, a study on the effect of [MX] (where MX = KBr) on the rate of hydrolysis of some esters (S) in the presence of ionic CTABr micelles was reported (Vera & Rodenas, 1986). The observed data (k_{obs} vs. [MX]) were discussed according to the PIE model coupled with an empirical equation (**Eq. 2.2**)

$$K_S = K_S^0 - L\,[MX] \qquad \textbf{(2.2)}$$

where K_S is the cationic CTABr micellar binding constant of S^-, $K_S^0 = K_S$ at [MX] = 0 and L is an empirical constant whose magnitude is the measure of the ability of X^- to expel S^- from the cationic CTABr micellar pseudophase to the aqueous phase (Khan, 2006).

The limitation of PIE model has been noticed in some cases, where the concentration of surfactant is very high or the salt (additive) contains (in excess) a strong hydrophilic counterion such as F^-, Cl^- and HO^- (Bunton, 1991; Bunton *et al.*, 1991; Bunton *et al.*, 1993; Khan & Ismail, 2001). This limitation arose due to the failure of one (or more) of those assumptions provided in the literature (Khan, 2006). Given this, several researchers (Abuin *et al.*, 1983; Blasko *et al.*, 1993) have discussed the probable cause(s) of the limitation and the possible adjustment (Khan, 2006).

2.8 Viscoelastic properties of micelles

Due to their various applications (Schubert *et al.*, 2003; Yang, 2002), aqueous viscoelastic surfactant micellar solutions have been reported to be used in pharmaceutical and health sectors (Ideta *et al.*, 2004; Kabanov *et al.*, 2002; Kataoka *et al.*, 2001; Nishiyama *et al.*, 2005; Nishiyama & Kataoka, 2006; Rangel-Yagui *et al.*, 2005; Sutton *et al.*, 2007) as well as petrochemical industries (Qi & Zakin, 2002). The distinctive characteristic of viscoelastic micelles, over polymers in solution, is their tendency to change and regain shapes and sizes when subjected to the external factors such as heat

and shear. Thus they are regarded as “living polymers” (Yang, 2002; Ziserman *et al.*, 2009). They also attain a certain level of stability under high temperature or high shear rate conditions (Davies *et al.*, 2006).

Though several studies (Ali & Makhloufi, 1997; Shikata *et al.*, 1987; Soltero *et al.*, 1996) have reported that addition of counterionic salts makes the formation of viscoelastic wormlike micelles easier, another study (Gamez-Corrales *et al.*, 1999), later, revealed their formation, in the absence of salts, in cationic surfactant solutions.

CHAPTER 3: INFLUENCE OF MIXED CTABr–$C_{16}E_{20}$ MICELLES/NANOPARTICLES ON RELATIVE COUNTERION BINDING CONSTANTS IN AQUEOUS SOLUTIONS OF INERT SALTS (2-$NaOC_6H_4CO_2Na$ AND NaBr): KINETIC AND RHEOMETRIC STUDY[1]

3.1 Introduction

Micellar substances are nanoparticles in nature, and their molecular, physical and chemical behaviours on the kinetic rate of reaction have been thoroughly investigated for almost sixty years ago (Fendler, 2012). Despite the fact that experimental and theoretical studies on the structure of mixed micelles have been published for the past 20 to 30 years, details of the reactions are not being discussed well when compared to pure ones. Studies on the influence of mixed micelles upon the rate of kinetic reactions began less than 25 years back (Eads & Robosky, 1999; Junquera & Aicart, 2002). Efforts were made to come up with highlights on the majority of data by the use of one of the two models, viz; (i) micellar models of pure surfactant solutions (Muñoz *et al.*, 2002; Zakharova *et al.*, 2003) or (ii) combination of (i) above and empirical equations (Frescura *et al.*, 1995; Lee & Nome, 2000).

Addition of nonionic micelles (C_nE_m) to cationic micellar-mediated reaction mixture lowers a number of counterions at the surfaces of ionic surfactants, and hence reduces the fraction of ionic surfactant coverage (β) (Bunton & Savelli, 1987; Larsen & Tepley, 1974). Moreover, the volume of the micellar pseudophase also increases (Vangeyte *et al.*, 2004), which in turn affects the amount of micellized reactant via dilution. The

[1]This chapter has been published, as journal article, by RSC Advances; Fagge, I. I., Khalid, K., Noh, M. A. M., Yusof, N. S., Zain, S. M., & Khan, M. N. (2016). Influence of mixed CTABr-$C_{16}E_{20}$ nanoparticles on relative counterion binding constants in aqueous solutions of inert salts (2-$NaOC_6H_4CO_2Na$ and NaBr): Kinetic and rheometric study. *RSC Advances*, 95504-95511. ISI indexed.

pseudophase (PP) micellar model coupled with **Eq. 3.1** have been used to analyse the data (Khan & Ismail, 2003).

$$K_S = K_S^0/(1 + K_{X/S}[MX]) \quad \textbf{(3.1)}$$

where K_S is the CTABr micellar binding constant of the anionic reactant, S^-, (and equals to K_S^0 in the absence of X^-), $K_{X/S}$ denotes empirical constant and its values indicate the ability of X^- to transfer anionic reactant, S^-, from pure CTABr micellar phase to bulk aqueous phase (Khalid *et al.*, 2016). Therefore, $K_{X/S}$ should be directly and inversely proportional to K_S and K_S^0, respectively (Khan & Fui, 2009).

Several efforts have been made to bring reliable clarification(s) for the viscoelastic nature of the micellar systems in the aqueous phase. However, almost all the clarifications are not enough for some systems such as those of CTABr with certain inert salts (Rao *et al.*, 1987). Moreover, there is a scarcity of quantitative and theoretical evidence(s) to confirm that addition of these salts in a surfactant solution results in the viscoelastic behavior of micelles.

The report in this chapter varies from previously reported ones (Khan & Fui, 2009; Khan & Ismail, 2004), due to the fact that it is designed to (i) deal with mixed cationic-nonionic surfactants (CTABr-$C_{16}E_{20}$) and a bimolecular reaction aimed at providing a quantitative elucidation on how the rate of CTABr-$C_{16}E_{20}$ micellar catalyzed organic reactions could be affected by the addition of sodium salicylate, (ii) to use rheological information to correlate the values of relative counterion binding constants (K_X^{Br} or R_X^{Br}) for CTABr/M_2X/H_2O solution (M_2X = 2-$NaOC_6H_4CO_2Na$) systems and CTABr micellar structural growth of CTABr/$C_{16}E_{20}$/M_2X/H_2O solution under different experimental conditions. The results obtained and their possible elaborations are presented in this chapter.

3.2 Methodology

Two types of experiments were involved in the study; the kinetic measurements for the reaction of piperidine with ionised phenyl salicylate, in the presence of salts and surfactants, which was monitored using a UV-Visible spectrophotometer. The other type was the rheometric study to support the findings from the former.

3.2.1 Materials

Reagent-grade substances, which are commercially available from different manufacturers, have been used. Phenyl salicylate (PSH) was bought from Fluka (% purity ≥ 98). Acetonitrile from Merk (an A.R. Grade) was used in preparing 0.01 M stock solution of PSH. The other reactant, piperidine (Pip), was also supplied by Merk (% purity ≥ 99). The cationic surfactant hexadecyltrimethylammonium bromide (in powdered form), denoted as CTABr, was provided by Sigma-Aldrich (%purity ≥ 99). The nonionic surfactant polyethylene glycol (20) hexadecyl ether [$C_{16}H_{33}(OCH_2CH_2)_{20}OH$ ($C_{16}E_{20}$)], also called "Brij 58", was purchased from Sigma-Aldrich. Sodium hydroxide, NaOH, with ≥ 99% purity was from Merk. The organic salt disodium salicylate, 2-$NaOC_6H_4CO_2Na$ (M_2X), with % purity ≥ 98, was brought by Sigma-Aldrich whereas the inorganic one, sodium bromide, NaBr (MX), was purchased from Merk with ≥ 99% purity. All these reagents were used without further purification. The stock solutions of 1.0 M Pip, 0.2 M CTABr, 0.2 M $C_{16}E_{20}$, 0.3 M NaOH, and 2.5 M NaBr were prepared by using distilled deionized water while the standard solution of 0.5 M M_2X (disodium salicylate, 2-$NaOC_6H_4CO_2Na$) was prepared by adding 0.55 M NaOH to 0.5 M solution of sodium salicylate.

3.2.2 Kinetic method

The thermoregulatory water bath and electronically temperature controlled cells compartments UV-Visible spectrophotometer (equipment model; Perkin Elmer Double

Beam Lambda 25) was used to carry out the kinetic experiments. The measurements were performed to observe the disappearance of ionised phenyl salicylate, PS^-, in a solution containing 0.10 M Pip, > 0.03 M NaOH, and NaBr as well as 2-$NaOC_6H_4CO_2Na$, at 370 nm and 35 °C (in the presence of pure CTABr and mixed CTABr-$C_{16}E_{20}$ micelles. Distilled deionized water was used as a blank before the measurements. Volumetric flasks, of 25 mL each, containing 4.9 mL mixture of different concentration of the reagents (except PSH) were immersed into a water-bath at 35 °C for at least 15 minutes. Followed by the addition of 0.1 mL of 0.2 mM substrate (PSH) to the flask (total volume became five mL) to initiate the reaction. This went simultaneously with starting the kinetic measurement in the Lambda 25 computer software. The solution was then transferred to the cuvette followed by putting it in the cell compartment. The rate was monitored at different concentrations of MX and M_2X.

3.2.2.1 Product characterization of piperidinolysis of PS^-

The rate and product characterization study on the alkaline piperidinolysis of PS^- in an aqueous solvent containing 2% v/v CH_3CN, as described in the earlier study (Khan & Fui, 2009), revealed the brief reaction step as represented by **Scheme 3.1.**

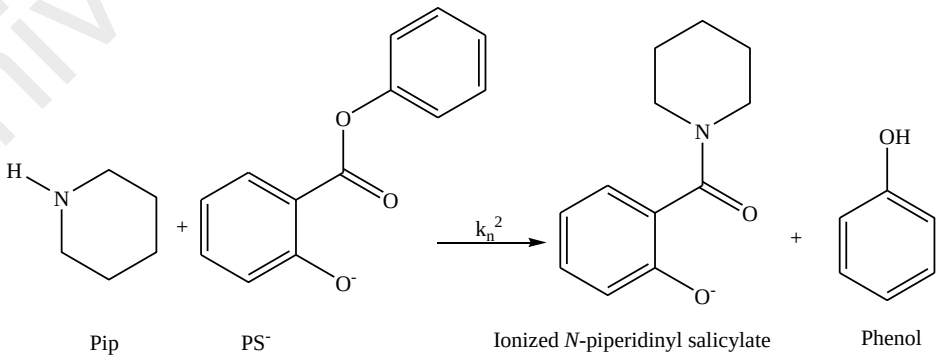

Scheme 3.1: Chemical equation for the aqueous piperidinolysis of PS^-.

In **Scheme 3.1,** k_n^2 represents nucleophilic second-order rate constant for the reaction of Pip with anionic PSH (PS^-). The piperidinolysis of PS^- has been shown to involve nonionic PS^- (PSH) and Pip as the reactants and under the experimental condition the

reaction of PSH and Pip is concluded to be kinetically insignificant (Khan, 1991; Khan & Fui, 2009).

The experiment was fixed to fit pseudo first order rate law throughout, by making sure that the ratio of total concentrations of Pip and PS^- ($[Pip]_T : [PS^-]_T$) is 500 : 1 where $[\ ]_T$ stands for the total concentration. The steps for the order of the reaction are illustrated as follows;

$$S \xrightarrow{k_{obs}} P \qquad \textbf{(3.2)}$$

where S and P represent the reactant and the product, and the k_{obs} is the pseudo first order reaction rate constant for the reaction. The rate law, **Eq. 3.2**, can be presented as follows;

$$\text{Rate} = \frac{-d[S]}{dt} = \frac{-d[Pip]}{dt} = \frac{+d[P]}{dt} = k_{obs}[S] \qquad \textbf{(3.3)}$$

or

$$\text{Rate} = \frac{-d[S]}{dt} = k_{obs}[S] \qquad \textbf{(3.4)}$$

Integrating **Eq. 3.3** or **3.4** results in **Eq. 3.5**

$$[S] = [S_0] \exp(-k_{obs}t) \qquad \textbf{(3.5)}$$

with $[S_0]$ and [S] representing, respectively, the concentration of S at initial stage (time = 0) and at time, t. Considering A_{obs} to be the observed absorbance, then

$$A_{obs} = \delta_S[S] + \delta_P[P] \qquad \textbf{(3.6)}$$

where δ_S and δ_P stand for the molar absorptivities of S and P, respectively.

Recalling **Eq. 3.2**,

$$[S_0] = [S] - [P] \quad \textbf{(3.7)}$$

and

$$[P] = [S_0] + [S] \quad \textbf{(3.8)}$$

Relating **Eqs. 3.6** and **3.8**,

$$A_{obs} = \delta_S[S] + \delta_P([S_0] - [S]) \quad = (\delta_S - \delta_P)[S] + \delta_P[S_0] \quad \textbf{(3.9)}$$

If $\delta_P([S_0] = A_\infty$ and $(\delta_S - \delta_P = \delta_{app}$ **Eq. 3.9** can be modified to **Eq. 3.10**

$$A_{obs} = \delta_{app}[S] + A_\infty \quad \textbf{(3.10)}$$

Substituting **Eq. 3.5** into **Eq. 3.10** gives

$$A_{obs} = [S_0]\delta_{app} \exp(-k_{obs}t) + A_\infty \quad \textbf{(3.11)}$$

Eq. 3.11 shows the relationship between the absorbance (A_{obs}) and the reaction time (t) for the reaction, and it was used to calculate the values of δ_{app} (apparent molar absorptivity), k_{obs} and A_∞ ($A_{obs} = A_\infty$ at $t = \infty$) and the results were analyzed as described elsewhere (Khan & Ismail, 2003). The values of k_{obs} were obtained in the presence of pure $[CTABr]_T$ and mixed $[CTABr]_T$-$[C_{16}E_{20}]_T$ micelles at different [MX]. Different values of k_{obs}, in the absence of CTABr, were also determined and are required in the use of the SEK method. Details of this technique and explanations of the reaction mechanisms were according to what was described in the earlier report (Khan & Ismail, 2003).

3.2.3 Determination of relative counterion binding constants (K_X^{Br} or R_X^{Br}) for X = $^-OC_6H_4CO_2Na$ using the semi empirical kinetics technique

Semi empirical kinetic (SEK) method which requires the use of appropriate reaction kinetic probe, has been used experimentally to determine the values of K_X^{Br} or R_X^{Br} for pure

CTABr (Khan & Sinasamy, 2011; Yusof & Khan, 2012). The effect of the concentrations of the inert counterionic salts ([MX] and [M_2X]) on the values of k_{obs}, for the nucleophilic reaction of Pip with PS^- at constant concentration of pure CTABr and 35 °C, has been used as a kinetic probe to use the SEK method (Yusof *et al.*, 2013). The determination of K_X^{Br} or R_X^{Br} by the use of the SEK method requires the values of kinetic parameters, $K_{X/S}^n$, for $X = X^-$ (test counterions) and Br^- (reference counterion), at a constant $[CTABr]_T$. The values of $K_{X/S}^n$ were determined by the use of K_S^0 (= CTABr micellar binding constant of PS^- at [MX] or [M_2X] = 0). The reported value of K_S^0 (7000 M^{-1}) (Khan & Arifin, 1996) was used to calculate the values of $K_{X/S}^n$. Details of this technique and explanations of the reaction mechanisms are as according to what was described in earlier reports (Khan, 2010; Khan & Ismail, 2003; Khan & Sinasamy, 2011).

3.2.4 Rheological measurements

In these measurements, the total volume of the sample used (for kinetic measurements explained in section 3.2.2), was doubled (i.e. 10 mL). Two different sets of desired samples were prepared, viz; (i) Pure CTABr micellar solution containing a constant volume of > 0.03 M NaOH, 0.10 M Pip, 2 x 10^{-4} M PSH and 0.015 M CTABr at various [M_2X] ([M_2X] within the range of 0.006 to 0.120 M). (ii) Mixed CTABr-$C_{16}E_{20}$ micellar solution containing constant volume of > 0.03 M NaOH, 0.10 M Pip, 2 x 10^{-4} PSH and $[CTABr]_T$-$[C_{16}E_{20}]_T$ (with $[CTABr]_T$ = 0.015 M and $[C_{16}E_{20}]_T$ = 0.006 M) at various [M_2X] ([M_2X] within the range of 0.006 to 0.120 M). The rheological measurements were conducted at 25 and 35 °C using Anton Paar MCR301 rheometer, with a double gap cylinder (DG26.7/T200/SS having 26.661 mm external diameter and 24.656 mm internal diameter). The values of steady-shear viscosity (η), during the flow curve measurement, were obtained within the range of 0.010-1000 s^{-1} of shear rates. The details of the experiment were the same described in the previous study (Yusof *et al.*, 2013).

3.3 Results

3.3.1 Effect of [NaBr] on k_{obs} for the piperidinolysis of PS^- at constant concentration of pure $C_{16}E_{20}$ and 35 °C

Certain kinetic runs were carried out to study the influence of pure $C_{16}E_{20}$ on k_{obs} on the reaction of 0.10 M Pip with 2 x 10^{-4} M PS^- and 0.030 M NaOH at various concentrations of NaBr ([NaBr] within the range of 0.000-0.700 M). The experiment was achieved by adding 0.001 M $C_{16}E_{20}$ at 35 °C and 370 nm. Similar observations were obtained by increasing $[C_{16}E_{20}]_T$ to 0.003, 0.006, 0.008, 0.010 and 0.015 M. The values of k_{obs}, δ_{app} and A_∞ at $[C_{16}E_{20}]_T$ = 0.001, 0.003 and 0.006, and 0.008, 0.010 and 0.015 M are presented, respectively, as **Appendices A** and **B**.

3.3.2 Effect of mixed CTABr-$C_{16}E_{20}$ on k_{obs} for the piperidinolysis of PS^- at various [NaBr] and 35 °C

Several kinetic runs were conducted to study the effects of mixed CTABr-$C_{16}E_{20}$ on k_{obs} for the reaction of 0.10 M Pip, with 2 x 10^{-4} M PS^- and 0.030 M NaOH in the presence of NaBr (within the concentration range of 0.000–0.700 M). These data were used to obtain parameters required to find the value of K_X^{Br} or R_X^{Br}. The experiments were carried out by adding three different $[CTABr]_T$ (= 0.006, 0.010 and 0.015 M) at 0.006 M $C_{16}E_{20}$, 35 °C and 370 nm. Similar observations were obtained by increasing $[C_{16}E_{20}]$ to 0.010 M and 0.015 M. The values of k_{obs}, are presented in **Tables 3.1, 3.2** and **3.3.**

3.3.3 Effect of [2-$NaOC_6H_4CO_2Na$] on k_{obs} for the piperidinolysis of PS^- at constant concentration of pure CTABr and 35 °C

Several kinetic experiments were conducted at 0.006 M CTABr, 0.10 M Pip, 2 x10^{-4} M PSH, > 0.03 M NaOH and various [2-$NaOC_6H_4CO_2Na$] (0.00–0.14 M). Complementary results were found by increasing the concentration of CTABr to 0.010

M and 0.015 M. The values of k_{obs} obtained within [2-$NaOC_6H_4CO_2Na$] range are presented graphically in **Figure 3.1**.

3.3.4 Effect of [2-$NaOC_6H_4CO_2Na$] on k_{obs} for piperdinolysis of PS^- at constant concentration of pure $C_{16}E_{20}$ and 35 °C

Other kinetic experiments for the reaction of 0.10 M Pip with 0.20 mM PS^- and 0.030 M NaOH at various [2-$NaOC_6H_4CO_2Na$] (ranging from 0.00 to 0.12 M) in the presence 0.001 M $C_{16}E_{20}$ were conducted. Similar observations were obtained by increasing $[C_{16}E_{20}]_T$ to 0.003, 0.005, 0.006, 0.007, 0.008, 0.010, 0.012 and 0.015 M.

The observed data, k_{obs} versus [2-$NaOC_6H_4CO_2Na$] as well as δ_{app} and A_∞, at $[C_{16}E_{20}]_T$ = 0.001, 0.003, 0.006, 0.008, 0.010 and 0.015 M are presented, respectively, as **Appendices C** and **D**.

3.3.5 Effect of mixed CTABr-$C_{16}E_{20}$ on k_{obs} for piperidinolysis of PS^- at various [2-$NaOC_6H_4CO_2Na$] and 35 °C

To study the influence of mixed CTABr-$C_{16}E_{20}$ micelles ($[CTABr]_T$ = 0.006, 0.010 and 0.015 M + 0.006 M $C_{16}E_{20}$) on the reaction between Pip, PS^- and NaOH, different kinetic experiments were conducted in the presence of [2-$NaOC_6H_4CO_2Na$] (0.00-0.15 M). Similar results were obtained by increasing $[C_{16}E_{20}]_T$ to 0.010 M and 0.015 M. The values of k_{obs} are outlined and presented, respectively, in **Figures 3.2, 3.3** and **3.4.**

3.3.6 Rheological behavior of aqueous pure CTABr and mixed CTABr-$C_{16}E_{20}$ micelles in the presence of various [2-$NaOC_6H_4CO_2Na$] at 25 and 35 °C

Rheological measurements of solutions (in aqueous form) containing 0.015 M CTABr, constant 0.1 M Pip, 2 x 10^{-4} M PS^- and > 0.03 M NaOH and different values of [2-$NaOC_6H_4CO_2Na$] were conducted at the steady-shear rheological response, and 25 and 35°C. The values of shear viscosity (η) at various shear rates ($\dot{\gamma}$) were determined at this

condition. These results are presented, using log-log plots of η vs $\dot{\gamma}$ at various [2-$NaOC_6H_4CO_2Na$], in **Figures 3.5 (a)** and **(b)** at, respectively, 25 and 35 °C. Measurements on aqueous solutions containing mixed 0.015 M CTABr and 0.006 M $C_{16}E_{20}$, with other conditions similar to one mentioned above were also conducted. The values of η at various $\dot{\gamma}$ were also determined. Different observations were obtained at the two different temperatures (25 and 35 °C) and the results are presented in **Figures 3.6 (a)** and **(b).**

Table 3.1: Pseudo-first-order rate constants ($^{m}k_{obs}$) for the reaction of piperidine with anionic phenyl salicylate (PS^-) at 0.006 M CTABr in the presence of 0.006, 0.010, and 0.015 M $C_{16}E_{20}$ and different [MX] (= NaBr).[a]

[MX][b] (M)	[CTABr]$_T$[c] = 0.006 M [$C_{16}E_{20}$]$_T$[d] = 0.006 M		0.006 M 0.010 M		0.006 M 0.015 M	
	$10^4\ {}^{m}k_{obs}$[e] s^{-1}	$10^4\ {}^{m}k_{calcd}$[f] s^{-1}	$10^4\ {}^{m}k_{obs}$[e] s^{-1}	$10^4\ {}^{m}k_{calcd}$[f] s^{-1}	$10^4\ {}^{m}k_{obs}$[e] s^{-1}	$10^4\ {}^{m}k_{calcd}$[f] s^{-1}
0.00	25.3 ± 0.4[g]		31.3 ± 0.5[g]		30.1 ± 0.3[g]	
0.01	26.7 ± 0.7	25.0	39.3 ± 0.4	34.3	32.5 ± 0.3	32.5
0.03	33.0 ± 0.4	29.8	44.9 ± 0.4	39.7	38.1 ± 0.3	37.0
0.06	37.0 ± 0.4	36.1	51.6 ± 0.5	46.3	47.1 ± 0.5	42.9
0.10	40.0 ± 0.7	42.8	52.0 ± 0.4	53.2	48.2 ± 0.2	49.4
0.12	44.9 ± 0.6	45.7	54.9 ± 0.9	56.1	48.5 ± 0.7	52.3
0.15	48.9 ± 0.3	49.5	56.7 ± 0.4	59.9	54.2 ± 0.4	56.1
0.18	51.8 ± 0.5	52.9	61.1 ± 0.4	63.0	61.8 ± 0.4	59.5
0.20	54.8 ± 0.5	54.9	61.7 ± 0.5	64.9	62.2 ± 0.6	61.5
0.25	60.1 ± 0.8	59.2	64.2 ± 0.9	68.9	68.0 ± 0.4	66.0
0.30	65.3 ± 0.8	62.8	75.9 ± 0.6	72.2	69.9 ± 0.5	69.8
0.35	66.7 ± 0.8	65.8	77.5 ± 0.5	74.9	72.8 ± 0.8	73.0
0.40	67.8 ± 0.9	68.4	79.8 ± 1.0	77.1	73.0 ± 0.5	75.8
0.50	71.9 ± 0.7	72.5	81.9 ± 0.6	80.7	78.5 ± 1.0	80.4
0.60	76.1 ± 1.0	75.8	84.8 ± 0.9	83.4	89.1 ± 0.6	84.0
0.70	77.8 ± 1.0	78.3	82.5 ± 0.6	85.6	84.9 ± 0.7	86.9

[a]$[PSH]_0$ = 0.2 mM, [Pip] = 0.1 M, [NaOH] = 0.03 M, λ = 370 nm and aqueous reaction mixture for each kinetic run contains 2% v/v acetonitrile. [b]Total concentration of NaBr. [c]Total concentration of CTABr. [d]Total concentration of $C_{16}E_{20}$. [e]Observed pseudo first order rate constant. [f]Pseudo first order rate constant calculated from **Eq. 3.13** with parameters listed in **Table 3.5**, $\theta = F_{X/S}k^{W}_{obs}$ and $K^{X/S} = K_{X/S}/(1+K^{0}_{S}[CTABr]_T)$. [g]Error limits are standard deviations.

Table 3.2: Pseudo-first-order rate constants (k_{obs}) for the reaction of piperidine with anionic phenyl salicylate (PS^-) at 0.010 M CTABr in the presence of 0.006, 0.010 and 0.015 M $C_{16}E_{20}$ and different [MX] (= NaBr).[a]

[MX][b] (M)	[CTABr]$_T$[c] = 0.010 M		0.010 M		0.010 M	
	[$C_{16}E_{20}$]$_T$[d] = 0.006 M		0.010 M		0.015 M	
	10^4 $^m k_{obs}$[e] s^{-1}	10^4 $^m k_{calcd}$[f] s^{-1}	10^4 $^m k_{obs}$[e] s^{-1}	10^4 $^m k_{calcd}$[f] s^{-1}	10^4 $^m k_{obs}$[e] s^{-1}	10^4 $^m k_{calcd}$[f] s^{-1}
0.00	23.0 ± 0.4[g]		17.5 ± 0.4[g]		28.7 ± 0.3[g]	
0.01	24.2 ± 0.4	24.0	18.1 ± 0.7	18.0	29.4 ± 0.2	29.0
0.03	26.3 ± 0.6	26.5	20.1 ± 0.3	20.4	30.8 ± 0.4	31.1
0.06	29.8 ± 0.5	29.8	22.8 ± 0.6	23.4	34.0 ± 0.4	34.0
0.10	33.4 ± 0.4	33.3	26.8 ± 0.4	26.6	26.8 ± 0.4	37.6
0.12	34.7 ± 0.5	34.9	28.4 ± 0.3	27.9	38.1 ± 0.3	39.2
0.15	36.5 ± 0.5	37.0	30.3 ± 0.5	29.7	38.8 ± 0.5	41.4
0.18	38.8 ± 0.5	38.8	30.9 ± 0.6	31.2	41.3 ± 0.4	43.4
0.20	39.9 ± 0.4	39.8	31.7 ± 0.3	32.1	44.6 ± 0.4	44.6
0.25	42.1 ± 0.5	42.2	33.6 ± 0.4	34.1	48.2 ± 0.3	47.5
0.30	44.6 ± 0.4	44.2	35.6 ± 0.6	35.7	49.5 ± 0.3	50.0
0.35	46.4 ± 0.5	45.8	37.3 ± 0.5	37.5	51.6 ± 0.5	52.2
0.40	47.0 ± 0.5	47.3	37.7 ± 0.4	38.2	54.4 ± 0.3	54.2
0.50	50.4 ± 0.5	49.6	40.4 ± 0.4	40.0	57.7 ± 0.4	57.6
0.60	50.8 ± 0.7	51.4	41.4 ± 0.4	41.4	59.5 ± 0.5	60.4
0.70	52.5 ± 0.6	52.9	43.3 ± 0.5	44.6	62.6 ± 0.2	62.8

Footnotes *a*, *b*, *c*, *d*, *e*, *f*, and *g* are the same as in **Table 3.1.**

Table 3.3: Pseudo-first-order rate constants (k_{obs}) for the reaction of piperidine with anionic phenyl salicylate (PS^-) at 0.015 M CTABr in the presence of 0.006, 0.010 and 0.015 M $C_{16}E_{20}$ and different [MX] (= NaBr).[a]

[MX][b] (M)	[CTABr]$_T$[c] = 0.015 M		0.015 M		0.015 M	
	[$C_{16}E_{20}$]$_T$[d] = 0.006 M		0.010 M		0.015 M	
	$10^4\ {}^m k_{obs}$[e] s^{-1}	$10^4\ {}^m k_{calcd}$[f] s^{-1}	$10^4\ {}^m k_{obs}$[e] s^{-1}	$10^4\ {}^m k_{calcd}$[f] s^{-1}	$10^4\ {}^m k_{obs}$[e] s^{-1}	$10^4\ {}^m k_{calcd}$[f] s^{-1}
0.00	21.8 ± 0.3[g]		17.9 ± 0.4[g]		23.22 ± 0.4[g]	
0.01	22.4 ± 0.4	22.0	18.4 ± 0.5	18.0	24.18 ± 0.4	23.0
0.03	23.9 ± 0.4	23.9	20.1 ± 0.5	19.4	24.69 ± 0.4	24.8
0.06	26.1 ± 0.3	26.2	20.8 ± 0.6	21.4	27.32 ± 0.4	27.1
0.10	28.8 ± 0.4	28.7	23.8 ± 0.5	23.6	29.30 ± 0.3	29.7
0.12	30.3 ± 0.2	29.7	24.9 ± 0.5	24.6	29.94 ± 0.3	30.9
0.15	30.9 ± 0.3	31.1	26.3 ± 0.6	26.0	32.37 ± 0.3	32.5
0.18	31.8 ± 0.3	32.3	26.8 ± 0.7	27.3	33.82 ± 0.3	33.9
0.20	33.1 ± 0.6	33.0	28.2 ± 0.4	28.1	34.55 ± 0.2	34.7
0.25	34.2 ± 0.6	34.5	29.1 ± 0.5	29.9	37.04 ± 0.2	36.7
0.30	35.7 ± 0.8	35.8	30.5 ± 0.5	31.4	39.14 ± 0.3	38.3
0.35	37.3 ± 0.6	36.8	33.2 ± 0.4	32.8	39.92 ± 0.3	39.7
0.40	38.5 ± 0.6	37.7	34.1 ± 0.2	34.0	40.71 ± 0.4	40.9
0.50	38.9 ± 0.7	39.1	35.8 ± 0.3	36.1	42.56 ± 0.5	43.0
0.60	39.5 ± 0.8	40.2	37.9 ± 0.6	37.7	44.61 ± 0.3	44.6
0.70	40.7 ± 0.8	41.0	38.8 ± 0.5	39.1	44.54 ± 0.3	45.9

Footnotes *a*, *b*, *c*, *d*, *e*, *f* and *g* are the same as in **Table 3.1.**

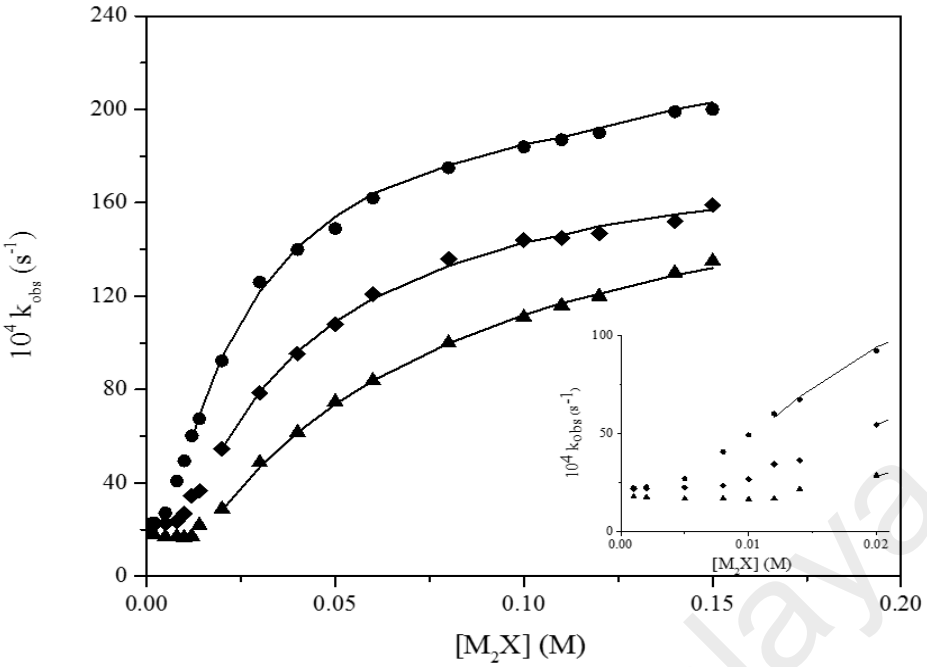

Figure 3.1: Plot of k_{obs} against [2-$NaOC_6H_4CO_2Na$] for the piperidinolysis of PS^- at 35 °C in the presence of $[CTABr]_T$/M = 0.006 (●), 0.010 (♦) and 0.015 (▲). The solid curves are sketched via the calculated values of the rate constant (k_{calcd}). Insert: The plots at magnified scale for the data points at lower values of [M_2X].

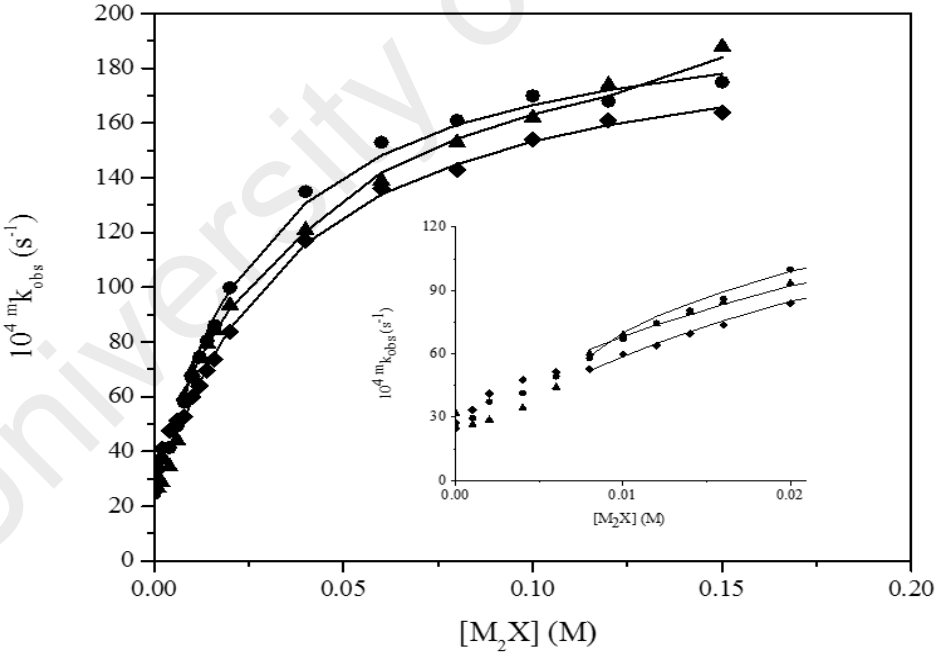

Figure 3.2: Plots of $^mk_{obs}$ (where superscript "m" represents mixed micelles) against [2-$NaOC_6H_4CO_2Na$] for the piperidinolysis of PS^- at $[CTABr]_T$ + $[C_{16}E_{20}]_T$/M = 0.006 + 0.006 (●), 0.006 + 0.010 (♦) and 0.006 + 0.015 (▲) and 35 °C. The solid curves represent the calculated values of rate constant (k_{calcd}). Insert: The enlarged plots for the concentrations of M_2X at lower values.

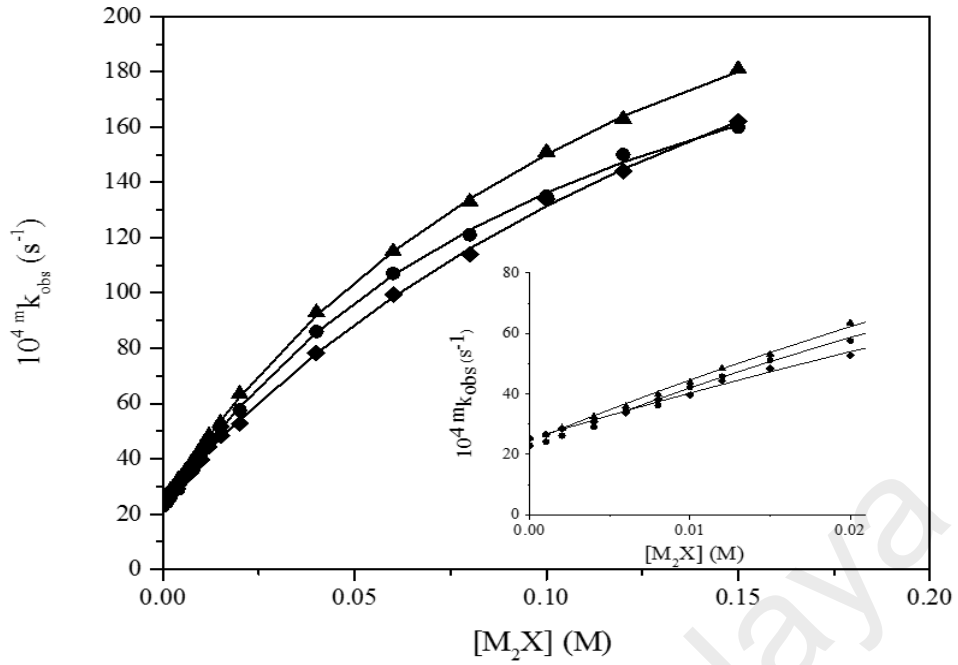

Figure 3.3: Plots of ${}^m k_{obs}$ (where superscript "m" represents mixed micelles) against [2-$NaOC_6H_4CO_2Na$] for the piperidinolysis of PS^- at $[CTABr]_T$ + $[C_{16}E_{20}]_T$/M = 0.010 + 0.006 (●), 0.010 + 0.010 (♦) and 0.010 + 0.015 (▲) and 35 °C. The solid curves are sketched via the calculated values of rate constant (k_{calcd}). Insert: The enlarged plots for the concentrations of M_2X at lower values.

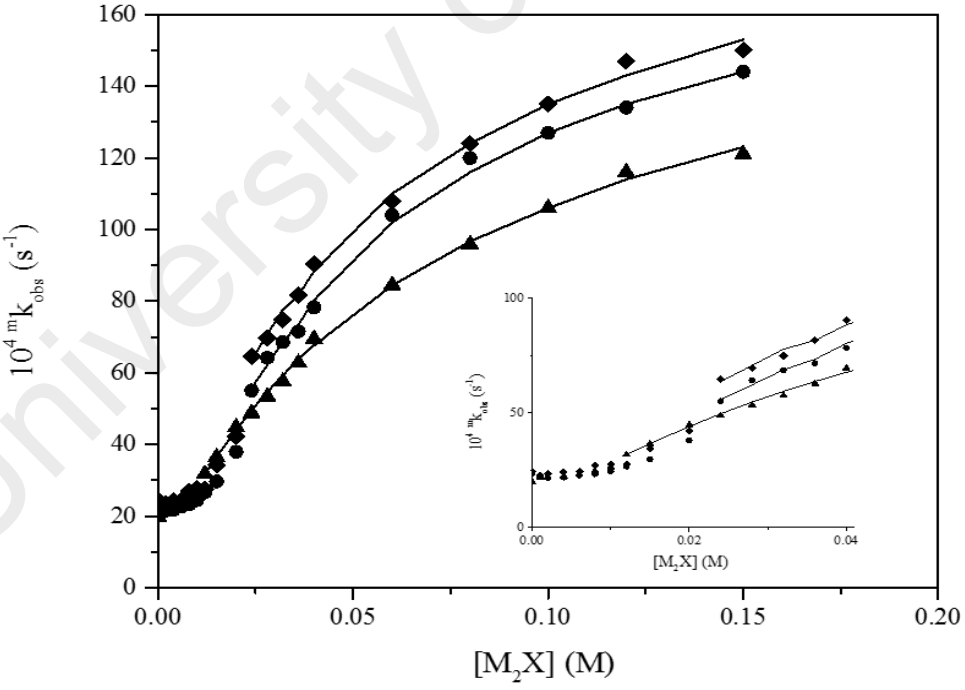

Figure 3.4: Plots of ${}^m k_{obs}$ (where superscript "m" represents mixed micelles) against [2-$NaOC_6H_4CO_2Na$] for the piperidinolysis of PS^- at $[CTABr]_T$ + $[C_{16}E_{20}]_T$/M = 0.015 + 0.006 (●), 0.015 + 0.010 (♦) and 0.015 + 0.015 (▲) and 35 °C. The solid curves are sketched via the calculated values of rate constant (k_{calcd}). Insert: The enlarged plots for the concentrations of M_2X at lower values.

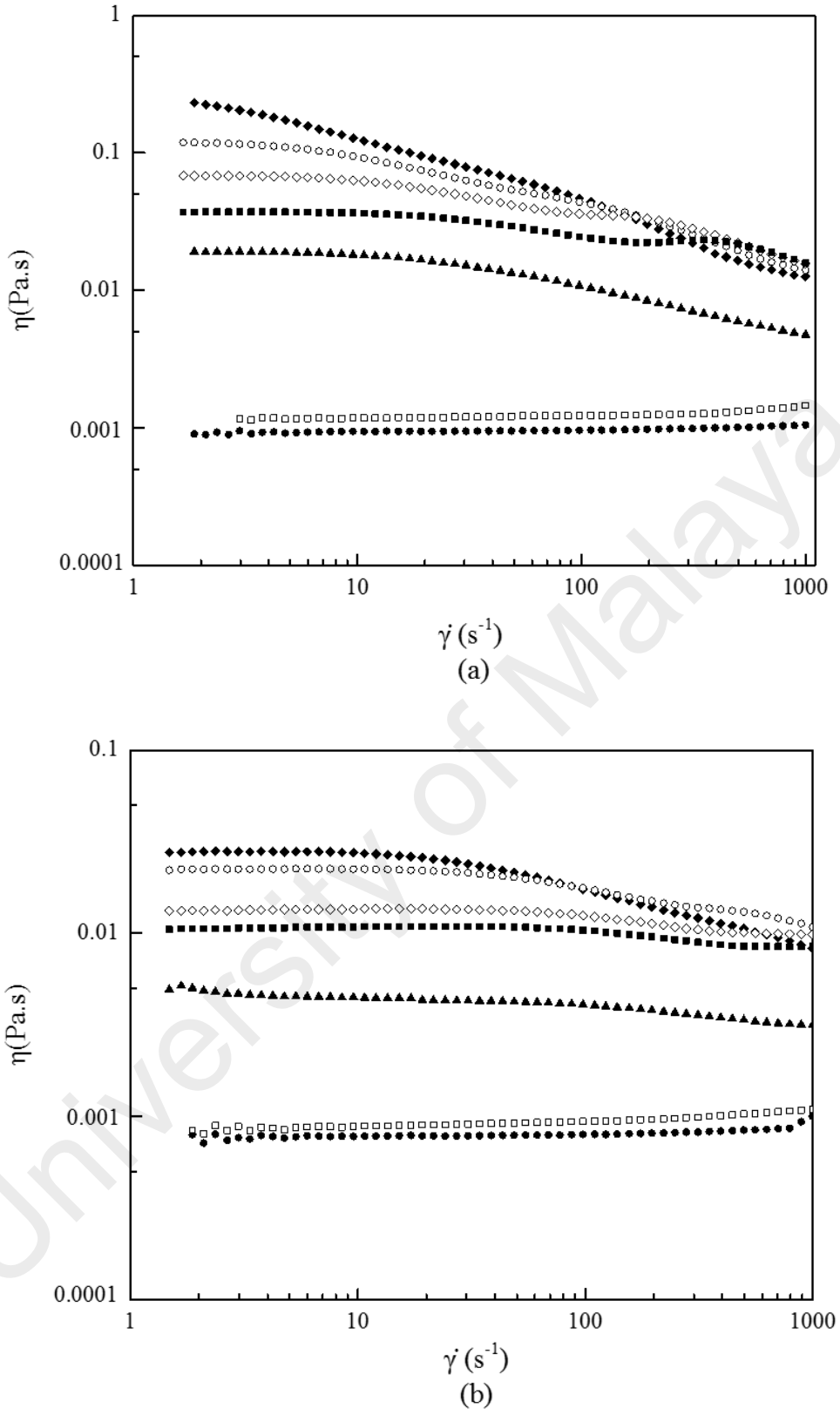

Figure 3.5: Graphs of shear viscosity (η) against shear rates (γ̇) for the piperidinolysis of PS^- containing 0.015 M CTABr and [2-$NaOC_6H_4CO_2Na$]/M = (a) 0.006 (•) 0.008 (□) 0.012 (▲) 0.020 (♦) 0.040 (○) 0.08 (◊) and 0.120 (■) at 25 °C and (b) 0.006 (•) 0.008 (□) 0.0120 (▲) 0.020 (♦) 0.040(○) 0.080 (◊) and 0.120 (■)at 35 °C.

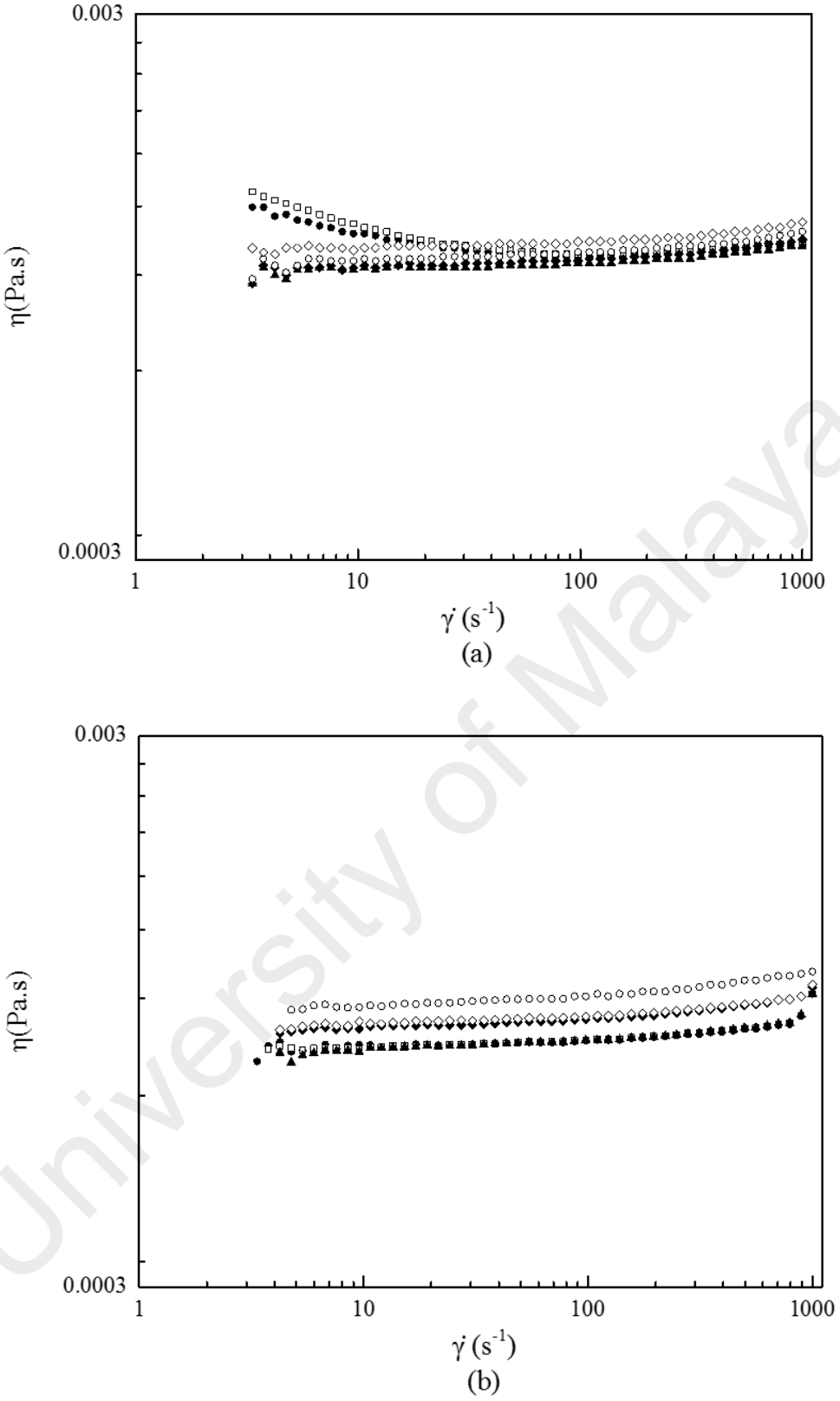

Figure 3.6: Plots of shear viscosity (η) against shear rate (γ̇) for the piperidinolysis of PS^- containing 0.015 M CTABr, 0.006 M $C_{16}E_{20}$ and [2-$NaOC_6H_4CO_2Na$]/M = (a) 0.006 (•) 0.008 (□) 0.0120 (▲) 0.020 (♦) 0.040 (○) and 0.120 (◊) at 25 °C and (b) 0.006 (•) 0.008 (□) 0.0120 (▲) 0.020 (♦) 0.040 (○) and 0.120 (◊) at 35 °C.

3.4 Discussion

3.4.1 Explanation of kinetic observations for the piperidinolysis of PS^- in the presence of pure $C_{16}E_{20}$ micelles at various [MX] or [M_2X] and 35 °C

The data obtained revealed that the values of k_{obs} at various values of [MX] (MX = NaBr) or [M_2X] (M_2X = 2-$NaOC_6H_4CO_2Na$) = 0 (or average of higher values of k_{obs} (k^0_{obs})) and those of k_{obs} at maximum value [MX] or [M_2X] ($k^{MX\ (max)}_{obs}$ or $k^{M_2X\ (max)}_{obs}$), decrease with the increase in $[C_{16}E_{20}]_T$ ($[C_{16}E_{20}]_T$ = 0.001, 0.003, 0.006, 0.008, 0.010 or 0.015 M). These are similar to the reported results in the past (Khan & Ismail, 2004). The presence of $C_{16}E_{20}$ shows a negative salt effect (NSE) and the values of k^0_{obs} and $k^{MX\ (max)}_{obs}$ were used to calculate the percent negative salt effect (%NSE); values presented in **Table 3.4**, using **Eq. 3.12**. These values were found to decrease with the increase in $[C_{16}E_{20}]_T$.

$$\%NSE = (k^0_{obs} - k^{MX\ (max)}_{obs})/k^0_{obs} \times 100$$

or

$$\%NSE = (k^0_{obs} - k^{M_2X\ (max)}_{obs})/k^0_{obs} \times 100 \quad \textbf{(3.12)}$$

where k^0_{obs} = k_{obs} at [MX] or [M_2X] = 0 (or average values of higher values of k_{obs}) and $k^{MX\ (max)}_{obs}$ or $k^{M_2X\ (max)}_{obs}$ = k_{obs} at the maximum value of [MX] or [M_2X].

3.4.2 Explanation of kinetic observations for the piperidinolysis of PS^- in the presence of pure CTABr and mixed CTABr-$C_{16}E_{20}$ micelles at various [MX] or [M_2X] and 35 °C

The values of k_{obs} obtained in the presence of a constant concentration of pure CTABr at various [MX] or [M_2X] (where M_2X = 2-$NaOC_6H_4CO_2Na$) were related to **Eq. 3.13** (Khan *et al.*, 2010).

$$k_{obs} = \frac{k_0+\theta K^{X/S}([MX] - [MX]_0^{op})}{1+ K^{X/S}([MX] - [MX]_0^{op})}$$

or

$$k_{obs} = \frac{k_0+\theta K^{X/S}([M_2X] - [M_2X]_0^{op})}{1+ K^{X/S}([[M_2X] - [M_2X]_0^{op})} \quad \textbf{(3.13)}$$

where k_0 stands for k_{obs} in the absence of MX or M_2X with, respectively, $[MX]_0^{op}$ or $[M_2X]_0^{op}$ (represent the optimum values of [MX] (= NaBr) or [M_2X] at which further increase in [MX] or [M_2X] is believed to have no effect on ion exchange X^-/HO^- and X^-/Br^- occurring in the CTABr micellar phase) (Khan, 2010). The values of $[MX]_0^{op}$ or $[M_2X]_0^{op}$, at various $[CTABr]_T$, were determined by an iterative technique as described in detail in the previously published reports (Khan & Ismail, 2003; Khan & Ismail, 2009). Parameters θ and $K^{X/S}$ represent the empirical constants and their values were calculated from **Eq. 3.13** using nonlinear least-squares relationship, considering k_0 to have known value. Different k_0 (= k_{obs} at [MX] = $[MX]_0^{op}$ = 0 or [M_2X] = $[M_2X]_0^{op}$ = 0) were determined by conducting kinetic experiments at typical $[CTABr]_T$ as well as $[CTABr]_T$ + $[C_{16}E_{20}]_T$ and their values are shown in **Tables 3.1, 3.2** and **3.3.**

Table 3.4: Values of kinetic parameters for the reaction of Pip and PS^- in the presence of inert salts MX or M_2X at different $[C_{16}E_{20}]_T$ and 35 °C.[a]

	MX = NaBr			M_2X = 2-$NaOC_6H_4CO_2Na$		
$[C_{16}E_{20}]_T$[b] M	k_{obs}^0[c] s^{-1}	$k_{obs}^{MX\ (max)}$[d] s^{-1}	%NSE[e]	k_{obs}^0[c] s^{-1}	$k_{obs}^{M_2X\ (max)}$[d] s^{-1}	%NSE[e]
0.001	279	193	31	276	177	36
0.003	254	188	26	254	204	20
0.006	227	181	22	229	204	11
0.008	210	176	16	173	166	4.0
0.010	191	173	09	276	177	36
0.015	177	165	07	239	202	14

[a] $[PSH]_0$ = 0.20 mM, [NaOH] = 0.03 M, [Pip] = 0.10 M, λ = 370 nm and aqueous reaction mixture for each kinetic run contains 2% v/v acetonitrile. [b]Total cncentration of $C_{16}E_{20}$. [c] k_{obs}^0 = k_{obs} at [MX] or [M_2X] = 0 (or average value of similar values of k_{obs} at various [MX] or [M_2X]). [d] $k_{obs}^{MX\ (max)}$ or $k_{obs}^{M_2X\ (max)}$ = k_{obs} at maximum value of [MX] or [M_2X]. [e]Percent negative salt effect, %NSE caculated from **Eq. 3.12.**

The values of k_{obs} obtained in the presence of mixed CTABr-$C_{16}E_{20}$ micelles within the concentration range of 0.006-0.015 M $C_{16}E_{20}$ surfactants were also found to fit to **Eq. 3.13**. The values of fraction of micellized S ion transferred from the CTABr micellar phase to aqueous phase, through the occurrence of ion exchange S^-/PS^-, is denoted as $F_{X/S}$. The relationship between θ and $F_{X/S}$ is expressed in **Eq. 3.14**.

$$\theta = F_{X/S}k_{obs}^{W} \qquad \textbf{(3.14)}$$

where k_{obs}^{W} $(= k_W^2[Pip]_T)$ denotes k_{obs} at different $[C_{16}E_{20}]_T$ (= 0.006, 0.010 and 0.015 M) and [MX] or $[M_2X]$ = [CTABr] = 0 with k_W^2 representing the nucleophilic second order rate constant in nonionic $C_{16}E_{20}$ micellar phase. The values of $K^{X/S}$, presented in **Tables 3.5, 3.6** and **3.7,** at various concentrations of pure CTABr micelles as well as mixed CTABr-$C_{16}E_{20}$ micelles, were determined by the use of **Eq. 3.13** (Khan & Arifin, 1996). The values of $K_{X/S}$, obtained for pure CTABr micelles (**Table 3.6**), were calculated from **Eq. 3.15** with the value of K_S^0 as 7000 M^{-1} obtained from the literature (Khan & Arifin, 1996).

$$K_{X/S} = K^{X/S}\left(1+K_S^0[CTABr]_T\right) \qquad \textbf{(3.15)}$$

The results obtained at various constant concentrations of pure CTABr and mixed CTABr-$C_{16}E_{20}$, in the presence of different [MX] and $[M_2X]$ (MX= NaBr and M_2X = $NaOC_6H_4CO_2Na$), are presented in **Tables 3.5, 3.6** and **3.7.** Symbolic modification of parameters was done to differentiate between those obtained in the presence of pure micelles and mixed micelles. Therefore, k_{obs}, k_0, k_{obs}^{W}, k_W^2 θ, $K_{X/S}$, $K^{X/S}$, K_S^0, $F_{X/S}$ and $K_{X/S}^n$ are considered as ${}^mk_{obs}$, ${}^mk_0$, ${}^mk_{obs}^{W}$, ${}^mk_W^2$, ${}^m\theta$, ${}^mK_{X/S}$, ${}^mK^{X/S}$, ${}^mK_S$, ${}^mF_{X/S}$ and ${}^mK_{X/S}^n$. The small letter "m" (superscript) was used to imply that the parameters obtained in the of mixed micellar solutions throughout the text.

The values of k_{obs}, in the presence of 0.006, 0.010 and 0.015 M pure CTABr, at various [2-$HOC_6H_4CO_2Na$] (**Figure 3.1**) has been observed to decrease with the increase in total concentration of CTABr. The understandings of the complex headgroups for $C_{16}E_{20}$ micelles with regards to the change in its structure have not yet been reported. The hydrophilic parts of CTABr in CTABr-$C_{16}E_{20}$ surfactants mixture are covered within the larger sized hydrophilic $C_{16}E_{20}$ micellar parts of the same mixed surfactants (Gao *et al.*, 2002). Thus, it appears acceptable that the combination of ionic surfactants (C_nIM) and nonionic ones (C_nE_m) with $n \leq m$ is related to incomplete dehydration of hydrophilic part of C_nIM (comprising the outermost portion of headgroups) which causes the ion exchange, leading to changes in structure of micelles from spherical to wormlike (Geng *et al.*, 2006).

It is clearly demonstrated from **Eq. 3.15** that as the concentration of pure CTABr increases, the values of $K^{X/S}$ decrease provided the values of $K_{X/S}$ are independent of $[CTABr]_T$. This prediction coincides well with what is presented in **Table 3.6** (the values of $K^{X/S}$ = 39, 26 and 13 for 0.006, 0.010 and 0.015 M CTABr, respectively).

The optimum values of [2-$NaOC_6H_4CO_2Na$], ($[M_2X]_0^{op}$), for the mixed CTABr-$C_{16}E_{20}$ micelles (**Table 3.7**) decreased compared to that of the pure CTABr (**Table 3.6**). But the values of parameters k_0, θ and $K^{X/S}$ remain independent of whether the micellar system is pure or mixed, and it was observed that the lowest value of the concentration of CTABr is more than 20-fold larger than the corresponding value of $[M_2X]_0^{op}$ (**Table 3.7**) in the presence of 0.006 M $C_{16}E_{20}$.

The magnitude of normalised values of $K_{X/S}$ ($K^n_{X/S} = F_{X/S}K_{X/S}$) is related to values of cationic micellar binding constants, K_X (for counterion X), and K_S, (for counterion S with $S^- = PS^-$) with the relationship; $K^n_{X/S} = \Omega_S K_X/K_S$ where Ω_S is denoting a proportionality constant (Khan, 2010). Similarly, for another ion exchange (with the reference counterion

Br^-) Br/S, the magnitude of normalised values of $K_{Br/S}$ ($K^n_{Br/S} = F_{Br/S}/K_{Br/S}$) has the relationship; $K^n_{Br/S} = \Omega_S K_{Br}/K_S$ (Khan, 2010). The values of $K^n_{X/S}$, summarised in **Table 3.6**, and the reported value of $K^n_{Br/S}$ (= 25 M^{-1}) (Khan, 1997a; Khan *et al.*, 2000; Khan & Ismail, 2007) were used to calculate the values of conventional ion exchange constant/relative counterion binding constants, K^{Br}_X, using **Eq. 3.16.** The values of K^{Br}_X (presented in **Table 3.6**) are 48.8, 45.0 and 33.1 at, respectively, $[CTABr]_T$ = 0.006, 0.010 and 0.015 M. These results are relatively more reliable as the mean value of K^{Br}_X (= 42) is similar to the one presented in the previous study (K^{Br}_X = 44) (Khan *et al.*, 2010).

$$K^{Br}_X = K_X/K_{Br} = K^n_{X/S}/K^n_{Br/S} \qquad \textbf{(3.16)}$$

Eq. 3.16 holds only if the values of $K^n_{X/S}$ and $K^n_{Br/S}$ are determined in the presence of micelles with the same structural behavior/feature (such as spherical or wormlike micelles or vesicles). However, if the values of $K^n_{X/S}$ and $K^n_{Br/S}$ have been determined in the presence of respective nonspherical and spherical micelles, then K^{Br}_X should represent R^{Br}_X (= K^{nsp}_X/K^{sp}_{Br} with K^{nsp}_X and K^{sp}_{Br} representing non-spherical and spherical micellar binding constants of X^- and Br^-, respectively) with the relationship represented by **Eq. 3.17**

$$R^{Br}_X = ({}^nK_{X/S})^{nsp}/ ({}^nK_{Br/S})^{sp} \qquad \textbf{(3.17)}$$

The conditions to use either of the relationships (**Eqs. 3.16** and **3.17**) have been reported in detail in the previous report (Khan *et al.*, 2010). It is perhaps noteworthy that **Eqs. 3.16** and **3.17** are applicable for both M_2X (= 2-$NaOC_6H_4CO_2Na$) and MX (= NaBr).

The observed data ($^mk_{obs}$ versus [MX] with superscript "m" representing mixed micelles) obtained in mixed micelles, CTABr-$C_{16}E_{20}$, were found to follow **Eq. 3.13** which is also applicable for observed data obtained in the presence of pure CTABr micelles. It is therefore assumed that **Eqs. 3.16** and **3.17** should be applicable for data in

the mixed micelles, CTABr-$C_{16}E_{20}$, with symbols K_X^{Br}, K_X, K_{Br}, $K_{X/S}^n$, $K_{Br/S}^n$, R_X^{Br}, $({}^nK_{X/S})^{nsp}$ and $({}^nK_{Br/S})^{sp}$ replaced by respective ${}^mK_X^{Br}$, ${}^mK_X$, ${}^mK_{Br}$, ${}^mK_{X/S}^n$, ${}^mK_{Br/S}^n$, ${}^mR_X^{Br}$, $({}^{m\,n}K_{X/S})^{nsp}$ and $({}^{m\,n}K_{Br/S})^{sp}$. The values of ${}^mK_{X/S}$ and ${}^mK_{Br/S}$ could not be calculated because the values of K_S^0 for mixed CTABr-$C_{16}E_{20}$ surfactants are not available for the present study. Consequently, the values of ${}^mK_{X/S}^n$, ${}^mK_{Br/S}^n$, $({}^{m\,n}K_{X/S})^{nsp}$ and $({}^{m\,n}K_{Br/S})^{sp}$ could not be calculated. In this case, **Eq. 3.16** or **3.17** could not be applied in determining the respective values of ${}^mK_X^{Br}$ or ${}^mR_X^{Br}$.

However, it can be easily shown, in view of **Eq. 3.15,** that

$$ {}^mK_{X/S}^n = {}^{m\,n}K^{X/S}\,(1+ {}^mK_S^0\,[CTABr]_T) \qquad \textbf{(3.18)} $$

and

$$ {}^mK_{Br/S}^n = {}^{m\,n}K^{Br/S}\,(1+ {}^mK_S^0\,[CTABr]_T) \qquad \textbf{(3.19)} $$

The relationships in **Eqs. 3.18** and **3.19** give **Eq. 3.20.**

$$ {}^mK_X^{Br} = {}^{m\,n}K^{X/S} / {}^{m\,n}K^{Br/S} \qquad \textbf{(3.20)} $$

with ${}^{m\,n}K^{X/S} = {}^mF_{X/S}\,{}^mK^{X/S}$ and ${}^{m\,n}K^{Br/S} = {}^mF_{Br/S}\,{}^mK^{Br/S}$.

Table 3.5: Values of empirical constants, $^{m}\theta$, $^{m}F_{X/S}$ and $^{m}K^{X/S}$ calculated from **Eqs. 3.13** and **3.14** for MX = NaBr at different concentrations of mixed CTABr-$C_{16}E_{20}$.[a]

$[CTABr]_T$	$[C_{16}E_{20}]_T$	$10^4\ ^{m}k_0$[d]	$10^3\ ^{m}\theta$	$^{m}K^{X/S}$	$^{m}F_{X/S}$	$^{m\ n}K^{X/S}$
M	M	s^{-1}	s^{-1}	M^{-1}		M^{-1}
0.006[b]	0.006[c]	25.3 ± 0.4[e]	10.1 ± 0.3[e]	3.4 ± 0.3[e]	0.4[f]	1.4[g]
0.006	0.010	31.3 ± 0.5	10.3 ± 0.9	4.4 ± 0.8	0.5	2.2
0.006	0.015	30.1 ± 0.3	11.4 ± 0.6	3.0 ± 0.4	0.6	1.8
0.010	0.006	23.0 ± 0.4	6.6 ± 0.1	3.2 ± 0.1	0.3	1.0
0.010	0.010	17.5 ± 0.4	5.2 ± 0.6	3.7 ± 0.1	0.3	1.1
0.010	0.015	28.7 ± 0.3	8.5 ± 0.1	1.8 ± 0.7	0.5	0.9
0.015	0.006	21.8 ± 0.3	4.8 ± 0.1	3.8 ± 0.2	0.2	0.8
0.015	0.010	17.9 ± 0.4	5.4 ± 0.1	2.1 ± 0.1	0.3	0.6
0.015	0.015	23.2 ± 0.4	5.9 ± 0.2	2.6 ± 0.2	0.3	0.8

[a] $[PSH]_0$ = 0.2 mM, [Pip] = 0.1 M, [NaOH] = 0.03 M, λ = 370 nm and aqueous reaction mixture for each kinetic run contains 2% v/v acetonitrile. [b] Total concentration of CTABr. [c] Total concentration of $C_{16}E_{20}$. [d] $^{m}k_0 = {}^{m}k_{obs}$ at $[MX] = [MX]_0^{op}$. [e] Error limits are standard deviations. [f] $^{m}F_{X/S} = {}^{m}\theta/{}^{m}k_{obs}^{W}$; with $^{m}k_{obs}^{W} = {}^{m}k_{obs}$ ($= {}^{m}k_W^2[Pip]_T$) = 240 x 10^{-4}, 193.2 x 10^{-4} and 184.2 x 10^{-4} s^{-1} at constant $[C_{16}E_{20}]_T$ (0.006, 0.010 and 0.015 M $[C_{16}E_{20}]$ respectively) and [MX] = [CTABr] = 0. [g] $^{m\ n}K^{X/S} = {}^{m}F_{X/S}\ {}^{m}K^{X/S}$.

Table 3.6: Values of empirical constants, θ, $F_{X/S}$ and $K^{X/S}$ obtained using **Eqs. 3.13** and **3.14** with the $[M_2X]_0^{op}$ values for M_2X = 2-$NaOC_6H_4CO_2Na$ at different $[CTABr]_T$.[a]

$[CTABr]_T$ M	$10^4\ k_0$[c] s^{-1}	$[M_2X]_0^{op}$ M	$10^3\ \theta\ s^{-1}$	$K^{X/S}\ M^{-1}$	$K_{X/S}\ M^{-1}$	$F_{X/S}$	$K^n_{X/S}\ M^{-1}$	K_X^{Br} or R_X^{Br}
0.006[b]	23.0 ± 0.2[d]	0.007	23.1 ± 0.1[d]	39.4 ± 5.6[d]	1694.2[e]	0.72[f]	1219.8[g]	48.8[h]
0.010	21.2 ± 0.4	0.011	19.4 ± 0.6	26.4 ± 2.4	1874.4	0.60	1124.6	45.0
0.015	16.4 ± 0.4	0.016	19.6 ± 0.4	13.0 ± 0.6	1378.0	0.60	0826.8	33.1

[a]$[PSH]_0$ = 0.2 mM, [NaOH] > 0.03 M, [Pip] = 0.1 M, λ = 370 nm and aqueous reaction mixture for each kinetic run contains 2% v/v acetonitrile. Footnote *b* is the same as in **Table 3.5**. [c]$k_0 = {}^m k_{obs}$ at $[MX] = [MX]_0^{op}$. [d]Error limits are standard deviations. [e]$K_{X/S} = K^{X/S}(1 + K_S^0 [CTABr]_T)$, where $K_S^0 = 7 \times 10^3\ M^{-1}$. [f]$F_{X/S} = \theta/(k_W^2 [Pip]_T)$, where $k_W^2 = k_{obs}$ at $[CTABr]_T = [C_{16}E_{20}]_T = 0$ and $[Pip]_T$ = 0.1 M and the values of k_W^2, under such conditions is 0.322 s^{-1}. [g]$K^n_{X/S} = F_{X/S}\ K_{X/S}$. [h]$K_X^{Br}$ or $R_X^{Br} = K^n_{X/S} / K^n_{Br/S}$, where $K^n_{Br/S} = 25\ M^{-1}$.

Table 3.7: Values of empirical constants, $^{m}\theta$, $^{m}F_{X/S}$ and $^{m}K^{X/S}$ calculated from **Eqs. 3.13** and **3.14** with the $[M_2X]_0^{op}$ values for M_2X = $2NaOC_6H_4CO_2Na$ at different concentrations of mixed CTABr-$C_{16}E_{20}$[a]

$[CTABr]_T$ M	$[C_{16}E_{20}]$ M	$10^4\ ^{m}k_0$[d] s^{-1}	$[M_2X]_0^{op}$ M	$10^3\ ^{m}\theta$ s^{-1}	$^{m}K^{X/S}$ M^{-1}	$^{m}F_{X/S}$	$^{m\ n}K^{X/S}$ M^{-1}	$^{m\ n}K^{Br/S}$ M^{-1}	$^{m}K_X^{Br}$ or $^{m}R_X^{Br}$
0.006[b]	0.006[c]	24.7 ± 0.5[e]	0.00028	20.8 ± 0.4[e]	34.8 ± 2.2[e]	0.87[f]	30.3[g]	1.4[h]	21.6[i]
0.006	0.010	27.2 ± 0.5	0.00201	19.9 ± 0.2	28.1 ± 0.9	1.03	28.9	2.2	13.1
0.006	0.015	14.1 ± 0.1	0.00000	21.7 ± 0.5	24.6 ± 1.5	1.18	29.9	1.8	16.6
0.010	0.006	22.9 ± 0.8	0.00000	26.5 ± 0.5	8.82 ± 0.4	1.10	09.7	1.0	09.7
0.010	0.010	25.3 ± 0.4	0.00006	35.0 ± 1.1	4.87 ± 0.2	1.82	08.9	1.1	08.1
0.010	0.015	25.3 ± 0.5	0.00047	32.3 ± 0.5	7.26 ± 0.2	1.75	12.7	0.9	14.1
0.015	0.006	23.6 ± 0.2	0.01085	19.6 ± 0.4	16.8 ± 0.8	0.82	13.8	0.8	17.3
0.015	0.010	24.5 ± 0.3	0.00768	20.6 ± 0.4	16.8 ± 0.9	0.86	14.5	0.6	24.2
0.015	0.015	19.9 ± 0.4	0.00560	18.0 ± 0.4	12.4 ± 0.6	0.98	12.2	0.8	15.3

Footnote *a* is the same as in **Table 3.6**. Footnotes *b*, *c*, *d*, *e* and *f* are the same in **Table 3.5**. [g] $^{m\ n}K^{X/S} = {}^{m}F_{X/S}\ {}^{m}K^{X/S}$. [h] $^{m\ n}K^{Br/S} = {}^{m}F_{Br/S}\ {}^{m}K^{Br/S}$ (for the reference salt, MX = NaBr). [i] $^{m}K_X^{Br}$ or $^{m}R_X^{Br} = {}^{m\ n}K^{X/S}/\ {}^{m\ n}K^{Br/S}$.

The coditions to use **Eq. 3.20** are also the same as in the case of **Eq. 3.16.** Furthermore, if the conditions fail, **Eq. 3.21** should be used instead.

$$ {}^{m}R_{X}^{Br} = ({}^{m\ n}K^{X/S})^{nsp} / ({}^{m\ n}K^{Br/S})^{sp} \quad \textbf{(3.21)} $$

with $({}^{m\ n}K^{X/S})^{nsp} = ({}^{m}F_{X/S})^{nsp}({}^{m}K^{X/S})^{nsp} / ({}^{m\ n}K^{Br/S})^{sp} = ({}^{m}F_{Br/S})^{sp}({}^{m}K^{Br/S})^{sp}$.

In general, **Eqs. 3.16** and **3.20** are applicable if the values of $K^{n}_{X/S}$ and $K^{n}_{Br/S}$ (for pure micelles) and ${}^{m\ n}K^{X/S}$ and ${}^{m\ n}K^{Br/S}$ (for mixed micelles) are determined in the presence of micelles with the same structural behavior/feature respectively. But **Eqs. 3.17** and **3.21** are applicable if the values of $K^{n}_{X/S}$ and $K^{n}_{Br/S}$ (for pure micelles) and ${}^{m\ n}K^{X/S}$ / ${}^{m\ n}K^{Br/S}$ (for mixed micelles) have been determined in the presence of respective nonspherical and spherical micelles.

The presence of mixed CTABr-$C_{16}E_{20}$ micelles revealed the increase in the values of ${}^{m}F_{X/S}$ for M_2X = 2-$NaOC_6H_4CO_2Na$ (**Table 3.6**).

3.4.3 Explanation of rheological measurements for the piperidinolysis of PS^- in the presence of pure CTABr and mixed CTABr-$C_{16}E_{20}$ micelles at various [M_2X]

In the presence pure CTABr micelles, all flow curves in **Figures 3.5 (a)** and **(b)** at ≥ 0.012 M 2-$NaOC_6H_4CO_2Na$ and at both, 25 and 35 °C show the Newtonian fluid behavior at their beginning with the exception of 0.006 and 0.008 M 2-$NaOC_6H_4CO_2Na$ while showing the shear thinning behavior at the end. This behavior of CTABr surfactant, with a constant concentration in the presence of different [2-$NaOC_6H_4CO_2Na$], indicates the possible presence of elongated micelles (Lu *et al.*, 2008; Qiao *et al.*, 2011). As the [2-$NaOC_6H_4CO_2Na$] increases from 0.006 to 0.012 M, the values of critical shear rate (γ_{cr}) decrease and also shift to lower values with increase in zero shear viscosity (η_o). This critical shear rate is the specific shear rate at which the values of shear viscosity (η) begin

to decrease (shear thinning). However, further increase in [2-$NaOC_6H_4CO_2Na$] (0.02-0.12 M) increases the values of γ_{cr} with a decrease in η_o. It implies, therefore, the CTABr micellar structure is getting networked to a great extent, and to a lesser degree at > 0.008 to 0.012 M and 0.02 to 0.12 M range of 2-$NaOC_6H_4CO_2Na$ respectively. This is a typical rheological behavior of wormlike micelles (Yusof & Khan, 2013; Yusof *et al.,* 2013). Almost all of the flow curves in **Figures 3.6 (a)** and **(b)** (0.006-0.12 M 2-$NaOC_6H_4CO_2Na$) at 25 and 35 °C, in the presence of mixed CTABr-$C_{16}E_{20}$ (with fixed concentration of both CTABr-$C_{16}E_{20}$), show Newtonian fluid systems.

The graphs of η_o at constant shear rate ($\dot{\gamma}$) against [2-$HOC_6H_4CO_2Na$] at both 25 and 35 °C are shown in **Figure 3.7.** Typical single asymmetrical maxima at [CTABr] = 0.015 M, [$C_{16}E_{20}$] = 0, and 25 and 35 °C (represented by respectively □ and ◊ in **Figure 3.7**) were obtained at the same value of [2-$HOC_6H_4CO_2Na$]$_{sp}$ (= 0.02 M). The values of specific concentration of 2-$HOC_6H_4CO_2Na$, [2-$HOC_6H_4CO_2Na$]$_{sp}$, at which the viscosity maximum occurs at a constant $\dot{\gamma}$, [CTABr], and both 25 and 35 °C remained unchanged. This observation agreed with previously reported studies (Abdel-Rahem, 2008; Davies *et al.,* 2006) where the maxima obtained at fixed concentration of cationic surfactant in solution and various [MX] (where MX stands for counterionic salt) reveals the possibility of the existence of wormlike micelles. Despite the fact that the presence of, at least, single maximum in such a plot is no longer unusual (Abdel-Rahem, 2008; Ali & Makhloufi, 1999; Davies *et al.*, 2006; Dreiss, 2007; Lin *et al.*, 2009; Oelschlaeger *et al.*, 2008; Rehage & Hoffmann, 1991; Schubert *et al.*, 2004), the molecular mechanism for the cause of such a maximum is still not fully understood even at a fundamental molecular level (Davies *et al.*, 2006; Ziserman *et al.,* 2009). However, it has turned out to be practically certain from several studies (Abdel-Rahem, 2008; Ali & Makhloufi, 1999; Davies *et al.*, 2006; Dreiss, 2007; Lin *et al.*, 2009; Oelschlaeger *et al.*, 2008; Rehage & Hoffmann, 1991; Schubert *et al.*, 2004) that the occurrence of a viscosity maximum for a surfactant solution containing

a constant concentration of ionic micelle-forming surfactant and various concentration of counterionic salt is characteristic of the presence of WM/entangled WM in the surfactant solutions. In mixed CTABr-$C_{16}E_{20}$ micellar solution at 0.015 M CTABr, 0.006M $C_{16}E_{20}$ and 25 and 35 °C (represented by respectively Δ and ○ in **Figure 3.7**) however, no maxima were obtained. Hence, no significant changes in the respective values of shear viscosity at different values of $[2\text{-}HOC_6H_4CO_2Na]_{sp}$ were noticed.

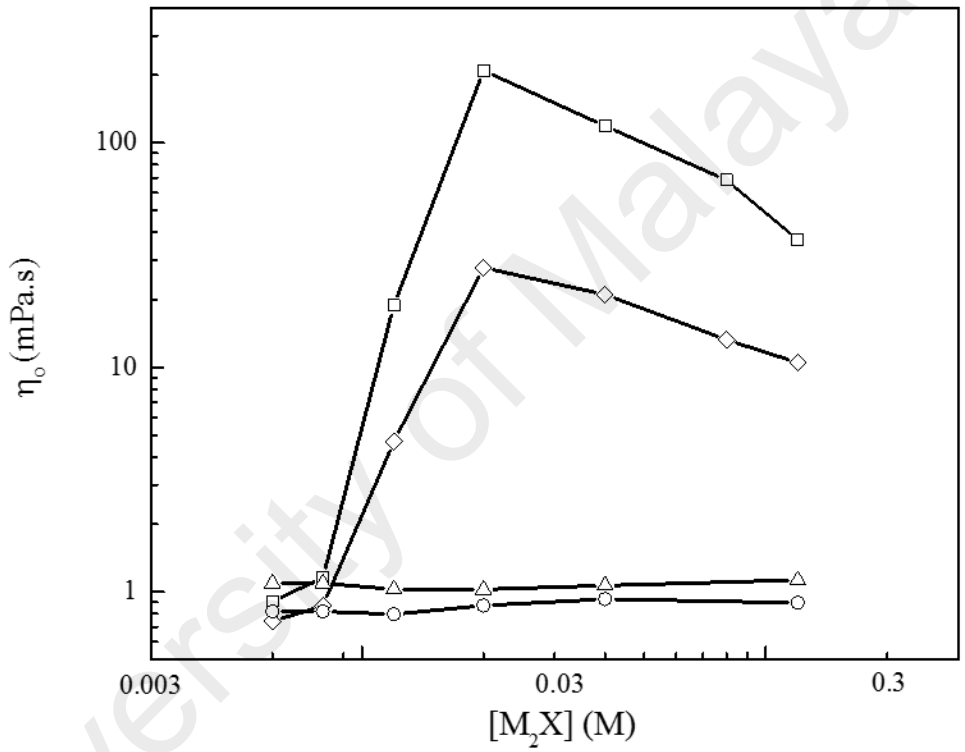

Figure 3.7: Graphs of zero shear viscosity (η_o) at a constant shear rate ($\dot{\gamma}$) against [2-$HOC_6H_4CO_2Na$] with 0.015 M CTABr in absence of $C_{16}E_{20}$ at 25°C (□) and 35 °C (◊), and presence of 0.006 M $C_{16}E_{20}$ at 25 °C (Δ) and 35 °C (○).

3.5 Conclusion

It is known from the literature that the CTABr micellar binding constant of salicylate ion is nearly 100-fold larger in the presence of CTABr micelles compared to that in the presence of $C_{16}E_{20}$ (Khan & Ismail, 2004). It is now common belief that the viscoelastic behavior of aqueous CTABr micellar solution containing sodium salicylate is caused by the strong CTABr micellar binding of sodium salicylate. However, the perception has never been supported by the quantitative determination of such binding constant. The new

and interesting finding described in this chapter is that CTABr/M_2X/H_2O micellar solution (with K_X^{Br} or R_X^{Br} ≈ 42) contains wormlike micelles whereas CTABr/M_2X/$C_{16}E_{20}$/H_2O micellar solution (with ${}^{m}K_X^{Br}$ or ${}^{m}R_X^{Br}$ ≈ 16) contains spherical micelles, with M_2X = disodium salicylate. This presents a quantitative correlation between the magnitude of counterion (X) binding constant with CTABr (K_X^{Br} or R_X^{Br}) and X-induced CTABr micellar growth. It is also important to note that the structural feature, as well as viscosity of CTABr/M_2X/$C_{16}E_{20}$/H_2O micellar solutions, can be manipulated by just changing the concentration of $C_{16}E_{20}$.

CHAPTER 4: STUDY OF CATIONIC AND NONIONIC MIXED MICELLES WITH NaBr AND 3,5-$Cl_2C_6H_3CO_2Na$ BY THE USE OF PROBE NUCLEOPHILIC REACTION OF PIPERIDINE WITH IONIZED PHENYL SALICYLATE[2]

4.1 Introduction

There is no dispute on the recent rises and needs for new and consistent scientific information in the field of research on micelles (Stang, 2012). Surface active substances (SAS), popularly called surfactants, form micelles of different characteristics and they have been discovered for the past 10 decades (Menger, 1979). It has also been unanimously believed that changes in cationic micellar behaviors, from one structural feature to another, are related to the counterion (X) affinity to their surfaces (Gravsholt, 1976; Oelschlaeger *et al.*, 2010; Penfold *et al.*, 2004; Rao *et al.*, 1987; Singh *et al.*, 2009; Vermathen *et al.*, 2002) and different investigations on qualitative NMR studies on the cationic micellar affinity of X ions have been reported (Rao *et al.*, 1987; Singh *et al.*, 2009; Vermathen *et al.*, 2002). Some di-substituted benzoate salts were studied based on NMR and the counterions X (including 3,5-$Cl_2C_6H_3CO_2^-$) were reported to be inserted into the micellar hydrophobic core/hydrophilic head interface (Kreke *et al.*, 1996). Rheological studies, small angle neutron scattering (SANS), and cryo-TEM images have also revealed the micellar growth and its formation for the X ions (Carver *et al.*, 1996).

There have been quite a number of reports that provided various kinetic models which were used to quantitatively correlate the observed data for the rate of micellar catalysed reactions (Khan, 2006). However, most of the studies were focused on the pure micellar system (Eads & Robosky, 1999) and very few were reported based on mixed micellar

[2]This chapter has been accepted for publication by *Journal of Oleo Science*, Vol. 67, No. 1 (2018); DOI: 10.5650/jos.ess17033. ISI indexed Journal.

system (Junquera & Aicart, 2002). Furthermore, theoretical studies on the structure of mixed micelles began a few decades ago (Goldsipe & Blankschtein, 2007) and the detail explanations on their characteristic features are not yet well cleared relative to those of pure micellar systems. There was an attempt, in 1998 (Davies & Foggo, 1998), to explain observations based upon the effects of mixed micelles on the kinetic reaction rate using Multiple Micellar Pseudophase (MMPP) models. But that was carried out to study the mixed anionic-nonionic micellar combination. Another study (Bunton *et al.*, 1993), however, presented the use of Pseudophase (PP) micellar model to explain the rate of reactions affected by mixed cationic-nonionic micellar system. The PP micellar model merged with an empirical equation (**Eq. 3.1**) (Khan & Ismail, 2003) was used to treat the results obtained in this study.

The behavior of pure cationic micelles (CTABr), for the reaction of piperidine with ionised phenyl salicylate, in the presence of MX, 3,5-dichlorosodium benzoate (3,5-$Cl_2C_6H_3CO_2Na$), was recently studied (Razak *et al.*, 2014). However, the study has not reported such behavior in the presence of mixed micelles. It has been known for nearly three decades that the counterionic salts affect the physicochemical properties of mixed aqueous ionic-nonionic surfactants (Dar *et al.*, 2010; Karayil *et al.*, 2016; Sidim, 2016). Effects of the concentrations of moderately hydrophobic counterions on the structural features of iomic micelles in mixed aqueous ionic-nonionic surfactants have been reported rarely, although such systems are very important industrially as well as technologically (Dar *et al.*, 2010). The effects of sodium benzoate (NaBz), sodium hexanoate (NaHx) and NaCl on the associated physicochemical properties of polymer-cationic surfactant mixed system have been studied and the qualitative interpretation of the findings is given in detail (Dar *et al.*, 2006; Dar *et al.*, 2010; Jan *et al.*, 2007; Mir *et al.*, 2009). A quantitative interpretation of these results (Dar *et al.*, 2006; Dar *et al.*, 2010; Jan *et al.*, 2007; Karayil *et al.*, 2016; Mir *et al.*, 2009; Sidim, 2016) and related studies

(Lin *et al.*, 2016; Wang *et al.*, 2015; Yan & Zhao, 2015; Zhang *et al.*, 2013) is difficult because of the unavailability of the values of the counterion binding constants with the ionic surfactants in the absence and presence of nonionic surfactant or polymer. In the continuation of the study on the determination of the hydrophilic and moderately hydrophobic counterions binding constants with CTABr in the absence and presence of $C_{16}E_{20}$ (Fagge *et al.*, 2016), the following new findings are reported on: (i) the effects of [$C_{16}E_{20}$] on the binding affinity of X^- with CTABr, (ii) the rheological study of mixed aqueous CTABr/MX/$C_{16}E_{20}$/H_2O (MX = 3,5-$Cl_2C_6H_3CO_2Na$) solution and (iii) the possible quantitative relationship between the values of ion exchange constants (R_X^{Br} or K_X^{Br}) and the structural features of CTABr/MX/$C_{16}E_{20}$/H_2O (MX = 3,5-$Cl_2C_6H_3CO_2Na$). The choice of MX as 3,5-$Cl_2C_6H_3CO_2Na$ was motivated by nearly 4-fold larger mean value of R_X^{Br} or K_X^{Br} for X = 3,5-$Cl_2C_6H_3CO_2^-$ than that for X = salicylate ion (Fagge *et al.*, 2016). The results and their plausible explanations are described in this chapter. It is perhaps noteworthy that this constitutes the second report where the effect of mixed micelles, CTABr-$C_{16}E_{20}$/H_2O, on the counterion binding constant have been studied quantitatively.

4.2 Methodology

4.2.1 Reagents and chemicals

All the reagents and chemicals mentioned in section 3.2.1, except M_2X (M_2X = disodium salicylate, 2-$NaOC_6H_4CO_2Na$), were the same in this section. Their methods of preparations, as well as concentrations, were also the same. Another salt, MX (3,5-$Cl_2C_6H_3CO_2Na$) brought by Sigma-Aldrich, with 97% purity, was used instead. The standard solutions of 0.2 M MX (3,5-$Cl_2C_6H_3CO_2Na$) were prepared by adding 0.25 M NaOH to 0.2 M solution of 3,5-dichlorobenzoic acid (3,5-$Cl_2C_6H_3CO_2H$) which was obtained from Aldrich with 97% purity and it was recrystallized before preparation.

4.2.2 Kinetic method

The details are the same as in section 3.2.2.

4.2.3 Use of semi empirical kinetic, SEK, method to find the values of relative counterion binding constants (K_X^{Br} or R_X^{Br}) for X = 3,5-$Cl_2C_6H_3CO_2^-$

The details are the same as in section 3.2.3.

4.2.4 Rheological study

The details are the same as in section 3.2.4.

4.3 Results

4.3.1 Effect of [NaBr] on k_{obs} for the piperidinolysis of PhS^- at lower concentrations of $C_{16}E_{20}$ in mixed CTABr-$C_{16}E_{20}$ and 35 °C

The kinetic experiments on the effects of [NaBr] for the reaction of 0.10 M Pip, 0.20 mM PSH and 0.030 M NaOH in the presence of pure CTABr and mixed CTABr-$C_{16}E_{20}$ on k_{obs} (with the NaBr concentration range from 0.00–0.700 M) were conducted at 35 °C and 370 nm. The value of $[CTABr]_T$ is 0.006 M with 0.00 M $C_{16}E_{20}$. Similar observations were obtained by increasing $[C_{16}E_{20}]$ to 0.6 μM and 0.06 mM. The results are presented graphically in **Figure 4.1**.

4.3.2 Effect of [3,5-$Cl_2C_6H_3CO_2Na$] on k_{obs} for the piperidinolysis of PS^- at a constant concentration of pure CTABr and 35 °C

Other kinetic experiments were also conducted at constant 0.10 M Pip, 0.20 mM PSH and 0.03 M NaOH in the presence of 0.006 M CTABr and various values [3,5-$Cl_2C_6H_3CO_2Na$] (0.00–0.08 M). Similar results were obtained by further increasing the concentration of CTABr to 0.010 and 0.015 M. The values of k_{obs} obtained are shown in **Table 4.1.**

4.3.3 Effect of [3,5-$Cl_2C_6H_3CO_2Na$] on k_{obs} for the piperidinolysis of PS^- at a constant concentration of $C_{16}E_{20}$ and 35 °C

Other kinetic experiments for the piperidinolysis of PS^- at various [3,5-$Cl_2C_6H_3CO_2Na$] (within the range of 0.00–0.20 M) and 0.030 M NaOH were carried out. They were performed at $[C_{16}E_{20}]_T$ = 0.001 M, 370 nm and 35 °C. The value of $[C_{16}E_{20}]_T$ was increased to 0.003, 0.006, 0.008, 0.010, and 0.015 M. The kinetic parameters obtained are presented in **Appendix E** (with $[C_{16}E_{20}]_T$ = 0.001, 0.003 and 0.006 M) and **Appendix F** (with $[C_{16}E_{20}]_T$ = 0.008, 0.0010 and 0.015 M).

4.3.4 Effect of [3,5-$Cl_2C_6H_3CO_2Na$] on k_{obs} for the piperidinolysis of PS^- at various concentrations of mixed CTABr-$C_{16}E_{20}$ and 35 °C

Two sets of kinetic experiments were conducted at constant 0.10 M Pip, 0.20 mM PS^-, 0.03 M NaOH and different [3,5-$Cl_2C_6H_3CO_2Na$] (0.00–0.04 M) in the presence of lower concentrations of $C_{16}E_{20}$ of the mixed CTABr-$C_{16}E_{20}$ micelles ($[CTABr]_T$ = 0.006 M with $[C_{16}E_{20}]_T$ = 6.0 μM).

Similar results were obtained upon increasing $[C_{16}E_{20}]_T$ to 0.06 mM and the observed data are presented in **Table 4.2.**

Three sets of kinetic experiments were also conducted at constant 0.10 M Pip, 0.20 mM PS^-, 0.03 M NaOH, and different [3,5-$Cl_2C_6H_3CO_2Na$] (0.00–0.08 M) in the presence of higher concentrations of $C_{16}E_{20}$ of the mixed CTABr-$C_{16}E_{20}$ micelles ($[CTABr]_T$ = 0.006, 0.010 and 0.015 M with 0.006 M $C_{16}E_{20}$). Similar results were obtained upon increasing $[C_{16}E_{20}]_T$ to 0.010 and 0.015 M and the plots of k_{obs} against [3,5-$Cl_2C_6H_3CO_2Na$] are presented in **Figures 4.2, 4.3** and **4.4,** respectively.

4.3.5 Rheological characteristics of aqueous pure CTABr micellar solutions at various [3,5-$Cl_2C_6H_3CO_2Na$], 25 and 35 °C

Aqueous solution mixtures containing constant [Pip], [PS^-], and [NaOH] in the presence of 0.015 M CTABr and different [3,5-$Cl_2C_6H_3CO_2Na$] were rheologically measured. The experiments were conducted at the steady-shear response and two distinct temperatures (25 and 35 °C). Different values of shear viscosity (η) at various shear rates ($\dot{\gamma}$) were determined. The results are presented, using log-log sketches of η vs $\dot{\gamma}$, in **Figures 4.5 (a)** and **(b)** at, respectively, 25 and 35 °C.

4.3.6 Rheological characteristics of aqueous mixed CTABr-$C_{16}E_{20}$ micellar solutions at various [3,5-$Cl_2C_6H_3CO_2Na$], 25 and 35 °C

To study the effects of mixed micelles, another aqueous solution mixtures of constant [Pip], [PS^-], [NaOH], and mixed 0.015 M CTABr and 0.006 M $C_{16}E_{20}$ at different [3,5-$Cl_2C_6H_3CO_2Na$], were subjected to rheometric measurements. The experimental conditions were similar as that in 4.3.5 above and different values of η at different $\dot{\gamma}$ were also determined. Different observations were obtained in the presence of 0.006 M $C_{16}E_{20}$ and the results are presented, using log–log sketches of η vs. $\dot{\gamma}$, in **Figures 4.6 (a)** and **(b)** at, respectively, 25 and 35 °C.

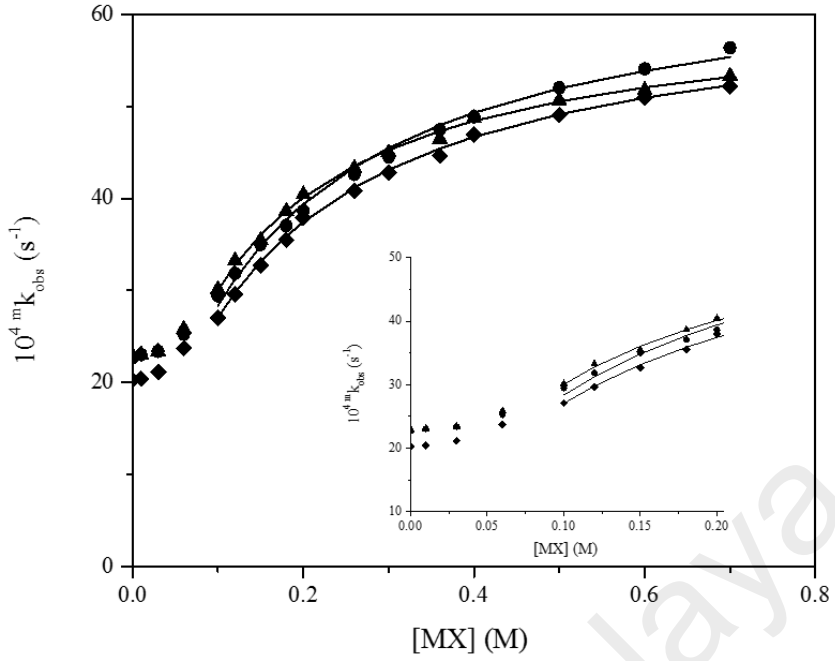

Figure 4.1: Plots showing the relationship between $^mk_{obs}$ (where superscript "m" represents mixed micelles) and [NaBr] for the reaction of Pip and PS^- at three different constant $[CTABr]_T + [C_{16}E_{20}]_T$ = 0.006 M + 0.00 M (●), 0.006 M + 0.6 μM (♦) and 0.006 M + 0.060 mM (▲), and 35 °C. The solid lines are drawn via the calculated values of the rate constant (k_{calcd}). Insert: The plots for magnified scale for the data points at lower values of [NaBr].

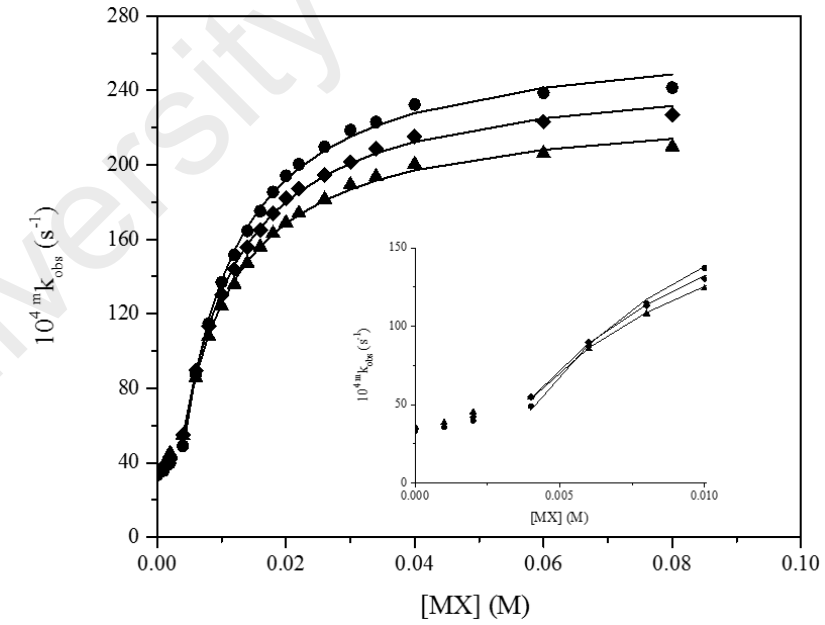

Figure 4.2: Plots showing the relationship between $^mk_{obs}$ (where superscript "m" represents mixed micelles) and [3,5-$Cl_2C_6H_3CO_2Na$] for the reaction of Pip and PS^- at three different constant $[CTABr]_T + [C_{16}E_{20}]_T$/M = 0.006 + 0.006 (●), 0.006 + 0.010 (♦) and 0.006 + 0.015 (▲), and 35 °C. The solid lines are drawn via the calculated values of the rate constant (k_{calcd}). Insert: The plots for magnified scale for the data points at lower values of [3,5-$Cl_2C_6H_3CO_2Na$].

Table 4.1: Pseudo first-order rate constants (k_{obs}) for the reaction of Pip with PS^- at 0.006, 0.010 and 0.015 M CTABr at different [3,5-$Cl_2C_6H_3CO_2Na$].[a]

[MX][b] M	[CTABr]$_T$[c] = 0.006 M		0.010 M		0.015 M	
	$10^4\ k_{obs}$[d] s^{-1}	$10^4\ k_{calcd}$[e] s^{-1}	$10^4\ k_{obs}$[d] s^{-1}	$10^4\ k_{calcd}$[e] s^{-1}	$10^4\ k_{obs}$[d] s^{-1}	$10^4\ k_{calcd}$[e] s^{-1}
0.00	28.7 ± 0.2[f]		26.6 ± 0.3[f]		25.4 ± 0.2[f]	
0.001	28.3 ± 0.4		26.8 ± 0.3		25.1 ± 0.3	
0.002	28.8 ± 0.2		27.3 ± 0.2		26.8 ± 0.2	
0.004	31.8 ± 0.3		29.2 ± 0.3		27.7 ± 0.2	
0.006	51.3 ± 0.6		42.4 ± 0.2	42.5	33.0 ± 0.3	31.5
0.008	94.4 ± 0.6	93.2	75.0 ± 0.6	73.0	54.5 ± 0.3	53.8
0.010	123.0 ± 1.3	123.2	98.3 ± 0.9	96.3	70.6 ± 0.6	72.2
0.012	143.9 ± 1.3	144.9	114.5 ± 1.5	114.7	86.3 ± 0.4	87.4
0.014	163.4 ± 1.4	161.3	127.8 ± 1.7	129.6	99.2 ± 0.7	100.3
0.016	176.7 ± 1.6	174.2	138.1 ± 1.7	142.0	110.4 ± 1.2	111.4
0.018	182.8 ± 1.9	184.6	149.3 ± 1.9	152.3	118.9 ± 1.1	121.1
0.020	192.3 ± 2.2	193.1	157.5 ± 2.1	161.1	127.5 ± 1.2	129.5
0.022	198.5 ± 2.2	200.3	166.7 ± 1.8	168.8	137.0 ± 1.2	136.9
0.026	212.0 ± 1.9	211.5	183.2 ± 2.0	181.3	149.6 ± 1.2	149.4
0.030	222.4 ± 1.4	220.0	196.2 ± 2.0	191.1	162.5 ± 1.4	159.6
0.034	229.8 ± 2.0	226.7	206.0 ± 2.1	199.0	172.1 ± 1.8	168.0
0.040	237.5 ± 1.8	234.3	211.7 ± 1.8	208.3	180.7 ± 1.5	178.1
0.060	247.3 ± 2.0	249.1	224.6 ± 2.7	227.3	198.0 ± 1.4	199.8
0.080	254.0 ± 1.7	256.7	233.1 ± 1.9	237.6	209.1 ± 1.6	212.1

[a]$[PSH]_0$ = 0.2 mM, [Pip] = 0.1 M, [NaOH] = 0.03 M, λ = 370 nm and aqueous reaction mixture for each kinetic run contains 2% v/v acetonitrile. [b]Total concentration of 3,5-$Cl_2C_6H_3CO_2Na$. [c]Total concentration of CTABr. [d]Observed pseudo first order rate constant. [e]Pseudo first order rate constant calculated from **Eq. 3.13** with parameters listed in **Table 4.4**, $\theta = F_{X/S}(k_W^2\ [Pip]_T)$ and $K^{X/S} = K_{X/S}/(1+ K_S^0[CTABr]_T)$. [f]Error limits are standard deviations.

Table 4.2: Pseudo-first-order rate constants ($^{m}k_{obs}$) for the reaction of piperidine with anionic phenyl salicylate (PS^{-}) at 0.006 M CTABr in the presence of 0.600 μM, and 0.060 mM $C_{16}E_{20}$ and different [3,5-$Cl_2C_6H_3CO_2Na$].[a]

[MX][b]	[CTABr]$_T$[c] = 0.006 M		0.006 M	
	[$C_{16}E_{20}$]$_T$[d] = 0.600 μM		0.060 mM	
M	$10^4\ ^{m}k_{obs}$[e] s^{-1}	$10^4\ ^{m}k_{calcd}$[f] s^{-1}	$10^4\ ^{m}k_{obs}$[e] s^{-1}	$10^4\ ^{m}k_{calcd}$[f] s^{-1}
0.00	20.3 ± 0.30[g]		21.1 ± 0.40[g]	
0.001	21.1 ± 0.29		21.3 ± 0.30	32.5
0.002	22.7 ± 0.32		21.5 ± 0.35	37.0
0.004	33.3 ± 0.38	32.7	29.4 ± 0.67	29.7
0.006	75.7 ± 0.47	78.3	73.5 ± 0.89	73.4
0.008	106.0 ± 0.55	106.5	101.1 ± 1.31	99.7
0.010	125.3 ± 0.63	125.7	118.3 ± 1.48	117.2
0.012	139.8 ± 0.72	139.6	129.8 ± 1.69	129.8
0.014	150.4 ± 0.43	150.2	137.6 ± 2.91	139.2
0.016	159.2 ± 0.53	158.4	146.0 ± 2.04	146.5
0.018	165.1 ± 0.75	165.1	151.0 ± 1.98	152.3
0.020	170.8 ± 1.10	170.5	156.2 ± 2.04	157.1
0.022	176.4 ± 0.92	175.1	161.4 ± 2.15	161.1
0.026	182.7 ± 1.20	182.3	165.5 ± 1.68	167.4
0.030	188.3 ± 1.14	187.7	170.5 ± 1.49	174.1
0.034	192.2 ± 1.31	192.0	176.8 ± 1.39	175.7
0.040	194.5 ± 1.64	196.9	180.6 ± 1.52	179.9

Footnote *a*, *b*, and *c* are the same as in **Table 4.1.** [d]Total concentration of $C_{16}E_{20}$. [e]Observed pseudo first order rate constant. [f]Pseudo first order rate constant calculated from **Eq. 3.13**. [g]Error limits are standard deviation.

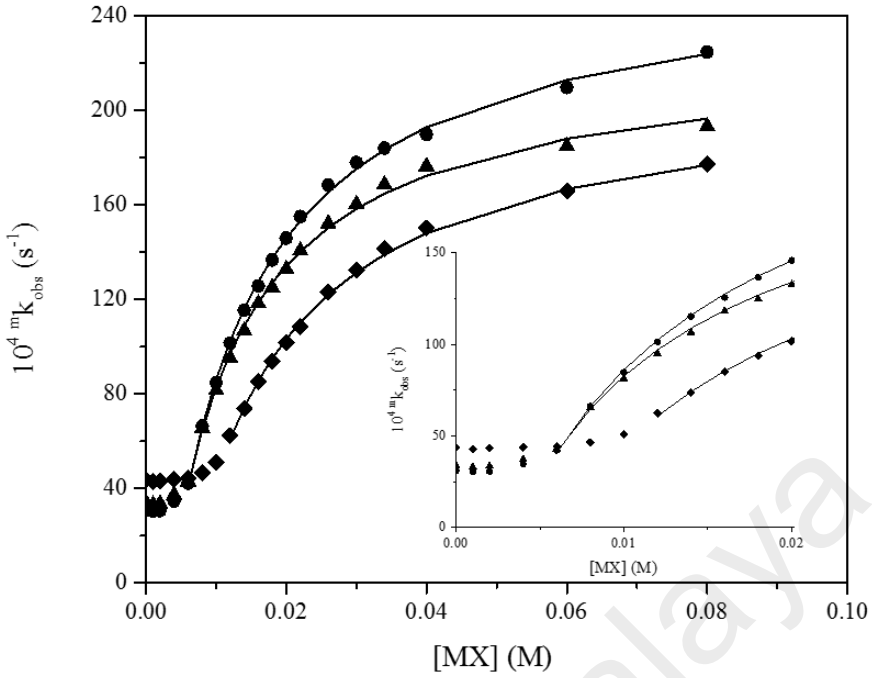

Figure 4.3: Plots showing the relationship between $^m k_{obs}$ (where superscript "m" represents mixed micelles) and [3,5-$Cl_2C_6H_3CO_2Na$] for the reaction of Pip and PS^- at three different constant $[CTABr]_T + [C_{16}E_{20}]_T$/M = 0.010 + 0.006 (●), 0.010 + 0.010 (♦) and 0.010 + 0.015 (▲), and 35 °C. The solid lines are drawn via the calculated values of the rate constant (k_{calcd}). Insert: The plots for magnified scale for the data points at lower values of [3,5-$Cl_2C_6H_3CO_2Na$].

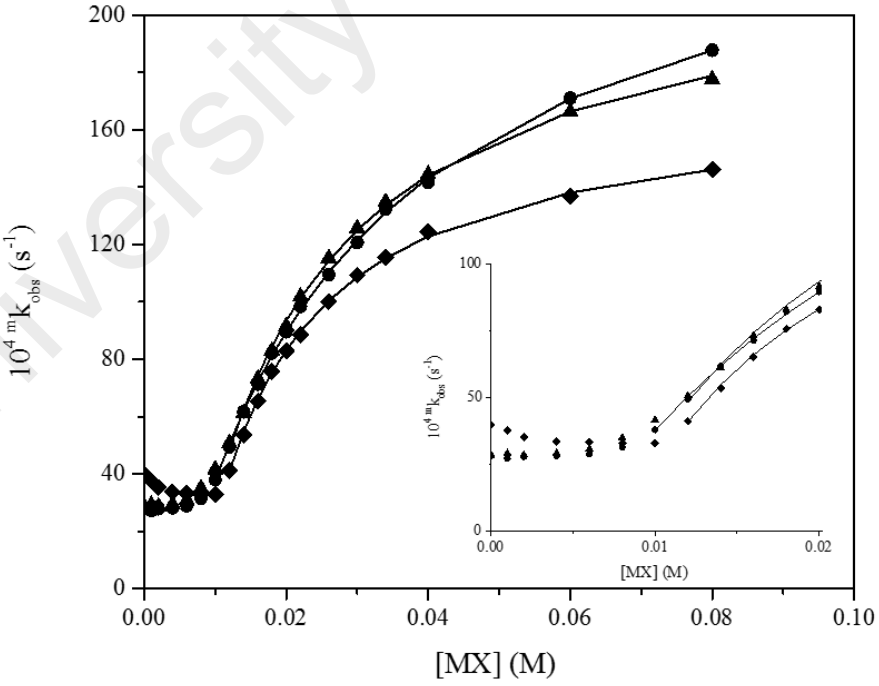

Figure 4.4: Plots showing the relationship between $^m k_{obs}$ (where superscript "m" represents mixed micelles) and [3,5-$Cl_2C_6H_3CO_2Na$] for the reaction of Pip and PS^- at of three different constant $[CTABr]_T + [C_{16}E_{20}]_T$/M = 0.015 + 0.006 (●), 0.015 + 0.010 (♦) and 0.015 + 0.015 (▲), and 35°C. The solid lines are drawn via the calculated values of the rate constant (k_{calcd}). Insert: The plots for magnified scale for the data points at lower values of [3,5-$Cl_2C_6H_3CO_2Na$].

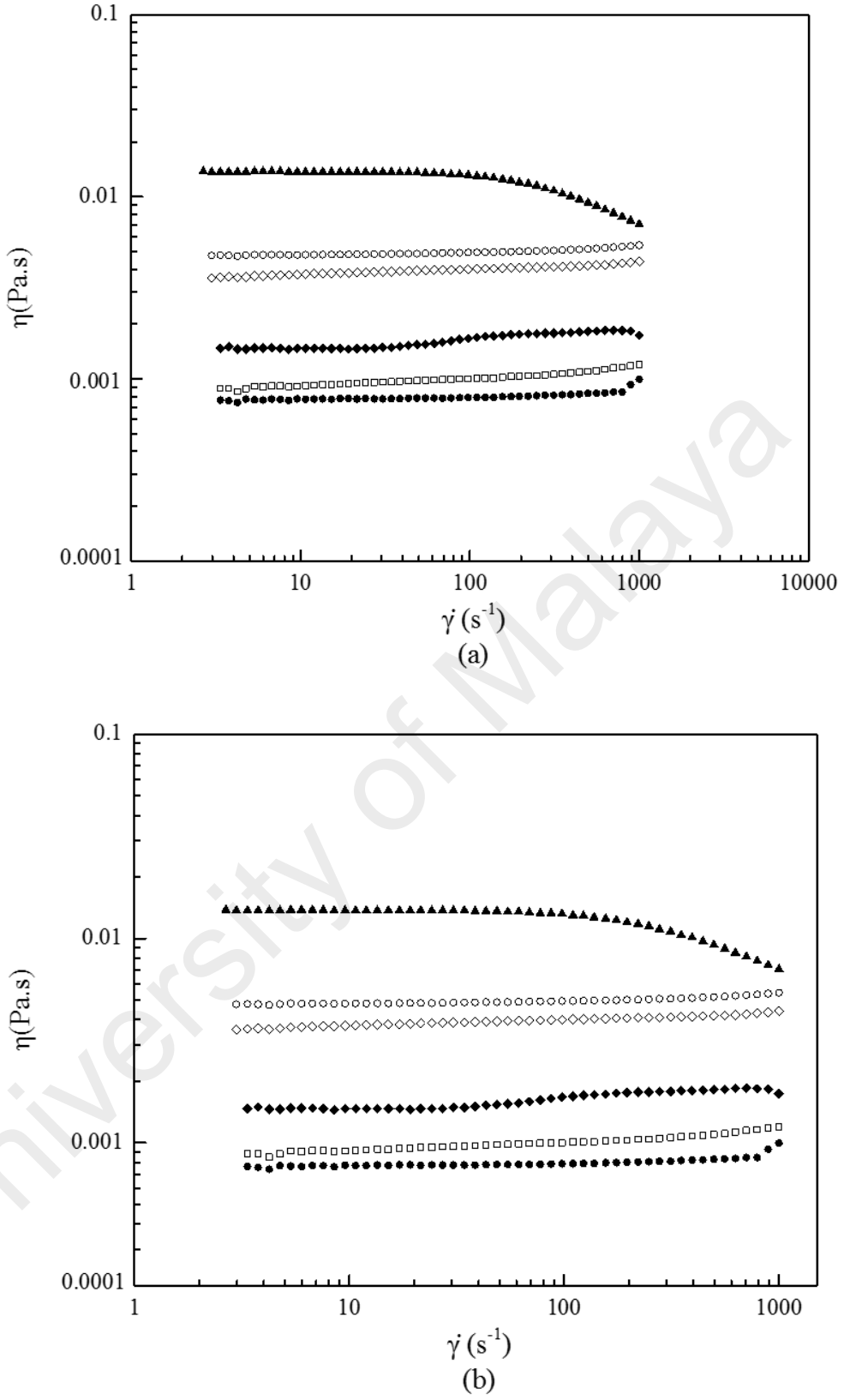

Figure 4.5: Plots representing shear viscosity (η) against shear rate (γ̇) for the piperidinolysis of PS^- containing 0.015 M CTABr and [3,5-$Cl_2C_6H_3CO_2Na$]/M = (a) 0.004 (•) 0.007 (□) 0.015 (▲) 0.025 (♦) 0.040 (○) and 0.070 (◊) at 25 °C and (b) 0.004 (•) 0.007 (□) 0.015 (▲) 0.025 (♦) 0.040 (○) and 0.070 (◊) at 35 °C.

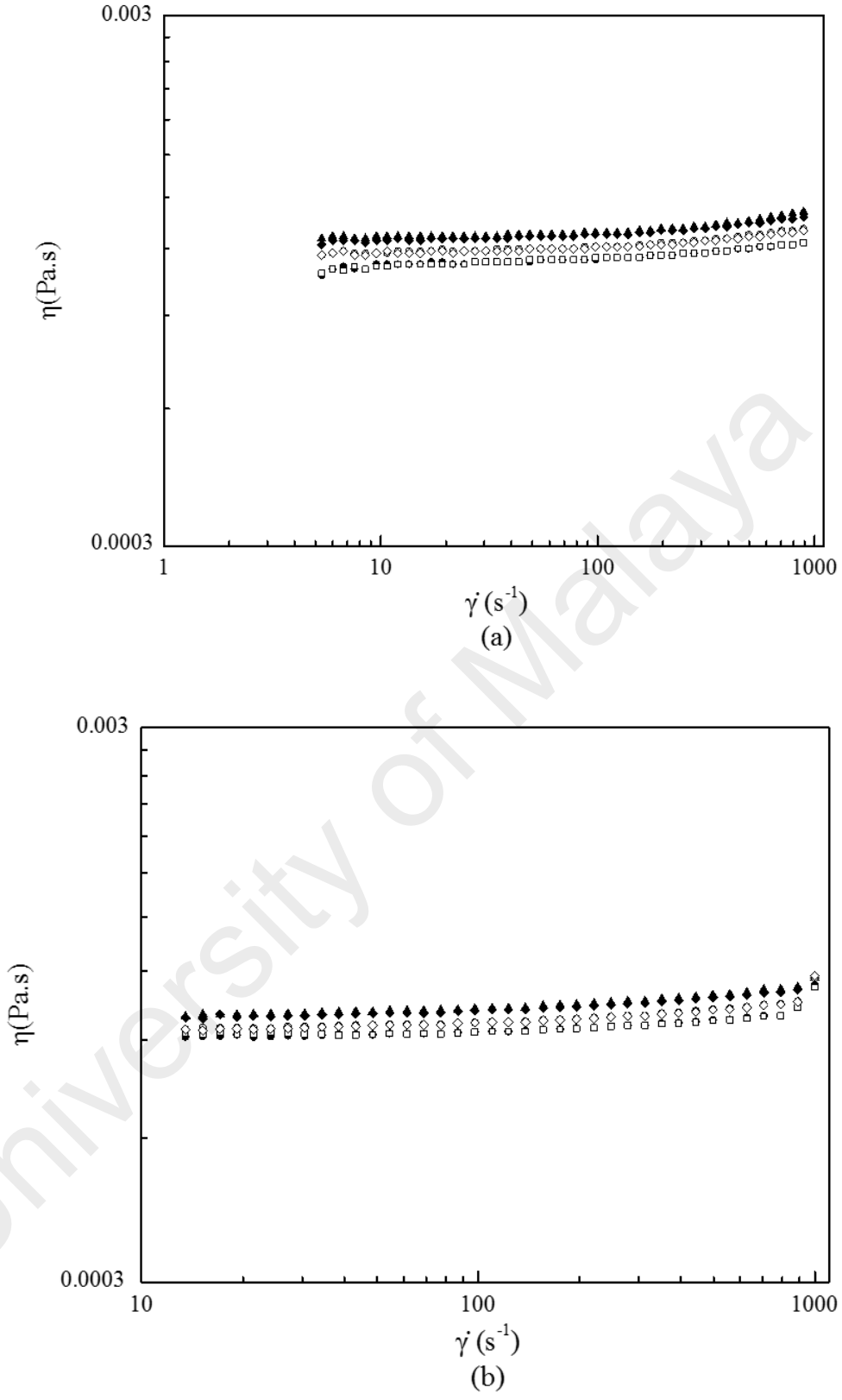

Figure 4.6: Plots representing shear viscosity (η) against shear rate (γ̇) for the piperidinolysis of PS^- containing 0.015 M CTABr, 0.006 M $C_{16}E_{20}$ and [3,5-$Cl_2C_6H_3CO_2Na$]/M = (a) 0.004 (•) 0.007 (□) 0.015 (▲) 0.025 (♦) 0.040 (○) and 0.070 (◊) at 25 °C and (b) 0.004 (•) 0.007 (□) 0.015 (▲) 0.025 (♦) 0.040 (○) and 0.070 (◊) at 35 °C.

4.4 Discussion

4.4.1 Explanation of kinetic observations for the piperidinolysis of PS^- in the presence of pure $C_{16}E_{20}$ micelles at various [MX] and 35 °C

The results obtained showed similar effect as explained in section 3.4.1 and the values of kinetic parameters are presented in **Table 4.3.**

Table 4.3: Values of kinetic parameters for the reaction of Pip and PS^- in the presence of 3,5-$Cl_2C_6H_4CO_2Na$ at different $[C_{16}E_{20}]_T$ and 35 °C.[a]

$[C_{16}E_{20}]_T$[b] M	k_{obs}^0[c] s^{-1}	$k_{obs}^{MX\ (max)}$[d] s^{-1}	%NSE[e]
0.001	268	155	42
0.003	233	142	39
0.006	217	146	33
0.008	201	142	29
0.010	153	120	22
0.015	123	107	13

[a]$[PSH]_0$ = 0.20 mM, [NaOH] = 0.03 M, [Pip] = 0.10 M, λ = 370 nm and aqueous reaction mixture for each kinetic run contains 2% v/v acetonitrile. [b]Total concentration of $C_{16}E_{20}$. [c]k_{obs}^0 = k_{obs} at [MX] = 0 (or average value of similar values of k_{obs} at various [MX]). [d]$k_{obs}^{MX\ (max)}$ = k_{obs} at the maximum value of [MX]. [e]Percent negative salt effect, %NSE calculated from **Eq. 3.12**

4.4.2 Explanation of kinetic results at constant concentration of pure CTABr micelles, various values of [3,5-$Cl_2C_6H_3CO_2Na$] and 35 °C

The values of k_{obs} for the reaction of 0.10 M Pip and 0.20 mM PSH in basic medium with $[CTABr]_T$ = 0.006, 0.010 or 0.015 M, $[C_{16}E_{20}]_T$ = 0, and different concentration of 3,5-$Cl_2C_6H_3CO_2Na$ (**Table 4.1**) obey semi empirical **Eq. 3.13.** The values of θ and $K^{X/S}$, obtained at different $[CTABr]_T$, were calculated using, respectively, **Eqs. 3.13** and **3.15,** and are presented in **Table 4.4.**

4.4.3 Ion exchange catalysis

Perhaps it is noteworthy that the observed data described in **Tables 4.1** and **4.2**, and the plots of **Figures 4.1–4.4** where the increase in k_{obs} with increasing [MX] represents catalytic effects of MX. The study carried out to discover the effects of MX (= sodium 4-chlorobenzoate) on k_{obs} for piperidinolysis of PS^- revealed the decrease of nearly 10% with the increase in [MX] from 0.0 to ≤ 0.2 M at constant [$C_{16}E_{20}$] within its range 5–15 mM and $[CTABr]_T = 0$ (Fagge & Khan, 2016). Thus, the observed results exhibited by **Tables 4.1, 4.2** and **Figures 4.1–4.4** cannot be attributed to ionic strength/salt effect. Similar observations have been presented in several reports on related studies where the nonlinear increase in k_{obs} with an increase in [MX] at a constant [cationic micelles] is ascribed to the occurrence of ion exchange process X^-/PS^- at the cationic micellar surface (Khalid *et al.*, 2016; Khan, 2006; Khan, 2010). This characteristic behavior of CTABr/MX/H_2O/$C_{16}E_{20}$ catalysis is referred to ion exchange catalysis, where the origin of catalysis of MX is the ion exchange X^-/PS^-.

It is evident from **Eq. 3.13** that $\theta K^{X/S}$ represents apparent catalytic constant ($^{X}k_{cat}$) of MX. Thus, the replacement of $\theta K^{X/S}$ in **Eq. 3.13** gives **Eq. 4.1.**

$$k_{obs} = \frac{k_0 + {}^{X}k_{cat}\,([MX] - [MX]_0^{op})}{1 + K^{X/S}([MX] - [MX]_0^{op})} \qquad \textbf{(4.1)}$$

where $k_0 = k_{obs}$ at $[MX] = [MX]_0^{op}$ and $[MX]_0^{op}$ represents the optimum values of [3,5-$Cl_2C_6H_3CO_2Na$] at which further increase in [MX] or [M_2X] is believed to have no effect on ion exchange X^-/HO^- and X^-/Br^- occurring in the CTABr micellar phase (Khan, 2010) and were obtained by the use of iterative method explained in detail in the literature (Khan & Ismail, 2003; Khan & Ismail, 2009). The values of $K^{X/S}$ and $^{X}k_{cat}$ were determined by the use of nonlinear least squares method. The values of k_0 were found experimentally by

carrying out kinetic runs at constant $[CTABr]_T$ and [MX] = 0 (**Table 4.4**). The optimum values of $[3,5\text{-}Cl_2C_6H_3CO_2Na]$ ($[MX]_0^{op}$) at various $[CTABr]_T$ were determined as described in the past (Khan & Ismail, 2003) and are presented in **Table 4.4.**

It has been described in detail elsewhere (Khan, 2010) that a plausible reaction mechanism in terms of psuedophase micellar model and empirical equation (**Eq. 3.13**) can lead to **Eq. 4.1** with $K^{X/S}$ and ${}^{X}k_{cat}$ represented by **Eqs 3.15** and **4.2,** respectively. It has been noticed from **Eq. 3.15** that increase in $[CTABr]_T$ results in the corresponding decrease in the values of $K^{X/S}$ (so long as $K_{X/S}$ does not depend on $[CTABr]_T$). This observation agrees with the results in **Table 4.4** where $K^{X/S}$ = 128, 82 and 57 M^{-1} at respectively $[CTABr]_T$ = 0.006, 0.010 and 0.015 M. But the values of $K_{X/S}$ (**Table 4.4**) were determined using **Eq. 3.15.**

$$ {}^{X}k_{cat} = F_{X/S}(k_W^2[Pip]_T)K^{X/S} \qquad \textbf{(4.2)} $$

where $F_{X/S}$ is an empirical constant and its appearance in **Eq. 4.2** is described in detail elsewhere (Khan, 2010), k_W^2 represents second-order rate constant for the nucleophilic reaction of Pip with ionized PSH (PS^-).

Perhaps, it is noteworthy that the calculated values of $K^{X/S}$ and k_{calcd} were turned out to be exactly the same at a particular value of $[CTABr]_T$ which is evident from **Tables 4.1** and **4.2,** and the plots of **Figures 4.1–4.4** where the solid lines are drawn through the calculated values of the rate constant, k_{calcd}.

To determine the values of conventional ion exchange constant/relative counterion binding constant (K_X^{Br}), the normalised values of both $K_{X/S}$ ($K_{X/S}^n = F_{X/S}K_{X/S}$) and $K_{Br/S}$ ($K_{Br/S}^n = F_{Br/S}K_{Br/S}$) (as discussed in section in section 3.4.2) are required. The values of $K_{X/S}^n$ are presented in **Table 4.4.** The values of K_X^{Br} were calculated from **Eq. 3.16** and the

calculated values of $K^{n}_{X/S}$ and the reported value of $K^{n}_{Br/S}$ ((= 25 M^{-1}) (Khan, 1997a; Khan *et al.*, 2000; Khan & Ismail, 2007). Similarly, the values of R^{Br}_{X} were calculated from **Eq. 3.17** and the calculated values of $({}^{n}K_{X/S})^{nsp}$ and $({}^{n}K_{Br/S})^{sp}$ in **Table 4.4.** These calculated values of K^{Br}_{X} or R^{Br}_{X} are summarised in **Table 4.4**.

Apparent experimental proof reported that there exist a consistently respective increase and decrease in hydrophobicity and hydrophilicity of micellar phase when the separation between the interior and exterior regions of the micelles is increased (Laschewsky, 2003). The counterion X (3,5-$Cl_2C_6H_3CO_2^-$) has chloro substituents (Cl) and a carboxylate ion (COO^-) which are, respectively, hydrophobic and hydrophilic in nature. The two chloro substituents, at position 3 and 5 of X, are assumed to be in a micellar region of almost similar hydrophilic and hydrophobic character. Thus, considering the reported value of K^{Br}_{X} or R^{Br}_{X} (= 50) for 3-$ClC_6H_4CO_2^-$ (Razak *et al.*, 2014), the value of K^{Br}_{X} for 3,5-$Cl_2C_6H_3CO_2^-$ supposed to have been around 100 if, and only if, the free energy factor (at the expense of groups located at the aromatic segment) would be significant. However, the mean value of K^{Br}_{X} or R^{Br}_{X}, (**Table 4.4**) for 3,5-$Cl_2C_6H_3CO_2^-$ is 198. This prediction of K^{Br}_{X} or R^{Br}_{X}value, based upon the number of substituents and their locations in an aromatic region, has a probably failed assumption which depends only on structural behaviours of CTABr/MX. It has not taken into account the changes in shapes and sizes of MX/CTABr with the decrease or increase in values of K^{Br}_{X} or R^{Br}_{X} (Razak *et al.*, 2014). The published results show the existence of mixed vesicle-wormlike micelles at 0.006–0.015 M range of CTABr and various values of [3,5-$Cl_2C_6H_3CO_2Na$] (Razak & Khan, 2013).

4.4.4 Explanation of kinetic data at constant mixed CTABr-$C_{16}E_{20}$ micelles, various [3,5-$Cl_2C_6H_3CO_2Na$] and 35 °C

The mixed cationic-nonionic (CTABr-$C_{16}E_{20}$) micellar system is different from the pure micellar system. To differentiate between the parameters obtained in the mixed

CTABr-$C_{16}E_{20}$ micellar systems and those in the pure ones, a letter "m" is used as a superscript to represent those obtained in the presence of mixed CTABr-$C_{16}E_{20}$ micelles as elaborated in section 3.4.2. It has been explained in section 4.4.2 (the case of pure CTABr micelles) that the values of k_0 were determined at constant $[CTABr]_T$ and $[3,5\text{-}Cl_2C_6H_3CO_2Na] = 0$. However, in the case of mixed CTABr-$C_{16}E_{20}$, the condition has been changed by adding constant concentrations of $C_{16}E_{20}$ (6.0×10^{-7}, 6.0×10^{-5}, 6.0×10^{-3}, 1.0×10^{-2} and 1.5×10^{-2} M) and the corresponding values of $^{m}k_0$ are presented in **Table 4.5.** The values of $^{m}k_{obs}$ were also found to fit **Eq. 3.13.** The values of $^{m}[MX]_0^{op}$ (**Table 4.5**) were found to increase with the increase in $[CTABr]_T$ and almost independent of $[C_{16}E_{20}]_T$. However, these values are comparatively higher than those obtained in the presence of pure CTABr (**Table 4.4**).

The relationship between $^{m}\theta$ and $^{m}F_{X/S}$ is; $^{m}F_{X/S} = {}^{m}\theta/{}^{m}k_{obs}^{W}$, with $^{m}k_{obs}^{W} = {}^{m}k_{obs}$ at various $[C_{16}E_{20}]_T$ and $[CTABr]_T = [MX] = 0$ ($^{m}k_{obs}^{W} = {}^{m}k_W^2 Pip]_T$). The values of $^{m}k_{obs}^{W}$ are 303.5×10^{-4}, 273.0×10^{-4}, 240.0×10^{-4}, 193.2×10^{-4} and 184.2×10^{-4} s^{-1} at, respectively, 6.0×10^{-7}, 6.0×10^{-5}, 6.0×10^{-3}, 1.0×10^{-2} and 1.5×10^{-2} M constant $[C_{16}E_{20}]_T$. The values of $^{m}F_{X/S}$ (**Table 4.5**) are independent of the concentration of the mixed CTABr-$C_{16}E_{20}$ micelles. But these values of $^{m}F_{X/S}$ were found to be higher than $F_{X/S}$ in the presence of pure micelles (**Table 4.4**). The values of $^{m}\theta$ and $^{m}K^{X/S}$, summarised in **Table 4.5**, were also found to be independent of the concentration of the mixed CTABr-$C_{16}E_{20}$ micelles and were also calculated using **Eqs. 3.13** and **3.14.** As explained in section 3.4.2, the values of $^{m}K_{X/S}$ could not be calculated due to the fact that the values of $^{m}K_S^0$ for mixed CTABr-$C_{16}E_{20}$ surfactants are not available for the present study. Hence, **Eq. 3.20** should be used for the calculation of $^{m}K_X^{Br}$. In addition, the values of $^{m}R_X^{Br}$ were calculated using **Eq. 3.21** and are presented in **Table 4.5.**

It is evident that in an aqueous solution containing mixed cationic-nonionic surfactants (e.g CTABr-$C_{16}E_{20}$), the relatively large hydrophilic headgroup of $C_{16}E_{20}$ shields the small sized hydrophobic micellar parts of CTABr (Gao *et al.*, 2002).

4.4.5 Explanation of rheometric data in the presence of pure CTABr and mixed CTABr-$C_{16}E_{20}$ micelles at various [3,5-$Cl_2C_6H_3CO_2Na$]

Rheological data reveal that different flow curves show various micellar structural behaviours. For pure CTABr (0.015 M), at ≥ 0.004 to ≤ 0.007 M [3,5-$Cl_2C_6H_3CO_2Na$], there exist flow curves with mild shear thickening behavior at a reasonably high shear rate and at both 25 and 35 °C (**Figure 4.5 (a)** and **(b)**) which show unique characteristics of spherical micelles.

Table 4.4: Values of empirical constants, θ, and $K^{X/S}$ obtained using **Eqs. 3.13** and **3.14** with the $[MX]_0^{op}$ values for MX = 3,5-$Cl_2C_6H_3CO_2Na$ at different $[CTABr]_T$.[a]

$[CTABr]_T$ M	10^4 k_0[c] s^{-1}	$[MX]_0^{op}$ M	10^3 θ[d] s^{-1}	$K^{X/S}$[d,e] M^{-1}	10 $^Xk_{cat}$[e] $M^{-1}s^{-1}$	$F_{X/S}$	$K_{X/S}$ M^{-1}	$K^n_{X/S}$ M^{-1}	K^{Br}_X or R^{Br}_X
0.006[b]	28.7 ± 0.2[f]	0.00531	28.1 ± 0.2[f]	128.0 ± 3.1[f]	32.6 ± 0.7[f]	0.90[g]	5504[h]	4954.0[i]	198[j]
0.010	26.6 ± 0.3	0.00515	27.2 ± 0.4	81.7 ± 3.5	22.2 ± 0.7	0.87	5727	4982.7	199
0.015	25.4 ± 0.2	0.00552	25.6 ± 0.3	56.7 ± 1.8	14.5 ± 0.3	0.82	6010	4928.2	197

Footnote *a* is the same as in **Table 4.1.** [b]Total concentration of CTABr. [c]$k_0 = k_{obs}$ at [MX] = $[MX]_0^{op}$. [d]The values of θ and $K^{X/S}$ were calculated from **Eqs. 3.13** and **3.14**. [e]The values of $^Xk_{cat}$ and $K^{X/S}$ were calculated from **Eq. 4.1** with the replacement of $\theta K^{X/S}$ in **Eq. 3.13** by $^Xk_{cat}$. [f]Limits of error signifies standard deviations. [g]$F_{X/S} = \theta/(k_W^2\,[Pip]_T)$, where $k_W^2 = k_{obs}$ at $[CTABr]_T = [C_{16}E_{20}]_T = 0$ and $[Pip]_T = 0.10$ M and the value of k_W^2, under such conditions is 0.322 $M^{-1}s^{-1}$. [h]$K_{X/S} = K^{X/S}(1+ K_S^0[CTABr]_T)$, where $K_S^0 = 7 \times 10^3$ M^{-1}. [i]$K^n_{X/S} = F_{X/S}\,K_{X/S}$. [j]$K^{Br}_X$ or $R^{Br}_X = K^n_{X/S}/\,K^n_{Br/S}$, where $K^n_{Br/S} = 25$ M^{-1} (Yusof & Khan, 2010).

Table 4.5: Values of empirical constants, $^{m}\theta$, and $^{m}K^{X/S}$ obtained using **Eqs. 3.13** and **3.14** with the $[MX]_0^{op}$ values for MX = 3,5-$Cl_2C_6H_3CO_2Na$ at different concentrations of mixed CTABr-$C_{16}E_{20}$.[a]

$[CTABr]_T$[b] M	$[C_{16}E_{20}]_T$[c] M	$10^4\ ^{m}k_0$[d] s^{-1}	$^{m}[MX]_0^{op}$ M	$10^3\ ^{m}\theta$[e] s^{-1}	$^{m}K^{X/S}$[e,f] M^{-1}	$10\ ^{mX}k_{cat}$[f] $M^{-1}s^{-1}$	$^{m}F_{X/S}$	$^{m\ n}K^{X/S}$ M^{-1}	$^{m\ n}K^{Br/S}$[h] M^{-1}	$^{m}K_X^{Br}$ or $^{m}R_X^{Br}$
0.006	0.0000006	20.3 ± 0.3[g]	0.00311	22.7 ± 0.1[g]	178.2 ± 2.0[g]	40.4 ± 0.3[g]	0.8[h]	142.6[i]	1.4	102[k]
0.006	0.00006	21.1 ±0.4	0.00318	20.5 ± 0.1	192.6 ± 2.5	39.5 ± 0.4	0.8	154.1	1.8	85.1
0.006	0.006	33.4 ± 0.4	0.00352	27.2 ± 0.3	120.8 ± 4.2	32.9 ± 0.9	1.1	132.9	1.4[j]	81.5
0.006	0.010	34.5 ± 0.4	0.00317	25.4 ± 0.2	117.6 ± 3.5	29.8 ± 0.7	1.3	152.9	2.2[j]	60.0
0.006	0.015	35.7 ± 0.4	0.00318	23.3 ± 0.2	122.2 ± 3.3	28.5 ± 0.6	1.3	158.9	1.8[j]	73.9
0.010	0.006	30.9 ± 0.3	0.00534	26.2 ± 0.2	67.2 ± 1.7	17.6 ± 0.3	1.1	73.9	1.0[j]	85.9
0.010	0.010	43.4 ± 0.4	0.00989	21.2 ± 0.2	54.3 ± 1.9	11.5 ± 0.3	1.1	59.7	1.1[j]	61.1
0.010	0.015	33.8 ± 0.2	0.00547	22.5 ± 0.3	75.4 ± 3.0	17.0 ± 0.5	1.2	89.5	0.9[j]	105.3
0.015	0.006	28.3 ± 0.2	0.00866	25.7 ± 0.2	32.2 ± 0.5	8.3 ± 0.1	1.1	35.4	0.8[j]	46.6
0.015	0.010	39.8 ± 0.5	0.01185	17.2 ± 0.1	59.4 ± 1.4	10.2 ± 0.2	0.9	52.9	0.6[j]	85.3
0.015	0.015	28.5 ± 0.3	0.00964	22.3 ± 0.2	48.4 ± 1.3	10.7 ± 0.2	1.2	58.1	0.8[j]	73.5

Footnote *a* is the same as in **Table 4.1.** [b]Total concentration of CTABr. [c]Total concentration of $C_{16}E_{20}$. [d] $^{m}k_0 = {}^{m}k_{obs}$ at $[MX] = [MX]_0^{op}$. [e]The values of $^{m}\theta$ and $^{m}K^{X/S}$ were calculated from **Eqs. 3.13** and **3.14.** [f]The values of $^{mX}k_{cat}$ and $^{m}K^{X/S}$ were calculated from **Eq. 4.1** with the replacement of $^{m}\theta^{m}K^{X/S}$ in **Eq. 3.13** by $^{mX}k_{cat}$. [g]Limits of error signifies standard deviations. [h] $^{m}F_{X/S} = {}^{m}\theta/{}^{m}k_{obs}^{W}$; with $^{m}k_{obs}^{W} = {}^{m}k_{obs}(= {}^{m}k_W^2[Pip]_T) = 303.5 \times 10^{-4}, 273.0 \times 10^{-4}, 240 \times 10^{-4}, 193.2 \times 10^{-4}$ and $184.2 \times 10^{-4}\ s^{-1}$ at constant $[C_{16}E_{20}]_T$ (6×10^{-7}, 6×10^{-5}, 0.006, 0.010 and 0.015 M $[C_{16}E_{20}]$ respectively) and [MX] = [CTABr] = 0. [i] $^{m\ n}K^{X/S} = {}^{m}F_{X/S}{}^{m}K^{X/S}$. [j] $^{m\ n}K^{Br/S} = {}^{m}F_{Br/S}{}^{m}K^{Br/S}$ for MX = NaBr. [j]Data are obtained from reference (Fagge *et al.*, 2016). [k] $^{m}R_X^{Br} = {}^{m\ n}K^{X/S}/{}^{m\ n}K^{Br/S}$.

Some flow curves, at ≥ 0.015 to ≤ 0.025 M [3,5-$Cl_2C_6H_3CO_2Na$], experience shear thinning which indicates a non-Newtonian fluid system. This characteristic shows the possible existence of wormlike micelles (Lu *et al.*, 2008) in the solution. However, at ≥ 0.040 to ≤ 0.070 M [3,5-$Cl_2C_6H_3CO_2Na$], the system turned back to the shear thickening behavior with relatively higher viscosity values (**Figure 4.5 (a)** and **(b)**) (Qiao *et al.*, 2011). The presence of 0.006 M $C_{16}E_{20}$ in the mixed CTABr-$C_{16}E_{20}$ micelles gives different results at the same [3,5-$Cl_2C_6H_3CO_2Na$].

All the 12 flow curves in **Figure 4.6 (a)** and **(b)** give mild shear thickening behavior at a reasonably high shear rate under the entire experimental conditions. It has been concluded that very dilute solution with a very low shear viscosity at a very high shear rate exhibits what is called "Taylor effect" and these could be caused by the presence of $C_{16}E_{20}$ as a nonionic surfactant. These observations apparently revealed the presence of only spherical micelles under such experimental conditions.

The plot in **Figure 4.7** (representing η_o against 3,5-$Cl_2C_6H_3CO_2Na$) reveals the existence of two well-defined maxima in the absence of $C_{16}E_{20}$ at constant shear rate, 0.015 M CTABr and both 25 (□) and 35 °C (◊). These maxima appeared at specific values of [3,5-$Cl_2C_6H_3CO_2Na$], ([3,5-$Cl_2C_6H_3CO_2Na$]$_{sp}$); (i) 0.015 M (η_o = 31.2 mPas) and 0.040 M (η_o = 9.3 mPas) at 25 °C and (ii) 0.015 M (η_o = 13.5 mPas) and 0.040 M (η_o = 4.8 mPas) at 35 °C. It is clearly evident, therefore, that at both temperatures, the two maxima occurred at the same values of [3,5-$Cl_2C_6H_3CO_2Na$]$_{sp}$. But the increase in the temperature (from 25 to 35 °C) decreased the values of η_o from 31.2 to 13.9 mPas and 9.3 to 4.8 mPas, at respectively, 0.015 and 0.040 M values of [3,5-$Cl_2C_6H_3CO_2Na$]$_{sp}$.

Despite the fact that reports on the occurrence of maxima in the graph of shear viscosity against [MX] (for a solution of cationic surfactants) are almost common (Davies *et al.*, 2006; Dreiss, 2007; Lin *et al.*, 2009), the detailed explanation of the reaction for the source of those maxima has not yet been apprehended at the molecular level (Davies *et al.*, 2006; Ziserman *et al.*, 2009). Nonetheless, it has been accepted from previous reports (Abdel-Rahem, 2008; Davies *et al.*, 2006) that the appearance of these maxima (under such experimental conditions) is a sign of the presence of wormlike/twisted wormlike micelles in a solution. Contrarily, there was no existence of maxima (**Figure 4.7**) in the presence of mixed CTABr-$C_{16}E_{20}$ ($[CTABr]_T$ = 0.015 M and $[C_{16}E_{20}]_T$ = 0.006 M) at constant shear rate and both 25 (Δ) and 35 °C (○). But the values of η_o, not different from that of water, have also decreased due to the temperature variation from 25 to 35 °C.

Although specific ion effects on structural features of aqueous ionic surfactant aggregates have been known for the last nearly more than two decades and thousands of papers have been published, the basic forces responsible for such specific effect remain unclear both theoretically and experimentally (Romsted, 2007).

It is considered to be useful to develop reversible micelle-vesicle conversions by changing a physical parameter such as pH, temperature or pressure of the medium. Such approach might provide an understanding of fundamental principles of aqueous surfactants structural transitions from micelles to vesicles (Maeda *et al.*, 2006). The study described in this chapter reveals that the presence of 6 mM $C_{16}E_{20}$ has caused almost complete transformation of mixed vesicles and wormlike micelles to mere spherical micelles.

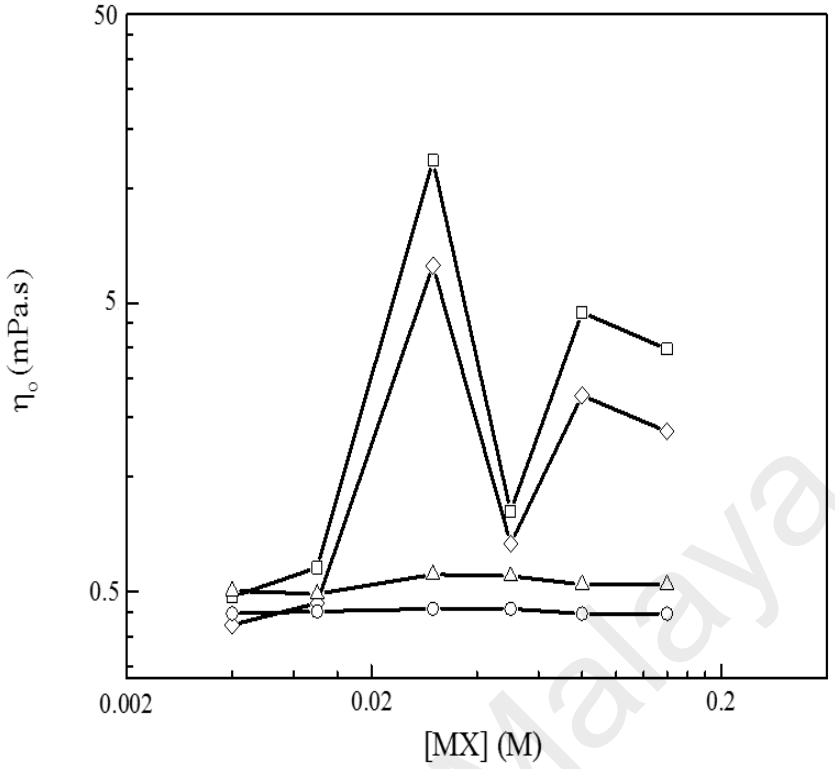

Figure 4.7: Plots representing zero shear viscosity (η_o at constant shear rate ($\dot{\gamma}$) against [3,5-$Cl_2C_6H_3CO_2Na$] with 0.015 M CTABr in the absence of $C_{16}E_{20}$ at 25 °C (□) and 35 °C (◊), and the presence of 0.006 M $C_{16}E_{20}$ at 25 °C (Δ) and 35 °C (○).

Similarly, the presence of 6 mM $C_{16}E_{20}$ reduced the values of R_X^{Br} or K_X^{Br} from 198 to 81**.** This is considered to be a quantitative correlation between the values of R_X^{Br} or K_X^{Br} and X-induced CTABr micellar growth. It is interesting to note that the similar effect of $C_{16}E_{20}$ could be observed (R_X^{Br} or K_X^{Br} = 102) at its concentration of 0.06 mM (**Table 4.3**).

4.5 Conclusion

Perhaps the most notable finding in this chapter is the reduction of the value of K_X^{Br} or R_X^{Br} from 198 to 78 due to presence of 0.06 mM $C_{16}E_{20}$ in the mixed aqueous solution containing 15 mM CTABr and different values of [NaX] with X = 3,5-$Cl_2C_6H_3CO_2^-$. The values of ${}^mK_X^{Br}$ or ${}^mR_X^{Br}$ remain independent of [$C_{16}E_{20}$] within the range of 0.06–15 mM. Varying the concentration of $C_{16}E_{20}$ could be a method to achieving changes in the structural as well as the viscoelastic behaviour of aqueous CTABr/$C_{16}E_{20}$/MX (MX = inert organic salt). It can be concluded that the nearly 2½-fold lower values of ${}^mR_X^{Br}$ or

$^{m}K_{X}^{Br}$ for the aqueous mixed CTABr/$C_{16}E_{20}$/3,5-$Cl_2C_6H_3CO_2Na$ micellar solution is related to the addition of a nonionic surfactant, $C_{16}E_{20}$. This quantitative correlation allows the prediction of structural behaviours of aqueous solutions of both pure CTABr and mixed CTABr-$C_{16}E_{20}$ surfactant at different [MX] on the basis of experimentally determined R_X^{Br} or K_X^{Br} values.

CHAPTER 5: KINETICS AND MECHANISM OF COUNTERIONIC SALT (4-$ClC_6H_4CO_2Na$)-CATALYZED PIPERIDINOLYSIS OF ANIONIC PHENYL SALICYLATE IN THE PRESENCE OF CATIONIC-NONIONIC MIXED MICELLES[3]

5.1 Introduction

Micelles (surfactant aggregates) have been drawing many attentions in nanoscience and nanotechnology fields of research for more than a century (Menger, 1979). Their numerous applications have been practiced, for instance, in district heating and cooling (DHC) systems as drag reducers (Ezrahi *et al.*, 2006; Yang, 2002) and petroleum industries (Walker, 2001). The structural growths in ionic micelles were believed to be dependent upon the strength of the counterion, X, binding to the cationic micelles (Oelschlaeger *et al.*, 2010; Rao *et al.*, 1987; Singh *et al.*, 2009). Kunz and his co-authors attempted to provide a qualitative correlation of X-induced micellar growth based upon the cationic micellar hydrophilic head and X interactions of Hofmeister anions (Kunz *et al.*, 2004). However, the limitations on the quantitative measurements of these bound counterions are yet to be solved (Geng *et al.*, 2006) especially when it comes to mixed surfactants systems. Perhaps it is worth to ask about the outcome of pure cationic micellar structure (example spherical, wormlike or vesicle) if nonionic surfactant (such as polyethylene glycol hexadecyl ether, $C_{16}E_{20}$) is added to the solution.

Several studies were published on the role of different inert salts in modifying the structural features of cationic micelles in aqueous solutions and, directly or indirectly, believed that these salts influence the micellar structural growth (Gravsholt, 1976; Harada *et al.*, 1988; Zhang *et al.*, 2007). In addition, some studies (Razak & Khan, 2013; Razak

[3]This chapter has been accepted for publication by *Progress in Reaction Kinetics and Mechanism;* ISI indexed Journal

et al., 2016; Yusof *et al.*, 2013) reported the possible quantitative correlations between the CTABr micellar binding constants and the counterion and/or temperature-induced micellar structural growth. These studies (Razak & Khan, 2013; Razak *et al.*, 2016; Yusof *et al.*, 2013) and some related ones (Khan, 1997b, 2010; Lajis & Khan, 1998) used semi empirical kinetic, SEK, method to determine the values of relative counterion binding constant, K_X^{Br} or R_X^{Br} (with $R_X^{Br} = K_X/K_{Br}$ where the values of CTABr micellar binding constants, K_{Br} and K_X, were derived from kinetic parameters obtained in the presence of micelles with different structural features) (Khan & Sinasamy, 2011). However, these reports lack information on the reliable mechanism(s) of the effects of nonionic surfactants in cationic micellar structural transition which opens up a possibility of optimising the use of mixed micelles in advanced technologies and industries nowadays (Yusof & Khan, 2013).

Khan reported (Khan, 2006) some studies where the data obtained for the cationic micellar mediated reactions were quantitatively correlated using several models. Davies and Foggo have also made a significant attempt to explain their findings (Davies & Foggo, 1998) on a mixed anionic-nonionic micellar system using Multiple Micellar Pseudo Phase (MMPP) models. In another report, Bunton and his co-authors have used the Pseudophase (PP) micellar model (Bunton *et al.*, 1993) to demonstrate on the reactions involving mixed cationic-nonionic micellar systems. This PP micellar model has been coupled with an empirical equation (**Eq. 3.1**) (Khan & Ismail, 2003) to treat the results of the present study.

We report, in this chapter; (i) the use of SEK method (described in detail elsewhere (Yusof & Khan, 2013)) and (ii) the rheometric observations, to correlate the relative counterion binding constants for CTABr/MX/H_2O solution (MX = 4-$ClC_6H_4CO_2Na$) systems and counterion-induced CTABr micellar structural growth in the presence of

$C_{16}E_{20}$ (CTABr/$C_{16}E_{20}$/MX/H_2O). The effort in providing some highlights on how the presence of nonionic surfactant, $C_{16}E_{20}$, influences the decrease in the mean values of relative counterion binding constant (K_X^{Br} or R_X^{Br}), as well as micellar structural growth, were also made. The observed results and their probable explanations are described in subsequent section.

5.2 Methodology

5.2.1 Reagents

All the reagents and chemicals used in section 3.2.1, except M_2X, were the same in this section. Their methods of preparations, as well as concentrations, were also the same. Another salt, MX = 4-$ClC_6H_4CO_2Na$, brought by Sigma-Aldrich with 99% purity, was used instead. The standard solutions of 0.2 M MX (4-$ClC_6H_4CO_2Na$) were prepared by adding 0.25 M NaOH to 0.2 M solution of 4-$ClC_6H_4CO_2H$ which was obtained from Sigma-Aldrich with 99% purity.

5.2.2 Kinetic and rheometric studies

The details of the kinetics and the rheometric studies are the same as in section 3.2.2 and 3.2.4 respectively.

5.2.3 Use of semi empirical kinetic, SEK, method for the determination of K_X^{Br} or R_X^{Br} for X = 4-$ClC_6H_4CO_2^-$

The details are the same as in section 3.2.3.

5.3 Results

5.3.1 5.3.1 Effect of [4-$ClC_6H_4CO_2Na$] on k_{obs} for the reaction of Pip with PS^- at constant concentration of pure CTABr and 35 °C

The kinetic investigations on the effects of [4-$ClC_6H_4CO_2Na$] on k_{obs} for the reaction of 0.10 M Pip, 0.20 mM PSH, in the presence of 0.006 M CTABr and different

concentrations of 4-$ClC_6H_4CO_2Na$ (0.00–0.20 M) were carried out at constant 0.03 M NaOH, 35 °C and 370 nm. Similar observations were obtained by increasing the concentration of CTABr to 0.010 and 0.015 M. The values of k_{obs} obtained are presented in **Table 5.1.**

5.3.2 Effect of [4-$ClC_6H_4CO_2Na$] on k_{obs} for the reaction of Pip with PS^- at constant concentration of pure $C_{16}E_{20}$ and 35 °C

Several kinetic runs for the reaction of 0.10 M Pip with 0.20 mM PS^- at various concentrations of 4-$ClC_6H_4CO_2Na$ (within the range of 0.00–0.20 M) and constant 0.030 M NaOH, and 0.001 M $C_{16}E_{20}$ were carried out. Similar observations were obtained by increasing $[C_{16}E_{20}]_T$ to 0.003, 0.006, 0.008, 0.010, and 0.015 M. The observed data, k_{obs} versus [4-$ClC_6H_4CO_2Na$] as well as δ_{app} and A_∞, at $[C_{16}E_{20}]_T$ = 0.001, 0.003, 0.006, 0.008, 0.010 and 0.015 M are presented, respectively, as **Appendices G** and **H** in the Appendix.

5.3.3 Effect of [4-$ClC_6H_4CO_2Na$] on k_{obs} for the reaction of Pip with PS^- in the presence of mixed CTABr-$C_{16}E_{20}$ at 35 °C

Other sets of kinetic experiments were also conducted at constant 0.10 M Pip, 0.20 mM PS^- and 0.03 M NaOH in the presence of CTABr ($[CTABr]_T$ = 0.006) at different [4-$ClC_6H_4CO_2Na$] (0.00–0.20 M). The concentrations of $C_{16}E_{20}$ were 0.006, 0.010 and 0.015 M. Similar results were obtained upon increasing $[CTABr]_T$ to 0.010 and 0.015 M and the sketches of k_{obs} against [4-$ClC_6H_4CO_2Na$] are presented in **Figures 5.1, 5.2** and **5.3,** respectively.

5.3.4 Rheological behavior of aqueous pure CTABr and mixed CTABr-$C_{16}E_{20}$ micelles in the presence of various [4-$ClC_6H_4CO_2Na$] at 25 and 35 °C

Two different rheometric investigations were conducted in the presence of pure CTABr (0.015 M) and mixed CTABr-$C_{16}E_{20}$ (0.015 M CTABr + 0.006 M $C_{16}E_{20}$)

micelles at different [4-$ClC_6H_4CO_2Na$]. Both were in aqueous solutions of 0.1 M Pip, 0.2 mM PSH and 0.03 M NaOH. The experiments were achieved at the steady shear rheological response, 25 and 35 °C. Various values of shear viscosity at various shear rates were determined and the results are presented in **Figures 5.4 (a)** and **(b)** (in the presence of pure CTABr) and **Figures 5.5 (a)** and **(b)** (in the presence mixed CTABr-$C_{16}E_{20}$).

Table 5.1: Values of observed pseudo-first-order rate constant, k_{obs}, obtained for the piperidinolysis of PS^- at 0.006, 0.010 and 0.015 M CTABr and different [4-$ClC_6H_4CO_2Na$].[a]

[MX][b] M	[CTABr]$_T$[c] = 0.006 M		0.010 M		0.015 M	
	$10^4\ k_{obs}$[d] s^{-1}	$10^4\ k_{calcd}$ s^{-1}	$10^4\ k_{obs}$[d] s^{-1}	$10^4\ k_{calcd}$ s^{-1}	$10^4\ k_{obs}$[d] s^{-1}	$10^4\ k_{calcd}$ s^{-1}
0.000	24.1 ± 0.4[e]		21.2 ± 0.3[e]		21.9 ± 0.2[e]	
0.001	23.2 ± 0.2		20.9 ± 0.4		20.8 ± 0.3	
0.002	21.7 ± 0.4		19.8 ± 0.3		20.8 ± 0.3	
0.004	26.7 ± 0.3		19.9 ± 0.3		20.4 ± 0.2	
0.006	28.7 ± 0.4		20.9 ± 0.4		20.6 ± 0.1	
0.008	39.5 ± 0.4		21.4 ± 0.3		20.7 ± 0.3	
0.010	52.7 ± 0.5		25.3 ± 0.4		21.5 ± 0.2	
0.015	84.5 ± 0.5	82.4[f]	43.3 ± 0.4	82.4[f]	36.7 ± 0.3	
0.020	99.0 ± 0.7	103.1	57.4 ± 0.3	103.1	48.1 ± 0.3	43.6[f]
0.025	120.7 ± 0.7	118.4	68.6 ± 0.3	118.4	54.9 ± 0.3	56.2
0.030	129.3 ± 0.9	130.2	77.9 ± 0.6	130.2	63.8 ± 0.3	67.1
0.040	141.6 ± 1.3	147.3	93.5 ± 0.4	147.3	82.4 ± 0.3	84.9
0.050	158.5 ± 1.7	159.0	107.4 ± 0.6	159.0	96.0 ± 0.6	99.0
0.060	169.7 ± 1.8	167.6	123.9 ± 1.3	167.6	112.4 ± 0.9	110.3
0.070	178.3 ± 1.3	174.1	135.6 ± 1.0	174.1	120.8 ± 0.5	119.6
0.080	182.4 ± 1.6	179.2	143.5 ± 1.4	179.2	128.8 ± 1.1	127.4
0.100	188.1 ± 1.9	186.8	155.1 ± 1.3	186.8	142.7 ± 1.6	139.7
0.150	193.8 ± 1.2	197.6	165.9 ± 1.3	197.6	160.8 ± 1.8	159.4
0.200	202.3 ± 2.4	203.3	172.6 ± 1.2	203.3	166.5 ± 1.1	171.0

[a]$[PSH]_0$ = 0.20 mM, [Pip] = 0.10 M, [NaOH] = 0.03 M, λ = 370 nm and aqueous reaction mixture for each kinetic run contains 2% v/v acetonitrile. [b]Total concentration of 4-$ClC_6H_4CO_2Na$. [c]Total concentration of CTABr. [d]Observed pseudo first order rate constant. [e]Error limits are standard deviations. [f]Values of pseudo first order rate constant calculated from **Eq. 3.13.**

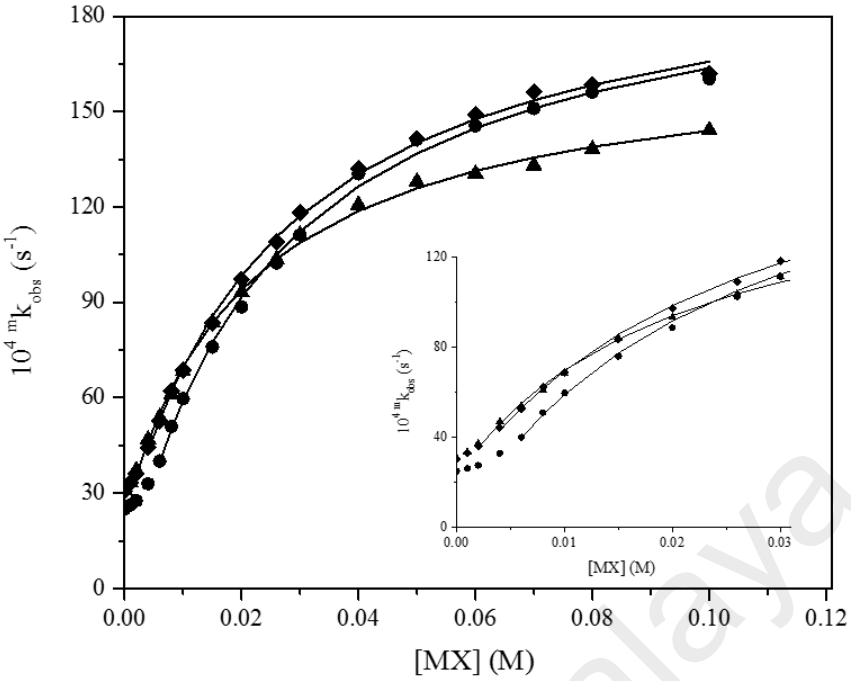

Figure 5.1: Plots showing the relationship between $^mk_{obs}$ (where superscript "m" represents mixed micelles) and [MX], MX = 4-$ClC_6H_4CO_2Na$, for the reaction of Pip and PS^- at three different constant $[CTABr]_T + [C_{16}E_{20}]_T$/M = 0.006 + 0.006 (●), 0.006 + 0.010 (♦) and 0.006 + 0.015 (▲), and 35 °C. The solid lines are drawn via the calculated values of the rate constant (k_{calcd}). Insert: The plots for magnified scale for the data points at lower values of [MX].

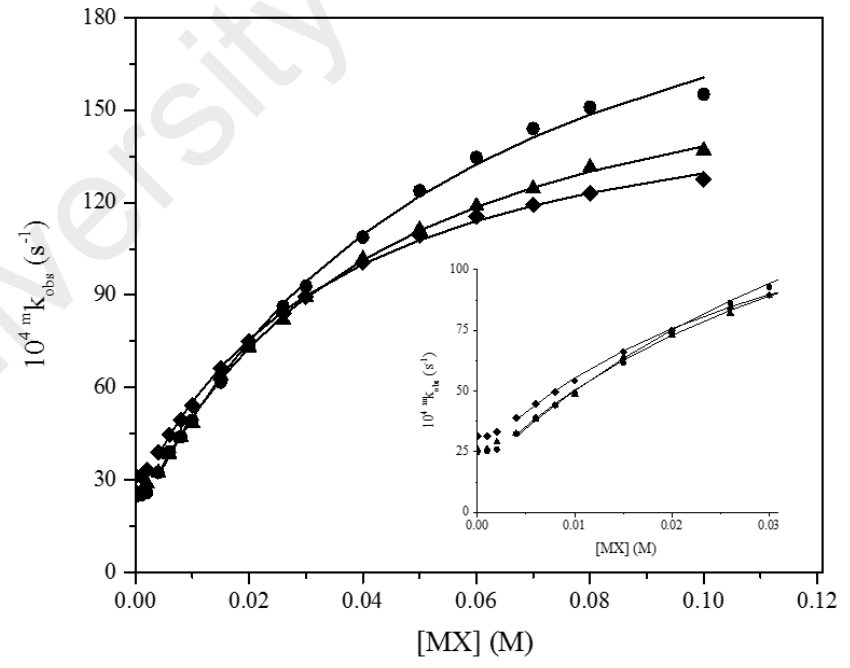

Figure 5.2: Plots showing the relationship between $^mk_{obs}$ (where superscript "m" represents mixed micelles) and [MX], MX = 4-$ClC_6H_4CO_2Na$, for the reaction of Pip and PS^- at three different constant $[CTABr]_T + [C_{16}E_{20}]_T$/M = 0.010 + 0.006 (●), 0.010 + 0.010 (♦) and 0.010 + 0.015 (▲), and 35 °C. The solid lines are drawn via the calculated values of the rate constant (k_{calcd}). Insert: The plots for magnified scale for the data points at lower values of [MX].

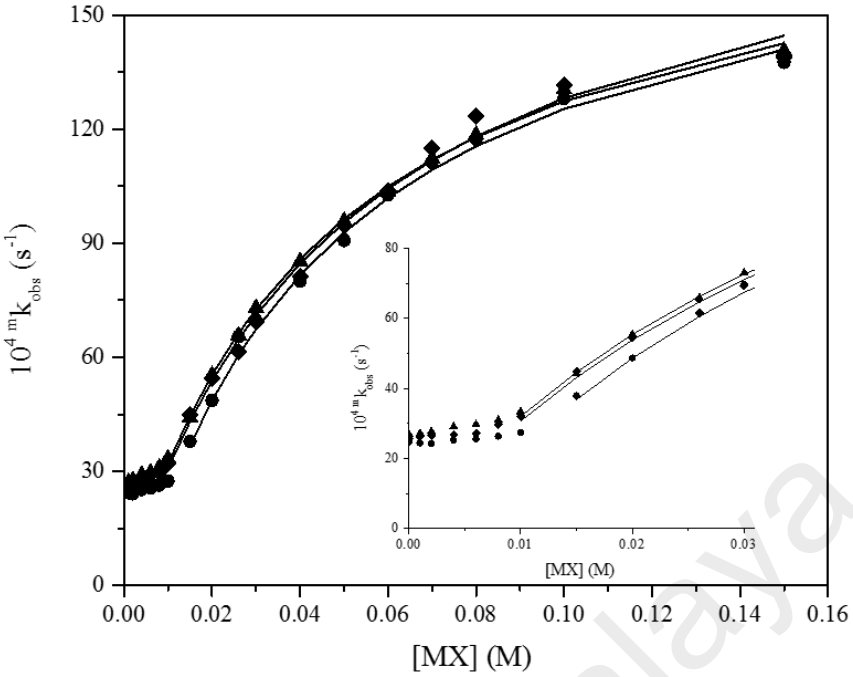

Figure 5.3: Plots showing the relationship between $^mk_{obs}$ (where superscript "m" represents mixed micelles) and [MX], MX = 4-$ClC_6H_4CO_2Na$, for the reaction of Pip and PS^- at three different constant $[CTABr]_T$ + $[C_{16}E_{20}]_T$/M = 0.015 + 0.006 (●), 0.015 + 0.010 (♦) and 0.015 + 0.015 (▲), and 35 °C. The solid lines are drawn via the calculated values of the rate constant (k_{calcd}). Insert: The plots for magnified scale for the data points at lower values of [MX].

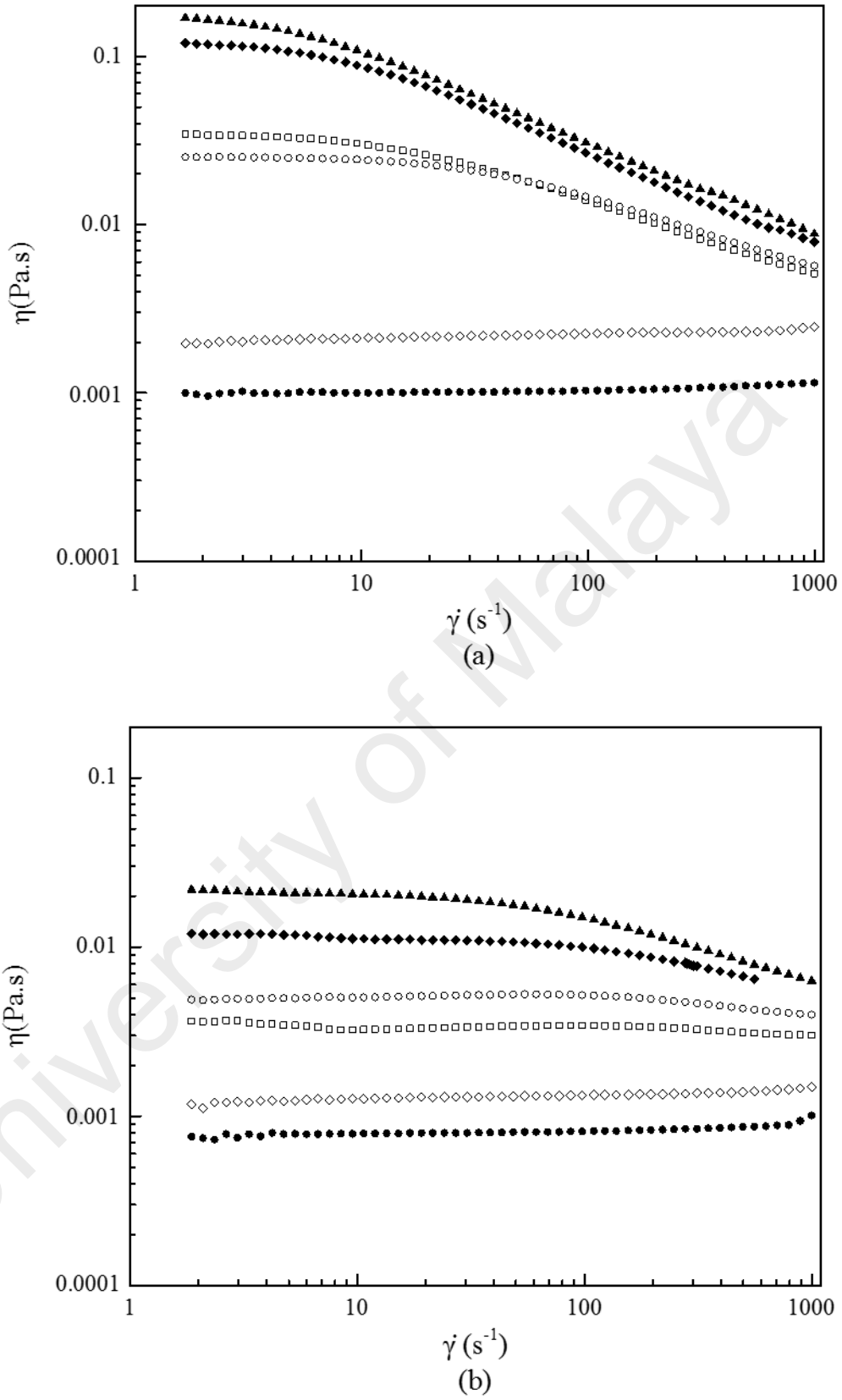

Figure 5.4: Graphs of shear viscosity (η) against shear rate (γ̇) for the piperidinolysis of PS^- containing 0.015 M CTABr and [4-$ClC_6H_4CO_2Na$]/M = **(a)** 0.008 (•) 0.015 (□) 0.030 (▲) 0.050 (♦) 0.080 (○) and 0.150 (◊) at 25 °C and **(b)** 0.008 (•) 0.015 (□) 0.030 (▲) 0.050 (♦) 0.080 (○) and 0.150 (◊) at 35 °C.

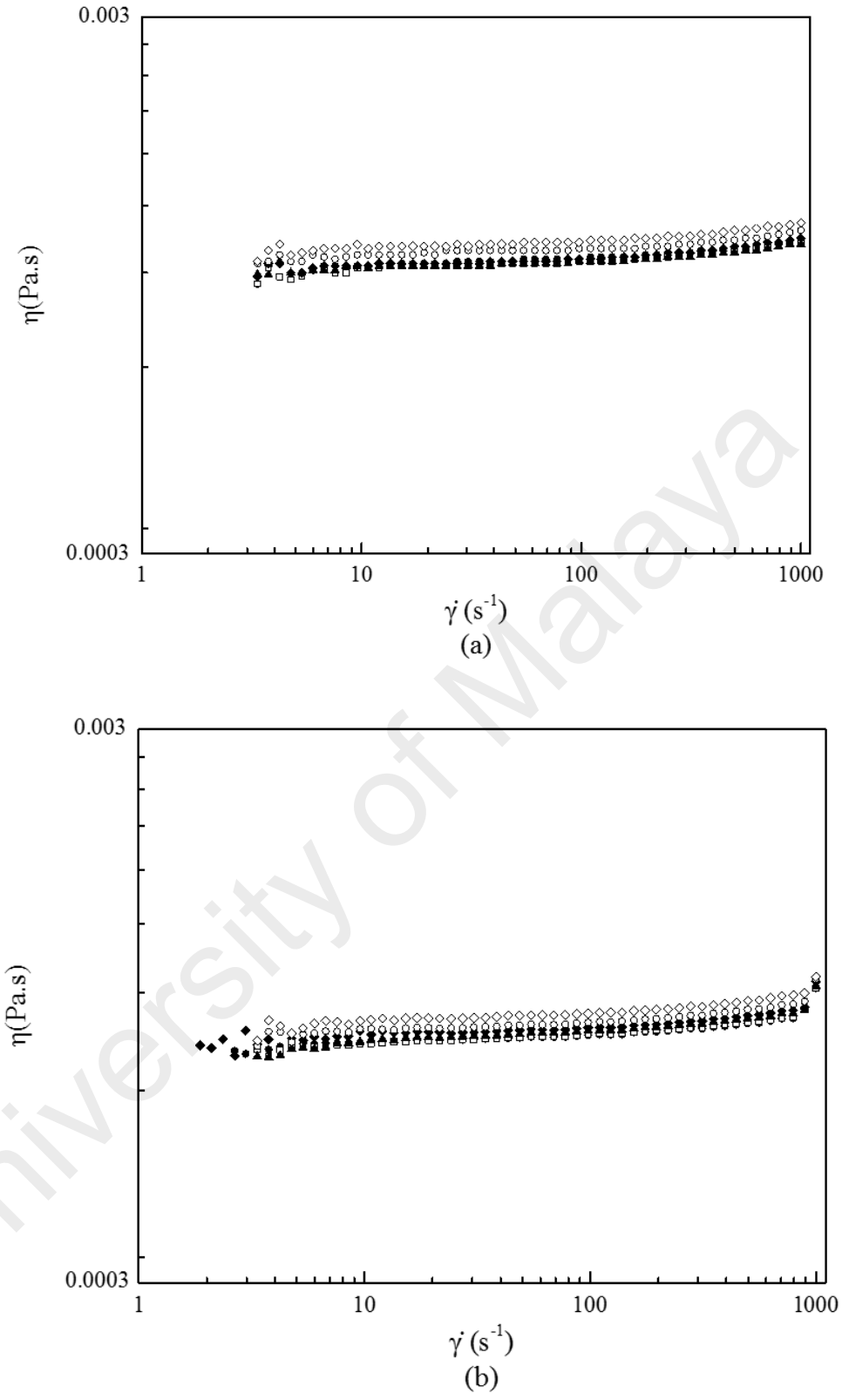

Figure 5.5: Graphs of shear viscosity (η) against shear rate (γ̇) for the piperidinolysis of PS^- containing 0.015 M CTABr, 0.006 M $C_{16}E_{20}$ and [4-$ClC_6H_4CO_2Na$]/M = **(a)** 0.008 (•) 0.015 (□) 0.030 (▲) 0.050 (♦) 0.080 (○) and 0.150 (◊) at 25 °C and **(b)** 0.008 (•) 0.015 (□) 0.030 (▲) 0.050 (♦) 0.080 (○) and 0.150 (◊) at 35 °C.

5.4 Discussion

5.4.1 Explanation of kinetic observations for the reaction of pip with PS^- in the presence of pure $C_{16}E_{20}$ at various [4-$ClC_6H_4CO_2Na$] and 35 °C

The results obtained showed similar effect as explained in section 3.4.1 and the values of kinetic parameters are presented in **Table 5.2.**

Table 5.2: Values of kinetic parameters for the reaction of Pip and PS^- in the presence of 4-$ClC_6H_4CO_2Na$ at different $[C_{16}E_{20}]_T$ and 35 °C.[a]

$[C_{16}E_{20}]_T$[b] M	k_{obs}^0[c] s^{-1}	$k_{obs}^{MX\ (max)}$[d] s^{-1}	%NSE[e]
0.001	288	202	30
0.003	277	226	18
0.006	265	233	12
0.008	235	208	11
0.010	197	205	-
0.015	160	178	-

[a]$[PSH]_0$ = 0.20 mM, [NaOH] = 0.03 M, [Pip] = 0.10 M, λ = 370 nm and aqueous reaction mixture for each kinetic run contains 2% v/v acetonitrile. [b]Total cncentration of $C_{16}E_{20}$. [c]k_{obs}^0 = k_{obs} at [MX] = 0 (or average value of similar values of k_{obs} at various [MX]). [d]$k_{obs}^{MX\ (max)}$ = k_{obs} at maximum value of [MX]. [e]Percent negative salt effect, %NSE caculated from **Eq. 3.12.**

5.4.2 Explanation of the effect of [4-$ClC_6H_4CO_2Na$] on k_{obs} for piperidinolysis of PS^- in the presence of pure CTABr and mixed CTABr-$C_{16}E_{20}$ micelles

The values of observed pseudo first order rate constants, k_{obs}, for the reaction of 0.10 M Pip with 0.20 mM PS^- (at 35 °C and 370 nm) and varying values of [MX] (MX = 4-$ClC_6H_4CO_2Na$) in the presence of constant concentration of pure CTABr and mixed CTABr-$C_{16}E_{20}$ were found to fit to **Eq. 3.13**. Various values of k_0 were obtained in the presence of different concentrations of pure CTABr as well as mixed CTABr-$C_{16}E_{20}$ at [MX] = 0 (**Tables 5.3** and **5.4**). To differentiate between the parameters determined in a

pure CTABr and mixed CTABr-$C_{16}E_{20}$ micellar systems, a small letter "m" is used as a superscript to represent those obtained in the presence of mixed CTABr-$C_{16}E_{20}$ micelles as elaborated in section 3.4.2. The values of $[MX]_0^{op}$ obtained in the presence of both pure CTABr and mixed CTABr-$C_{16}E_{20}$ are presented, respectively, in **Tables 5.3** and **5.4.**

The values of $F_{X/S}$ were obtained from **Eq. 3.14** and are summarized in **Tables 5.3** and **5.4** while the values of $K_{X/S}$ were determined by the use of **Eq. 3.15** as in section 3.4.2. These calculated values of $K_{X/S}$ are shown in **Table 5.3.**

The relationship between the normalized values of $K_{X/S}$ ($K^n_{X/S} = F_{X/S}/ K_{X/S}$) and $K_{Br/S}$ ($K^n_{Br/S} = F_{Br/S}/ K_{Br/S}$) are discussed in section 3.4.2. The calculated values of $K^n_{X/S}$, presented in **Table 5.3**, and the previously reported value of $K^n_{Br/S}$ (= 25 M^{-1}**)** (Khan, 1997a; Khan *et al.*, 2000; Khan & Ismail, 2007), were used to calculate the values of relative counterion binding constants, K^{Br}_X, (Khan, 2010) using **Eq. 3.16.** Similarly, the values of R^{Br}_X were calculated from **Eq. 3.17** and the calculated values of $({}^nK_{X/S})^{nsp}$ and $({}^nK_{Br/S})^{sp}$ in **Table 5.3.** These calculated values of K^{Br}_X or R^{Br}_X at $[CTABr]_T$ = 0.006, 0.010 and 0.015 M are also presented in **Table 5.3** and their mean value (= 50.3) was found to be almost similar to the recently reported one (= 47.9) where the same inert organic salt (4-$ClC_6H_4CO_2Na$) was used (Yusof & Khan, 2013). As explained in section 3.4.2, the values of ${}^mK_{X/S}$ could not be calculated due to the fact that the values of ${}^mK^0_S$ for mixed CTABr-$C_{16}E_{20}$ surfactants are not available for the present study. Hence, **Eq. 3.20** should be used for the calculation of ${}^mK^{Br}_X$. In addition, the values of ${}^mR^{Br}_X$ were calculated using **Eq. 3.21** and are presented in **Table 5.3.**

It is noteworthy that the values of ${}^mK^{Br}_X$ or ${}^mR^{Br}_X$ in the presence of mixed CTABr-$C_{16}E_{20}$ micelles (**Table 5.4**) were found to be independent of Y ($Y = [CTABr]_T/[C_{16}E_{20}]_T$) and their mean value (= 22) is 2.3-fold lower than that in the presence of pure CTABr

micelles **(=** 50**)**. This significant decrease is, perhaps, due to the existence of the bulky hydrated headgroups of $C_{16}E_{20}$ which results in the hydration of cationic CTABr surfactant headgroups and consequently yielding relatively more hydrated bulky CTABr micellar phase. Thus, causing the larger sized hydrophilic head of $C_{16}E_{20}$ to cover the smaller sized headgroup of CTABr surfactants in mixed micelles (Gao *et al.*, 2002).

5.4.3 5.4.3 Explanation of rheological behaviours for the reaction of Pip with PS^- in the presence of pure CTABr and mixed CTABr-$C_{16}E_{20}$ micelles at various [4-$ClC_6H_4CO_2Na$]

From the rheometric information presented in **Figures 5.4 (a)** (at 25 °C) and **(b)** (at 35 °C), the two flow curves obtained at the lower value of [4-$ClC_6H_4CO_2Na$] (0.008 M) and the higher [4-$ClC_6H_4CO_2Na$] (0.15 M) show non-Newtonian fluid characteristics (mild shear thickening behaviors) at the higher values of shear rates, which may be due to "Taylor's effect". This is the characteristic features of spherical micelles, with relative lower values of shear viscosity (η) (Qiao *et al.*, 2011). It has been recorded elsewhere (Acharya & Kunieda, 2006) that in a solution of ionic wormlike micelles containing certain salt, its viscoelastic nature could be changed at very high or low concentration of the added salt. However, the remaining four flow curves (at 0.015, 0.030, 0.050, and 0.15 M [4-$ClC_6H_4CO_2Na$]) with relatively higher values of η revealed Newtonian fluid characteristics at the lower shear rate and show shear thinning behaviours at the relatively higher shear rate. This behavior is attributed to possibility of the presence of wormlike micelles (Lu *et al.*, 2008). **Figures 5.5** (a) and **(b)** shows a contrasting result in which all the flow curves exhibit a mild shear thickening behavior at a very low shear viscosity and high shear rate which is merely due to Taylor's effect. This is a characteristic of spherical micelles and is directly related to the presence of a nonionic surfactant, $C_{16}E_{20}$ (Carver *et al.*, 1996).

The plots of values of zero shear viscosity, η_o, against different concentrations of 4-$ClC_6H_4CO_2Na$ are presented in **Figure 5.6**. Single symmetric maximum (η_o = 174.1 mPas) was obtained in the presence of pure CTABr micelles ($[CTABr]_T$ = 0.015 M and $[C_{16}E_{20}]_T$ = 0) at [4-$ClC_6H_4CO_2Na$] = 0.03 M and 25 °C (□). Increasing the temperature to 35 °C (◊) provided similar results (maximum at [4-$ClC_6H_4CO_2Na$] = 0.03 M) with decrease in the value of η_o (η_o = 21.4 mPas). These maxima indicate the possible existence of wormlike micelles (Abdel-Rahem, 2008; Davies *et al.*, 2006). As discussed earlier in this section, at very low [4-$ClC_6H_4CO_2Na$] (0.008 M) and high (0.15 M) with their respective values of η_o as 1.00 and 1.97 mPas, there were characteristic features of spherical micelles (Acharya & Kunieda, 2006) when the temperature was 25 °C (□). Increasing the temperature to 35 °C (◊) has also provided similar results with the decrease in the values of η_o from 1.00 and 1.97 mPas to 0.80 and 1.18 mPas, respectively.

In the presence of mixed CTABr-$C_{16}E_{20}$ ($[CTABr]_T$ = 0.015 M and $[C_{16}E_{20}]_T$ = 0.006 M), on the other hand, no maximum was observed at various values of [4-$ClC_6H_4CO_2Na$] (0.008, 0.015, 0.030, 0.050, 0.080, and 0.150 M) and both t 25 (Δ) and 35 °C (○).

Table 5.3: Values of empirical constants, θ, and $K^{X/S}$ obtained using **Eqs. 3.13 and 3.14** with the $[MX]_0^{op}$ values for MX = 4-$ClC_6H_4CO_2Na$ at different $[CTABr]_T$.[a]

$[CTABr]_T$ M	$10^4\ k_0$[c] s^{-1}	$[MX]_0^{op}$ M	$10^3\ \theta$ s^{-1}	$K^{X/S}$ M^{-1}	$F_{X/S}$	$K_{X/S}$ M^{-1}	$K^n_{X/S}$ M^{-1}	K_X^{Br}
0.*006*[b]	24.1 ± 0.4[d]	0.0065	22.2 ± 0.3[d]	49.1 ± 2.4[d]	0.69[e]	2111[f]	1456.8[g]	58[h]
0.010	21.2 ± 0.3	0.0100	21.4 ± 0.6	22.2 ± 1.6	0.67	1576	1056.1	42
0.015	21.9 ± 0.2	0.0129	21.6 ± 0.5	17.8 ± 1.1	0.67	1887	1264.2	51

[a] $[PSH]_0$ = 0.20 mM, [NaOH] = 0.03 M, [Pip] = 0.10 M, λ = 370 nm and aqueous reaction mixture for each kinetic run contains 2% v/v acetonitrile. [b]Total concentration of CTABr [c] $k_o = k_{obs}$ at [MX] = 0. [d]Limits of error signifies standard deviations. [e] $F_{X/S} = \theta/k_W^{MX}$ where $k_W^{MX} = k_W^2[pip]_T = k_{obs}$ at $[CTABr]_T = 0$ and the value of k_W^2, under such conditions is 0.322 $M^{-1}s^{-1}$. [f] $K_{X/S} = K^{X/S}(1+ K_S^0[CTABr]_T)$, where $K_S^0 = 7 \times 10^3\ M^{-1}$ (Khan & Arifin, 1996). [g] $K^n_{X/S} = F_{X/S}K_{X/S}$. [h] $K_X^{Br} = K^n_{X/S}/ K^n_{Br/S}$, where $K^n_{Br/S} = 25\ M^{-1}$ (Khan, 2010).

Table 5.4: Values of empirical constants, $^{m}\theta$ and $^{m}K^{X/S}$, obtained using **Eqs. 3.13 and 3.14** with the $[MX]_0^{op}$ values for MX = 4-$ClC_6H_4CO_2Na$ at different concentrations of mixed CTABr-$C_{16}E_{20}$.[a]

$[CTABr]_T$ M	$[C_{16}E_{20}]_T$[c] M	$10^4\ ^{m}k_0$[d] s^{-1}	$^{m}[MX]_0^{op}$ M	$10^3\ ^{m}\theta$ s^{-1}	$^{m}K^{X/S}$ M^{-1}	$^{m}F_{X/S}$	$^{m\ n}K^{X/S}$ M^{-1}	$^{m\ n}K^{Br/S}$[h] M^{-1}	$^{m}K_X^{Br}$ or $^{m}R_X^{Br}$
0.006[b]	0.006	25.0 ± 0.3[e]	0.00350	20.4 ± 0.4[e]	36.1 ± 2.0[e]	0.85[f]	30.7[g]	1.4[i]	21.9[j]
0.006	0.010	30.6 ± 0.4	0.00182	20.5 ± 0.2	35.0 ± 1.3	1.06	37.1	2.2[i]	16.9
0.006	0.015	31.0 ± 0.5	0.00109	17.0 ± 0.2	44.6 ± 1.7	0.92	41.0	1.8[i]	22.8
0.010	0.006	24.9 ± 0.4	0.00223	24.3 ± 0.8	16.8 ± 1.1	1.01	17.0	1.0[i]	17.0
0.010	0.010	31.3 ± 0.5	0.00201	16.6 ± 0.2	27.4 ± 0.8	0.86	23.6	1.1[i]	21.5
0.010	0.015	26.1 ± 0.4	0.00233	18.8 ± 0.2	23.0 ± 0.6	1.02	23.5	0.9[i]	26.1
0.015	0.006	24.7 ± 0.2	0.01065	18.6 ± 0.4	18.7 ± 1.1	0.78	14.6	0.8[i]	18.3
0.015	0.010	25.7 ± 0.3	0.00820	19.4 ± 0.8	17.0 ± 1.7	1.00	17.0	0.6[i]	28.6
0.015	0.015	26.9 ± 0.3	0.00820	18.7 ± 0.4	18.3 ± 0.9	0.98	17.9	0.8[i]	22.4

Footnote *a* and *b* are the same as in **Table 5.3.** [c]Total concentration of $C_{16}E_{20}$. [d] $^{m}k_0 = k_{obs}$ at [MX] = 0. [e]Limits of error signifies standard deviations. [f] $^{m}F_{X/S} = {}^{m}\theta/{}^{m}k_{obs}^{W}$; with $^{m}k_{obs}^{W} = {}^{m}k_{obs}$ ($= {}^{m}k_W^2[Pip]_T$) = 240 x 10^{-4}, 193.2 x 10^{-4} and 184.2 x 10^{-4} s^{-1} at constant $[C_{16}E_{20}]_T$ (0.006, 0.010 and 0.015 M $[C_{16}E_{20}]$, respectively) and [MX] = [CTABr] = 0. [g] $^{m\ n}K^{X/S} = {}^{m}F_{X/S}{}^{m}K^{X/S}$. [h] $^{m\ n}K^{Br/S} = {}^{m}F_{Br/S}{}^{m}K^{Br/S}$ for MX = NaBr. [i]Data are obtained from reference (Fagge *et al.*, 2016). [j] $^{m}K_X^{Br}$ or $^{m}R_X^{Br} = {}^{m\ n}K^{X/S}/{}^{m\ n}K^{Br/S}$.

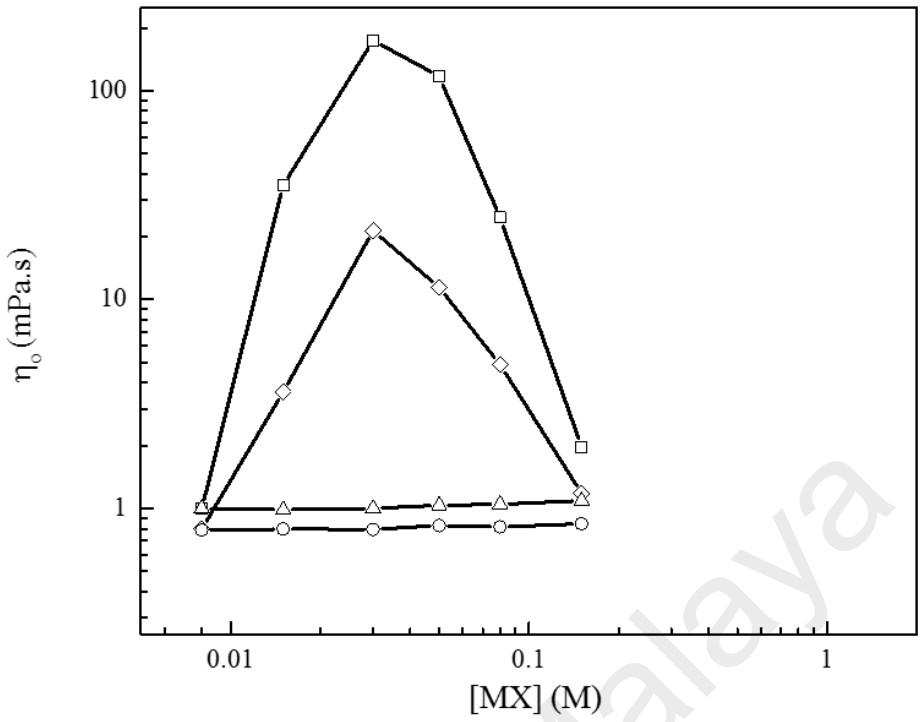

Figure 5.6: Plots of zero shear viscosity (η_o) against [4-$ClC_6H_4CO_2Na$] at a constant shear rate ($\dot{\gamma}$) with 0.015 M CTABr in the absence of $C_{16}E_{20}$ at 25 °C (□) and 35 °C (◊), and the presence of 0.006 M $C_{16}E_{20}$ at 25 °C (Δ) and 35 °C (○).

5.5 Conclusion

The mean values of relative counterion (4-$ClC_6H_4CO_2^-$) binding constants (K_X^{Br} or R_X^{Br}) in the present study (K_X^{Br} or R_X^{Br} = 50) and that of previously reported article (K_X^{Br} or R_X^{Br} = 47) for aqueous CTA^+/4-$ClC_6H_4CO_2^-$ is reduced to more than ½-fold ($^mK_X^{Br}$ or $^mR_X^{Br}$ = 22) when $C_{16}E_{20}$ (0.006 to 0.015 M) is added to the solution (CTA^+/$C_{16}E_{20}$/4-$ClC_6H_4CO_2^-$). Though wormlike micelles were found in aqueous CTA^+/4-$ClC_6H_4CO_2^-$ ($[CTABr]_T$ = 0.015 M) solution, spherical micelles also existed at very high and low concentrations of 4-$ClC_6H_4CO_2Na$ (which were revealed in CTA^+/$C_{16}E_{20}$/4-$ClC_6H_4CO_2^-$ solution). The significantly new findings in this chapter are; (i) K_X^{Br} or R_X^{Br} for 4-$ClC_6H_4CO_2^-$ in aqueous CTABr micellar solution could be reduced when certain amount of nonionic surfactant with larger sized hydrophilic tail is added (ii) 4-$ClC_6H_4CO_2^-$-induced CTABr micellar structural growth and viscoelasticity could skilfully be managed, not only by changing the counterion, X^-, (for instance 4-$ClC_6H_4CO_2^-$), pH, etc.,

but also by the addition of nonionic surfactant, such as $C_{16}E_{20}$. It is, therefore, concluded that the addition of small amount of $C_{16}E_{20}$ influences, significantly, the CTABr micellar structural transition.

CHAPTER 6: CONCLUSIONS AND FUTURE DIRECTIONS

6.1 Conclusion

The present research highlights the effect of polyethylene glycol hexadecyl ether, a nonionic surfactant ($C_{16}E_{20}$), on the relative counterion binding constants, K_X^{Br} or R_X^{Br}, and counterion-induced hexadecyltrimethylammonium bromide, CTABr, micellar structural growth. The semi empirical kinetics technique was used to correlate the values of K_X^{Br} or R_X^{Br} with the micellar structural behaviours. The data are ascertained by the rheometric results obtained in the second part of the experiments. The nonionic surfactant, as extensively discussed in chapter 3, 4, and 5, has been found to play an important role in the decrease of the values of K_X^{Br} or R_X^{Br}, as well as changes in the CTABr micellar structure.

The mean values of K_X^{Br} or R_X^{Br}, for CTABr/MX/H_2O, in the presence of different halo-substituted benzoate salts with counterions, X = 2-$NaOC_6H_4CO_2^-$, 3,5-$Cl_2C_6H_3CO_2^-$, and 4-$ClC_6H_4CO_2^-$ are, respectively, 42, 198, and 50. The mean values of K_X^{Br} or R_X^{Br} for CTABr/$C_{16}E_{20}$/MX/H_2O significantly dropped to 16 (X = 2-$NaOC_6H_4CO_2^-$**),** 78 (for X = 3,5-$Cl_2C_6H_3CO_2^-$**),** and 22 (for X = 4-$ClC_6H_4CO_2^-$) due to the presence of nonionic surfactant, $C_{16}E_{20}$. The rheometric investigations have been used in ascertaining the viscoelastic behaviours and structure of $CTA^+/X^-/H_2O$ micelles at $[CTABr]_T$ = 0.015 M, and the existence of wormlike micelles were obtained in the absence of $C_{16}E_{20}$. But the $CTA^+/C_{16}E_{20}/X^-/H_2O$ solution showed the presence of spherical micelles at $[CTABr]_T$ = 0.015 M and $[C_{16}E_{20}]_T$ = 0.006 M. It is now concluded that addition of a relatively small amount of nonionic surfactant (for instance $[C_{16}E_{20}]_T \geq 0.006$ M) to an aqueous solution of cationic CTABr surfactant could be a method of to change the CTABr micellar structure.

The new and interesting outcomes of this research work are; (i) The experimentally determined values of K_X^{Br} or R_X^{Br} for counterions 2-$NaOC_6H_4CO_2^-$, 3,5-$Cl_2C_6H_3CO_2^-$, and 4-$ClC_6H_4CO_2^-$ in the presence of mixed cationic-nonionic surfactants (CTABr-$C_{16}E_{20}$)−values were found to be significantly lower than those determined in the presence of pure CTABr micelles. (ii) The observations noted the quantitative correlation of the values of K_X^{Br} or R_X^{Br} obtained with the counterions-induced CTABr micellar structural change from wormlike (in $CTA^+/X^-/H_2O$ solution) to spherical (in $CTA^+/C_{16}E_{20}/X^-/H_2O$ solution). This correlation has been used to predict the cationic CTABr micellar structure (at $[CTABr]_T$ range of 0.006–0.015 M) and its counterion-induced structural changes in the presence of 0.006–0.015 M $[C_{16}E_{20}]_T$ at different values of certain inert salts. It has also been noted, perhaps for the first time, that the values of K_X^{Br} or R_X^{Br} are quantitatively correlated to the counterion-induced CTABr micellar structural changes (and ascertained by the rheometric evidence) in the presence of a nonionic surfactant, $C_{16}E_{20}$.

6.2 Future Directions

The present research focused on the influence of one nonionic surfactant on the relative counterion binding constant of cationic micelles and their induced micellar growth. It has also limited to three benzoate salts. The experiments conducted were kinetic and rheometric measurements using respectively, UV-Visible spectrophotometer and rheometer

It is recommended that the direction of future work should be towards the addition of other nonionic surfactants, with similar properties to $C_{16}E_{20}$ (those whose hydrophilic group is a polyethylene glycol chain), on CTABr micellar system. Studies on relative counterion binding constants, in the presence of different surfactant-cosurfactant combination, are also highly recommended. Different experiments such as cryo-TEM, SANS, etc and other benzoate salts should also be included in future studies.

REFERENCES

Abdel-Rahem, R. (2008). The influence of hydrophobic counterions on micellar growth of ionic surfactants. *Advances in Colloid and Interface Science, 141*(1), 24-36.

Abdel-Raouf, M., Maysour, N., Abdul-Raheim, A., El-Saeed, S. M., & Farag, R. (2011). Synthesis and study of the surface properties of alkylnaphthalene and alkylphenanthrene sulfonates. *Journal of Surfactants and Detergents, 14*(1), 23-30.

Abuin, E. B., Lissi, E., Araujo, P. S., Aleixo, R. M., Chaimovich, H., Bianchi, N., . . . Quina, F. H. (1983). Selectivity coefficients for ion exchange in micelles of hexadecyltrimethylammonium bromide and chloride. *Journal of Colloid and Interface Science, 96*(1), 293-295.

Acharya, D. P., & Kunieda, H. (2006). Wormlike micelles in mixed surfactant solutions. *Advances in Colloid and Interface Science, 123*, 401-413.

Ait Ali, A., & Makhloufi, R. (1999). Effect of organic salts on micellar growth and structure studied by rheology. *Colloid & Polymer Science, 277*(2), 270-275.

Alargova, R., Kochijashky, I., Sierra, M., Kwetkat, K., & Zana, R. (2001). Mixed micellization of dimeric (gemini) surfactants and conventional surfactants: II. CMC and micelle aggregation numbers for various mixtures. *Journal of Colloid and Interface Science, 235*(1), 119-129.

Ali, A., Malik, N. A., Uzair, S., Ali, M., & Ahmad, M. F. (2014). Hexadecyltrimethylammonium bromide micellization in glycine, diglycine, and triglycine aqueous solutions as a function of surfactant concentration and temperatures. *Russian Journal of Physical Chemistry A, 88*(6), 1053-1061.

Ali, A., & Makhloufi, R. (1997). Linear and nonlinear rheology of an aqueous concentrated system of cethyltrimethylammonium chloride and sodium salicylate. *Physical Review E, 56*(4), 4474.

Anacker, E., & Ghose, H. (1968). Counterions and micelle size. II. Light scattering by solutions of cetylpyridinium salts. *Journal of the American Chemical Society, 90*(12), 3161-3166.

Anand, P., Kunnumakkara, A. B., Newman, R. A., & Aggarwal, B. B. (2007). Bioavailability of curcumin: problems and promises. *Molecular Pharmaceutics, 4*(6), 807-818.

Aswal, V., Goyal, P., & Thiyagarajan, P. (1998). Small-angle neutron-scattering and viscosity studies of CTAB/NaSal viscoelastic micellar solutions. *The Journal of Physical Chemistry B, 102*(14), 2469-2473.

Batrakova, E. V., & Kabanov, A. V. (2008). Pluronic block copolymers: evolution of drug delivery concept from inert nanocarriers to biological response modifiers. *Journal of Controlled Release, 130*(2), 98-106.

Batrakova, E. V., Li, S., Brynskikh, A. M., Sharma, A. K., Li, Y., Boska, M., . . . Gendelman, H. E. (2010). Effects of pluronic and doxorubicin on drug uptake, cellular metabolism, apoptosis and tumor inhibition in animal models of MDR cancers. *Journal of Controlled Release, 143*(3), 290-301.

Bijma, K., Rank, E., & Engberts, J. B. (1998). Effect of counterion structure on micellar growth of alkylpyridinium surfactants in aqueous solution. *Journal of Colloid and Interface Science, 205*(2), 245-256.

Blasko, A., Bunton, C. A., Cerichelli, G., & McKenzie, D. C. (1993). A nuclear magnetic resonance study of ion exchange in cationic micelles: successes and failures of models. *The Journal of Physical Chemistry, 97*(43), 11324-11331.

Brown, W., Johansson, K., & Almgren, M. (1989). Threadlike micelles from cetyltrimethylammonium bromide in aqueous sodium naphthalenesulfonate solutions studied by static and dynamic light scattering. *The Journal of Physical Chemistry, 93*(15), 5888-5894.

Bunton, C. (1979). Reaction kinetics in aqueous surfactant solutions. *Catalysis Reviews Science and Engineering, 20*(1), 1-56.

Bunton, C. A. (1991). Micellar rate effects: what we know and what we think we know *Surfactants in Solution* (pp. 17-40): Springer.

Bunton, C. A. (1997). Reactivity in aqueous association colloids. Descriptive utility of the pseudophase model. *Journal of Molecular Liquids, 72*(1-3), 231-249.

Bunton, C. A., Nome, F., Quina, F. H., & Romsted, L. S. (1991). Ion binding and reactivity at charged aqueous interfaces. *Accounts of Chemical Research, 24*(12), 357-364.

Bunton, C. A., & Romsted, L. S. (1979). Test of pseudophase model of micellar catalysis: its partial failure. *Journal of American Chemical Society, 101*(5), 1253-1259.

Bunton, C. A., & Moffat, J. R. (1986). Ionic competition in micellar reactions: a quantitative treatment. *Journal of Physical Chemistry, 90*(4), 538-541.

Bunton, C. A., & Savelli, G. (1986). Organic reactivity in aqueous micelles and similar assemblies. *Advances in Physical Organic Chemistry, 22*, 213-309.

Bunton, C. A., & Savelli, G. (1987). Organic reactivity in aqueous micelles and similar assemblies. *Adv. Phys. Org. Chem, 22*, 213-309.

Bunton, C. A., Wright, S., Holland, P. M., & Nome, F. (1993). SN2 reactions of a sulfonate ester in mixed cationic/nonionic micelles. *Langmuir, 9*(1), 117-120.

Carver, M., Smith, T., Gee, J., Delichere, A., Caponetti, E., & Magid, L. (1996). Tuning of micellar structure and dynamics in aqueous salt-free solutions of cetyltrimethylammonium mono-and dichlorobenzoates. *Langmuir, 12*(3), 691-698.

Cates, M., & Candau, S. (1990). Statics and dynamics of worm-like surfactant micelles. *Journal of Physics: Condensed Matter, 2*(33), 6869.

Cetin, S., & Nasr-El-Din, H. (2017). *Rheological Study of a Novel Sulfobetaine Surfactant-Based Acid System.* Paper presented at the SPE Middle East Oil & Gas Show and Conference.

Chakraborty, T., Ghosh, S., & Moulik, S. P. (2005). Micellization and related behavior of binary and ternary surfactant mixtures in aqueous medium: cetyl pyridinium chloride (CPC), cetyl trimethyl ammonium bromide (CTAB), and polyoxyethylene (10) cetyl ether (Brij-56) derived system. *The Journal of Physical Chemistry B, 109*(31), 14813-14823.

Cheng, Y., Sun, L., & Luo, G. (2015). The effect of salts on micellization in C12. *Colloid Journal, 77*(4), 532-536.

Christian, S. D., & Scamehorn, J. F. (1995). *Solubilization in Surfactant Aggregates* (Vol. 55): CRC Press.

Clint, J. H. (1992). *Surfactant Aggregation,* Blackie, Glasgow.

Clint, J. H. (2012). *Surfactant Aggregation*: Springer Science & Business Media.

Crook, E., Trebbi, G., & Fordyce, D. (1964). Thermodynamic properties of solutions of homogeneous p, t-octylphenoxyethoxyethanols (OPE1-10). *The Journal of Physical Chemistry, 68*(12), 3592-3599.

Cullum, D. (1994). Surfactant types; classification, identification, separation. In Cullum, D. (ed.) *Introduction to Surfactant Analysis* (pp. 17-41): Springer.

Dar, A. A., Chatterjee, B., Rather, G. M., & Das, A. R. (2006). Mixed micellization and interfacial properties of dodecyltrimethylammonium bromide and tetraethyleneglycol mono-n-dodecyl ether in absence and presence of sodium propionate. *Journal of Colloid Interface Science, 298*(1), 395-405.

Dar, A. A., Garai, A., Das, A. R., & Ghosh, S. (2010). Rheological and fluorescence investigation of interaction between hexadecyltrimethylammonium bromide and methylcellulose in the presence of hydrophobic salts. *The Journal of Physical Chemistry A, 114*(15), 5083-5091.

Dar, A. A., Rather, G. M., & Das, A. R. (2007). Mixed micelle formation and solubilization behavior toward polycyclic aromatic hydrocarbons of binary and ternary cationic-nonionic surfactant mixtures. *The Journal of Physical Chemistry B, 111*(12), 3122-3132.

Davies, D. M., & Foggo, S. J. (1998). Kinetic treatment of the reaction of m-chloroperbenzoic acid and iodide in mixed anionic/non-ionic micelles. *Journal of the Chemical Society, Perkin Transactions 2*(2), 247-252.

Davies, T. S., Ketner, A. M., & Raghavan, S. R. (2006). Self-assembly of surfactant vesicles that transform into viscoelastic wormlike micelles upon heating. *Journal of the American Chemical Society, 128*(20), 6669-6675.

Deda, D. K., & Araki, K. (2015). Nanotechnology, Light and Chemical Action: an Effective Combination to Kill Cancer Cells. *Journal of the Brazilian Chemical Society, 26*(12), 2448-2470.

Doehlert, D. C., Moreau, R. A., Welti, R., Roth, M. R., & McMullen, M. S. (2010). Polar Lipids from Oat Kernels. *Cereal Chemistry, 87*(5), 467.

Dorshow, R., Briggs, J., Bunton, C., & Nicoli, D. (1982). Dynamic light scattering from cetyltrimethylammonium bromide micelles. Intermicellar interactions at low ionic strengths. *The Journal of Physical Chemistry, 86*(13), 2388-2395.

Dreiss, C. A. (2007). Wormlike micelles: where do we stand? Recent developments, linear rheology and scattering techniques. *Soft Matter, 3*(8), 956-970.

Drew, M. (2006). *Surfactant Science and Technology*. Hoboken: John Wiley & Sons.

Eads, C. D., & Robosky, L. C. (1999). NMR studies of binary surfactant mixture thermodynamics: molecular size model for asymmetric activity coefficients. *Langmuir, 15*(8), 2661-2668.

El Seoud, O. A., & Chinelatto, A. M. (1983). Acid-base indicator equilibria in aerosol-OT reversed micelles in heptane. The use of buffers. *Journal of Colloid and Interface Science, 95*(1), 163-171.

Esumi, K., Miyazaki, M., Arai, T., & Koide, Y. (1998). Mixed micellar properties of a cationic gemini surfactant and a nonionic surfactant. *Colloids and Surfaces A: Physicochemical and Engineering Aspects, 135*(1-3), 117-122.

Evans, D. F., & Wennerstrom, H. (1994). *The Colloid Domain, Where Physics, Chemistry, Biology and Technology Meet:* Wiley-VCH, New York.

Ezrahi, S., Tuval, E., & Aserin, A. (2006). Properties, main applications and perspectives of worm micelles. *Advances in Colloid and Interface Science, 128*, 77-102.

Fagge, I. I., Khalid, K., Noh, M. A. M., Yusof, N. S. M., Zain, S. M., & Khan, M. N. (2016). Influence of mixed CTABr–$C_{16}E_{20}$ nanoparticles on relative counterion binding constants in aqueous solutions of inert salts (2-$NaOC_6H_4CO_2Na$ and NaBr): kinetic and rheometric study. *RSC Advances, 6*(98), 95504-95511.

Fagge, I. I., & Khan, M. N. (2016). Role of non-ionic surfactants on the rate of piperidinolysis of ionized phenyl salicylate with the influence of 4-chlorosodium benzoate. Paper presented at the *4th International Congress on Nanoscience and Nanotechnology*, Kuala Lumpur.

Farías, T., De Menorval, L.-C., Zajac, J., & Rivera, A. (2009). Solubilization of drugs by cationic surfactants micelles: conductivity and 1 H NMR experiments. *Colloids and Surfaces A: Physicochemical and Engineering Aspects, 345*(1), 51-57.

Fendler, J. (2012). *Catalysis in Micellar and Macromoleular systems*: Elsevier.

Foley, P., Beach, E. S., & Zimmerman, J. B. (2012). Derivation and synthesis of renewable surfactants. *Chemical Society Reviews, 41*(4), 1499-1518.

Frescura, V. L., Marconi, D. M., Zanette, D., Nome, F., Blasko, A., & Bunton, C. A. (1995). Effects of sulfobetaine-sodium dodecanoate micelles on deacylation and indicator equilibrium. *The Journal of Physical Chemistry, 99*(29), 11494-11500.

Gamez-Corrales, R., Berret, J.-F., Walker, L., & Oberdisse, J. (1999). Shear-thickening dilute surfactant solutions: equilibrium structure as studied by small-angle neutron scattering. *Langmuir, 15*(20), 6755-6763.

Ganguly, R., Kunwar, A., Dutta, B., Kumar, S., Barick, K., Ballal, A., . . . Hassan, P. (2017). Heat-induced solubilization of curcumin in kinetically stable pluronic P123 micelles and vesicles: An exploit of slow dynamics of the micellar restructuring processes in the aqueous pluronic system. *Colloids and Surfaces B: Biointerfaces, 152*, 176-182.

Gao, H.-C., Zhao, S., Mao, S.-Z., Yuan, H.-Z., Yu, J.-Y., Shen, L.-F., & Du, Y.-R. (2002). Mixed micelles of polyethylene glycol (23) lauryl ether with ionic surfactants studied by proton 1D and 2D NMR. *Journal of Colloid and Interface Science, 249*(1), 200-208.

Geng, Y., Romsted, L. S., & Menger, F. (2006). Specific ion pairing and interfacial hydration as controlling factors in gemini micelle morphology. Chemical trapping studies. *Journal of the American Chemical Society, 128*(2), 492-501.

Ghosh, S., & Moulik, S. (1998). Interfacial and micellization behaviors of binary and ternary mixtures of amphiphiles (Tween-20, Brij-35, and sodium dodecyl sulfate) in aqueous medium. *Journal of Colloid and Interface Science, 208*(2), 357-366.

Goldsipe, A., & Blankschtein, D. (2007). Molecular-thermodynamic theory of micellization of multicomponent surfactant mixtures: 1. Conventional (pH-insensitive) surfactants. *Langmuir, 23*(11), 5942-5952.

Gravsholt, S. (1976). Viscoelasticity in highly dilute aqueous solutions of pure cationic detergents. *Journal of Colloid and Interface Science, 57*(3), 575-577.

Griffiths, P., Whatton, M., Abbott, R., Kwan, W., Pitt, A., Howe, A., . . . Heenan, R. (1999). Small-angle neutron scattering and fluorescence studies of mixed surfactants with dodecyl tails. *Journal of Colloid and Interface Science, 215*(1), 114-123.

Harada, S., Fujita, N., & Sano, T. (1988). Kinetic studies of the sphere-rod transition of micelles. *Journal of the American Chemical Society, 110*(26), 8710-8711.

Hatcher, H., Planalp, R., Cho, J., Torti, F., & Torti, S. (2008). Curcumin: from ancient medicine to current clinical trials. *Cellular and Molecular Life Sciences, 65*(11), 1631-1652.

Hayashi, S., & Ikeda, S. (1980). Micelle size and shape of sodium dodecyl sulfate in concentrated sodium chloride solutions. *The Journal of Physical Chemistry, 84*(7), 744-751.

Hentze, H.-P., Raghavan, S. R., McKelvey, C. A., & Kaler, E. W. (2003). Silica hollow spheres by templating of catanionic vesicles. *Langmuir, 19*(4), 1069-1074.

Hirata, H., Sato, M., Sakaiguchi, Y., & Katsube, Y. (1988). Small angle X-ray scattering study of an extremely elongated micelle system of CTAB-p-toluidine solution. *Colloid & Polymer Science, 266*(9), 862-864.

Hoffmann, H., & Pössnecker, G. (1994). The mixing behavior of surfactants. *Langmuir, 10*(2), 381-389.

Holland, P. M., & Rubingh, D. N. (1992). Mixed surfactant systems: ACS Publications.

Holmberg, K., Jönsson, B., Kronberg, B., & Lindman, B. (2002). Microemulsions. *Surfactants and Polymers in Aqueous Solution, Second Edition*, 139-155.

Ideta, R., Yanagi, Y., Tamaki, Y., Tasaka, F., Harada, A., & Kataoka, K. (2004). Effective accumulation of polyion complex micelle to experimental choroidal neovascularization in rats. *FEBS Letters, 557*(1-3), 21-25.

Ikeda, S., Ozeki, S., & Tsunoda, M.-A. (1980). Micelle molecular weight of dodecyldimethylammonium chloride in aqueous solutions, and the transition of micelle shape in concentrated NaCl solutions. *Journal of Colloid and Interface Science, 73*(1), 27-37.

Inoue, T., Inoue, Y., & Watanabe, H. (2005). Nonlinear rheology of CTAB/NaSal aqueous solutions: finite extensibility of a network of wormlike micelles. *Langmuir, 21*(4), 1201-1208.

Islam, M. N., & Kato, T. (2003a). Temperature dependence of the surface phase behavior and micelle formation of some nonionic surfactants. *The Journal of Physical Chemistry B, 107*(4), 965-971.

Islam, M. N., & Kato, T. (2003b). Thermodynamic study on surface adsorption and micelle formation of poly (ethylene glycol) mono-n-tetradecyl ethers. *Langmuir, 19*(18), 7201-7205.

Islam, M. N., Okano, T., & Kato, T. (2002). Surface Phase Behavior of a Mixed System of Anionic− Nonionic Surfactants Studied by Brewster Angle Microscopy and Polarization Modulation Infrared Reflection− Absorption Spectroscopy. *Langmuir, 18*(26), 10068-10074.

Jan, M., Dar, A. A., Amin, A., Rehman, N., & Rather, G. M. (2007). Clouding behavior of nonionic–cationic and nonionic–anionic mixed surfactant systems in presence of carboxylic acids and their sodium salts. *Colloid and Polymer Science, 285*(6), 631-640.

Junquera, E., & Aicart, E. (2002). Mixed micellization of dodecylethyldimethylammonium bromide and dodecyltrimethylammonium bromide in aqueous solution. *Langmuir, 18*(24), 9250-9258.

Kabanov, A. V., Batrakova, E. V., & Alakhov, V. Y. (2002). Pluronic® block copolymers as novel polymer therapeutics for drug and gene delivery. *Journal of Controlled Release, 82*(2), 189-212.

Kamada, M., Shimizu, S., & Aramaki, K. (2014). Manipulation of the viscosity behavior of wormlike micellar gels by changing the molecular structure of added perfumes. *Colloids and Surfaces A: Physicochemical and Engineering Aspects, 458*, 110-116.

Karayil, J., Kumar, S., Talmon, Y., Hassan, P., Tata, B., & Sreejith, L. (2016a). Micellar Growth in Cetylpyridinium Chloride/Alcohol System: Role of Long Chain Alcohol, Electrolyte and Surfactant Head Group. *Journal of Surfactants and Detergents, 19*(4), 849-860.

Karsa, D. R. (2006). What Are Surfactants? *Chemistry and Technology of Surfactants*, 1.

Kataoka, K., Harada, A., & Nagasaki, Y. (2001). Block copolymer micelles for drug delivery: design, characterization and biological significance. *Advanced Drug Delivery Reviews, 47*(1), 113-131.

Kern, F., Zana, R., & Candau, S. (1991). Rheological properties of semidilute and concentrated aqueous solutions of cetyltrimethylammonium chloride in the presence of sodium salicylate and sodium chloride. *Langmuir, 7*(7), 1344-1351.

Khalid, K., Noh, M. A. M., Zain, S. M., & Khan, M. N. (2016). Correlation of Kinetic and Rheological Data for Flexible Nanoparticle Catalysis in the Reaction of Piperidine with PS−. *Catalysis Letters, 146*(5), 960-967.

Khan, M. N. (1991). Catalytic effect of anionic micelles on alkaline hydrolysis of N‐hydroxyphthalimide. Evidence for the probable occurrence of the reaction in between Gouy‐Chapman and exterior boundary of Stern layers of the micelles. *International Journal of Chemical Kinetics, 23*(7), 567-578.

Khan, M. N. (1997a). Effects of [NaOH] and [KBr] on intramolecular general base-catalyzed methanolysis of ionized phenyl salicylate in the presence of cationic micelles. *The Journal of Organic Chemistry, 62*(10), 3190-3193.

Khan, M. N. (1997b). Effects of hydroxide ion, salts and temperature on the hydrolytic cleavage of ionized N-hydroxyphthalimide (NHPH) in the presence of cationic micelles. *Colloids and Surfaces A: Physicochemical and Engineering Aspects, 127*(1-3), 211-219.

Khan, M. N. (2006). Micellar Catalysis: Surfactant Science Series: CRC Press, Taylor and Francis Group LLC, Boca Raton, New York, London.

Khan, M. N. (2010). A new semi-empirical kinetic method for the determination of ion exchange constants for the counterions of cationic micelles. *Advances in Colloid and Interface Science, 159*(2), 160-179.

Khan, M. N. (2015). Kinetics and Mechanism of Mixed Micellar Catalysis, In *Encyclopedia of Surface and Colloid Science* (Third Edition, pp. 3502-3516): CRC Press, Taylor & Francis.

Khan, M. N., & Arifin, Z. (1996). Effects of cationic micelles on rates and activation parameters of intramolecular general base-catalyzed hydrolysis of ionized salicylate esters. *Journal of Colloid and Interface Science, 180*(1), 9-14.

Khan, M. N., Arifin, Z., Ismail, E., & Ali, S. F. (2000). Effects of [NaBr] on the rates of intramolecular general base-catalyzed reactions of ionized phenyl salicylate (PS-) with n-butylamine and piperidine in the presence of cationic micelles. *The Journal of Organic Chemistry, 65*(5), 1331-1334.

Khan, M. N., & Fui, C. T. (2009). Kinetic study on the effects of mixed nonionic–cationic micelles on the rate of alkaline hydrolysis of N-hydroxyphthalimide. *Journal of Molecular Liquids, 147*(3), 170-177.

Khan, M. N., & Ismail, E. (2001). An apparent weakness of the pseudophase ion-exchange (PIE) model for micellar catalysis by cationic surfactants with nonreactive counterions. *Journal of the Chemical Society, Perkin Transactions 2*(8), 1346-1350.

Khan, M. N., & Ismail, E. (2003). An empirical approach to study the anion selectivity at aqueous cationic micellar surface: Effects of inorganic salts on kinetically determined cationic micellar binding constant of ionized phenyl salicylate. *Journal of Molecular Liquids, 107*(1-3), 277-287.

Khan, M. N., & Ismail, E. (2004). Effects of non‐ionic and mixed non‐ionic–cationic micelles on the rate of aqueous cleavages of phenyl benzoate and phenyl salicylate in alkaline medium. *Journal of Physical Organic Chemistry, 17*(5), 376-386.

Khan, M. N., & Ismail, E. (2007). An empirical approach to study the occurrence of ion exchange in the alkaline hydrolysis of phthalimide in the presence of cationic micelles and inert salts. *Journal of Molecular Liquids, 136*(1), 54-63.

Khan, M. N., & Ismail, E. (2009). Kinetic evidence for the occurrence of independent ion-exchange processes in the cationic micellar-mediated reaction of piperidine with anionic phenyl salicylate. *The Journal of Physical Chemistry A, 113*(23), 6484-6488.

Khan, M. N., Ismail, E., & Yusof, N. S. M. (2010). A new empirical kinetic method for the determination of ion-exchange constants for the counterions of cationic micelles: The rate of piperidinolysis and hydrolysis of anionic phenyl salicylate as the kinetic probes. *Colloids and Surfaces A: Physicochemical and Engineering Aspects, 361*(1), 150-161.

Khan, M. N., & Sinasamy, S. (2011). A new semiempirical kinetic method for the determination of ion exchange constants for counterions of cationic micelles: Study of the rate of pH‐independent hydrolysis of phthalimide as the kinetic probe. *International Journal of Chemical Kinetics, 43*(1), 9-20.

Kim, W.-J., & Yang, S.-M. (2000). Microstructures and rheological responses of aqueous CTAB solutions in the presence of benzyl additives. *Langmuir, 16*(15), 6084-6093.

Kreke, P., Magid, L., & Gee, J. (1996). 1H and 13C NMR studies of mixed counterion, cetyltrimethylammonium bromide/cetyltrimethylammonium dichlorobenzoate, surfactant solutions: the intercalation of aromatic counterions. *Langmuir*, *12*(3), 699-705.

Kumar, S., Aswal, V. K., & Goyal, P. S. (1996). Effect of the addition of n-alkylamines on the growth of sodium decyl sulfate micelles. *Journal of the Chemical Society, Faraday Transactions*, *92*(13), 2413-2415.

Kunz, W., Henle, J., & Ninham, B. W. (2004). 'Zur Lehre von der Wirkung der Salze'(about the science of the effect of salts): Franz Hofmeister's historical papers. *Current Opinion in Colloid & Interface Science*, *9*(1), 19-37.

Kuperkar, K. C., Mata, J. P., & Bahadur, P. (2011). Effect of 1-alkanols/salt on the cationic surfactant micellar aqueous solutions-a dynamic light scattering study. *Colloids and Surfaces A: Physicochemical and Engineering Aspects*, *380*(1), 60-65.

Lajis, N. H., & Khan, M. N. (1998). Effects of ionic and non-ionic micelles on rate of hydroxide ion-catalyzed hydrolysis of securinine. *Journal of Physical Organic Chemistry*, *11*(3), 209-215.

Larsen, J. W., & Tepley, L. B. (1974). Effect of aqueous alcoholic solvents on counterion-binding to CTAB micelles. *Journal of Colloid and Interface Science*, *49*(1), 113-118.

Laschewsky, A. (2003). Polymerized micelles with compartments. *Current Opinion in Colloid & Interface Science*, *8*(3), 274-281.

Lee, B. S., & Nome, F. (2000). Effects of sulfobetaine-sodium decyl phosphate mixed micelles on deacylation and indicator equilibrium. *Langmuir*, *16*(26), 10131-10136.

Liang, X., Guo, C., Liao, C., Liu, S., Wick, L. Y., Peng, D., . . . Lin, Z. (2017). Drivers and applications of integrated clean-up technologies for surfactant-enhanced remediation of environments contaminated with polycyclic aromatic hydrocarbons (PAHs). *Environmental Pollution*, *225*, 129-140.

Lin, I., Moudgil, B., & Somasundaran, P. (1974). Estimation of the effective number of —CH_2-groups in long-chain surface active agents. *Colloid & Polymer Science*, *252*(5), 407-414.

Lin, Y., Qiao, Y., Yan, Y., & Huang, J. (2009). Thermo-responsive viscoelastic wormlike micelle to elastic hydrogel transition in dual-component systems. *Soft Matter*, *5*(16), 3047-3053.

Lin, Z., Zheng, Y., Talmon, Y., Maxson, A., & Zakin, J. L. (2016). Comparison of the effects of methyl-and chloro-substituted salicylate counterions on drag reduction and rheological behavior and micellar formation of a cationic surfactant. *Rheologica Acta*, *55*(2), 117-123.

Lipowsky, R., & Sackmann, E. (1995). *Structure and dynamics of membranes: I. from cells to vesicles/II. generic and specific interactions*: Elsevier.

Lu, T., Huang, J., Li, Z., Jia, S., & Fu, H. (2008). Effect of hydrotropic salt on the assembly transitions and rheological responses of cationic gemini surfactant solutions. *The Journal of Physical Chemistry B, 112*(10), 2909-2914.

Maeda, H., Tanaka, S., Ono, Y., Miyahara, M., Kawasaki, H., Nemoto, N., & Almgren, M. (2006). Reversible micelle-vesicle conversion of oleyldimethylamine oxide by pH changes. *The Journal of Physical Chemistry B, 110*(25), 12451-12458.

Mao, X., Jiang, R., Xiao, W., & Yu, J. (2015). Use of surfactants for the remediation of contaminated soils: a review. *Journal of Hazardous Materials, 285*, 419-435.

Mata, J., Aswal, V., Hassan, P., & Bahadur, P. (2006). A phenol-induced structural transition in aqueous cetyltrimethylammonium bromide solution. *Journal of Colloid and Interface Science, 299*(2), 910-915.

McBain, J. W. (1944). Solutions of soaps and detergents as colloidal electrolytes. *Alexanders Colloid Chem, 5*, 144.

Menger, F. M. (1979). The structure of micelles. *Accounts of Chemical Research, 12*(4), 111-117.

Menger, F. M., & Portnoy, C. E. (1967). Chemistry of reactions proceeding inside molecular aggregates. *Journal of the American Chemical Society, 89*(18), 4698-4703.

Mir, M. A., Dar, A. A., Amin, A., & Rather, G. M. (2009). Interaction of hydroxypropylcellulose with hexadecylbenzyldimethylammonium chloride in the absence and presence of hydrophobic salts. *Journal of Molecular Liquids, 150*(1), 86-91.

Muñoz, M., Rodríguez, A., Del Mar Graciani, M., & Luisa Moyá, M. (2002). Micellar medium effects on the hydrolysis of phenyl chloroformate in ionic, zwitterionic, nonionic, and mixed micellar solutions. *International Journal of Chemical Kinetics, 34*(7), 445-451.

Nemoto, N., & Kuwahara, M. (1993). Dynamic light scattering of CTAB/sodium salicylate long threadlike micelles in the semidilute regime: applicability of the dynamic scaling law. *Langmuir, 9*(2), 419-423.

Nishiyama, N., Bae, Y., Miyata, K., Fukushima, S., & Kataoka, K. (2005). Smart polymeric micelles for gene and drug delivery. *Drug Discovery Today: Technologies, 2*(1), 21-26.

Nishiyama, N., & Kataoka, K. (2006). Current state, achievements, and future prospects of polymeric micelles as nanocarriers for drug and gene delivery. *Pharmacology & Therapeutics, 112*(3), 630-648.

Niyaz Khan, M., & Ismail, E. (2003). An empirical approach to study the anion selectivity at aqueous cationic micellar surface: Effects of inorganic salts on kinetically

determined cationic micellar binding constant of ionized phenyl salicylate. *Journal of Molecular Liquids, 107*(1-3), 277-287.

Oelschlaeger, C., Schopferer, M., Scheffold, F., & Willenbacher, N. (2008). Linear-to-branched micelles transition: A rheometry and diffusing wave spectroscopy (DWS) study. *Langmuir, 25*(2), 716-723.

Oelschlaeger, C., Suwita, P., & Willenbacher, N. (2010). Effect of counterion binding efficiency on structure and dynamics of wormlike micelles. *Langmuir, 26*(10), 7045-7053.

Ojogun, V. A., Lehmler, H.-J., & Knutson, B. L. (2009). Cationic–anionic vesicle templating from fluorocarbon/fluorocarbon and hydrocarbon/fluorocarbon surfactants. *Journal of Colloid and Interface Science, 338*(1), 82-91.

Ortega, F., & Rodenas, E. (1987). An electrostatic approach for explaining the kinetic results in the reative counterion surfactants CTAOH and CTACN. *Journal of Physical Chemistry, 91*(5), 837-840.

Otzen, D. E. (2015). Proteins in a brave new surfactant world. *Current Opinion in Colloid & Interface Science, 20*(3), 161-169.

Pal, S., Vishal, G., Gandhi, K., & Ayappa, K. (2005). Ion exchange in reverse micelles. *Langmuir, 21*(2), 767-778.

Palous, J., Turmine, M., & Letellier, P. (1998). Mixtures of nonionic and ionic surfactants: determination of mixed micelle composition using cross-differentiation relations. *The Journal of Physical Chemistry B, 102*(30), 5886-5890.

Park, K.-H., Berrier, C., Lebaupain, F., Pucci, B., Popot, J.-L., Ghazi, A., & Zito, F. (2007). Fluorinated and hemifluorinated surfactants as alternatives to detergents for membrane protein cell-free synthesis. *Biochemical Journal, 403*(1), 183-187.

Patel, V., Dharaiya, N., Ray, D., Aswal, V. K., & Bahadur, P. (2014). pH controlled size/shape in CTAB micelles with solubilized polar additives: a viscometry, scattering and spectral evaluation. *Colloids and Surfaces A: Physicochemical and Engineering Aspects, 455*, 67-75.

Penfold, J., Tucker, I., Staples, E., & Thomas, R. (2004). Adsorption of Aromatic Counterions at the surfactant/water interface: A neutron reflectivity study of hydroxybenzoate and chlorobenzoate counterions at the hexadecyl trimethylammonium surfactant/water interface. *Langmuir, 20*(19), 8054-8061.

Qi, Y., & Zakin, J. L. (2002). Chemical and rheological characterization of drag-reducing cationic surfactant systems. *Industrial & Engineering Chemistry Research, 41*(25), 6326-6336.

Qiao, Y., Lin, Y., Wang, Y., Li, Z., & Huang, J. (2011). Metal-driven viscoelastic wormlike micelle in anionic/zwitterionic surfactant systems and template-directed synthesis of dendritic silver nanostructures. *Langmuir, 27*(5), 1718-1723.

Quina, F. H., & Chaimovich, H. (1979). Ion exchange in micellar solutions. 1. Conceptual framework for ion exchange in micellar solutions. *Journal of Physical Chemistry, 83*(14), 1844-1850.

Rangel-Yagui, C. O., Pessoa Jr, A., & Tavares, L. C. (2005). Micellar solubilization of drugs. *Journal of Pharmacy and Pharmaceutical Science, 8*(2), 147-163.

Rao, U., Manohar, C., Valaulikar, B., & Iyer, R. (1987). Micellar chain model for the origin of the visoelasticity in dilute surfactant solutions. *Journal of Physical Chemistry, 91*(12), 3286-3291.

Rathman, J. F. (1996). Micellar catalysis. *Current Opinion in Colloid & Interface Science, 1*(4), 514-518.

Rathman, J. F., & Scamehorn, J. F. (1984). Counterion binding on mixed micelles. *The Journal of Physical Chemistry, 88*(24), 5807-5816.

Razak, N. A., & Khan, M. N. (2013). Determination of flow activation energy at viscosity maximum for spherical and wormlike micelles of different lengths and flexibility. *Rheologica Acta, 52*(10-12), 927-937.

Razak, N. A., Yusof, N. S. M., & Khan, M. N. (2014). Kinetics and mechanism of nanoparticles (CTABr/MX/H_2O)-catalyzed piperidinolysis of ionized phenyl salicylate. 1. *Journal of the Taiwan Institute of Chemical Engineers, 45*(5), 2777-2785.

Razak, N. A., Yusof, N. S. M., & Khan, M. N. (2016). Rheological study on counter ion (X^{2-})-and temperature-induced cationic micellar growth: a quantitative correlation between X^{2-} binding affinity to cationic micelles and X^{2-}-and temperature-induced micellar growth. *Rheologica Acta, 55*(2), 125-136.

Rehage, H., & Hoffmann, H. (1991). Viscoelastic surfactant solutions: model systems for rheological research. *Molecular Physics, 74*(5), 933-973.

Romantsov, T., & Wood, J. (2016). Contributions of Membrane Lipids to Bacterial Cell Homeostasis upon Osmotic Challenge. *Biogenesis of Fatty Acids, Lipids and Membranes*, 1-22.

Romsted, L. S. (1977). A general kinetic theory of rate enhancements for reactions between organic substrates and hydrophilic ions in micellar systems. *Micellization, Solubilization, and Microemulsions* (pp. 509-530): Springer.

Romsted, L. S. (2007). Do amphiphile aggregate morphologies and interfacial compositions depend primarily on interfacial hydration and ion-specific interactions? The evidence from chemical trapping. *Langmuir, 23*(2), 414-424.

Rosen, M. J. (1986). Molecular interaction and synergism in binary mixtures of surfactants. *Phenomena in Mixed Surfactant Systems.*

Roy, J. C., Islam, M. N., & Aktaruzzaman, G. (2014). The effect of NaCl on the Krafft temperature and related behavior of cetyltrimethylammonium bromide in aqueous solution. *Journal of Surfactants and Detergents, 17*(2), 231-242.

Ruckenstein, E., & Beunen, J. (1988). Effect of counterion binding on micellization. *Langmuir, 4*(1), 77-90.

Sadegh, F., & Naghash, H. J. (2015). Synthesis of monoallyl-end-capped polydimethylsiloxane-based polymerizable surfactant. *Progress in Organic Coatings, 78*, 381-386.

Salager, J.-L. (2002). Surfactants types and uses. *FIRP booklet*(E300A).

Schramm, L. L., Stasiuk, E. N., & Marangoni, D. G. (2003). 2 Surfactants and their applications. *Annual Reports Section" C"(Physical Chemistry), 99*, 3-48.

Schubert, B. A., Kaler, E. W., & Wagner, N. J. (2003). The microstructure and rheology of mixed cationic/anionic wormlike micelles. *Langmuir, 19*(10), 4079-4089.

Schubert, B. A., Wagner, N. J., Kaler, E. W., & Raghavan, S. R. (2004). Shear-induced phase separation in solutions of wormlike micelles. *Langmuir, 20*(9), 3564-3573.

Shah, A., Shahzad, S., Munir, A., Nadagouda, M. N., Khan, G. S., Shams, D. F., . . . Rana, U. A. (2016). Micelles as Soil and Water Decontamination Agents. *Chemical Reviews, 116*(10), 6042-6074.

Shikata, T., Hirata, H., & Kotaka, T. (1987). Micelle formation of detergent molecules in aqueous media: viscoelastic properties of aqueous cetyltrimethylammonium bromide solutions. *Langmuir, 3*(6), 1081-1086.

Shiloach, A., & Blankschtein, D. (1998). Measurement and prediction of ionic/nonionic mixed micelle formation and growth. *Langmuir, 14*(25), 7166-7182.

Sidim, T. (2016). Salt Effect on Interfacial Properties of Cetyltrimethylammonium Bromide and Triton X-102 Mixed Surfactant System. *Asian Journal of Chemistry, 28*(2), 459-462.

Sigoillot, J.-C., & Nguyen, M.-H. (1992). Complete oxidation of linear alkylbenzene sulfonate by bacterial communities selected from coastal seawater. *Applied and Environmental Microbiology, 58*(4), 1308-1312.

Singh, K., Marangoni, D. G., Quinn, J. G., & Singer, R. D. (2009). Spontaneous vesicle formation with an ionic liquid amphiphile. *Journal of Colloid and Interface Science, 335*(1), 105-111.

Soltero, J., Puig, J., & Manero, O. (1996). Rheology of the cetyltrimethylammonium tosilate-water system. 2. Linear viscoelastic regime. *Langmuir, 12*(11), 2654-2662.

Stang, P. J. (2012). Abiological self-assembly via coordination: formation of 2D metallacycles and 3D metallacages with well-defined shapes and sizes and their chemistry. *Journal of the American Chemical Society, 134*(29), 11829-11830.

Sutton, D., Nasongkla, N., Blanco, E., & Gao, J. (2007). Functionalized micellar systems for cancer targeted drug delivery. *Pharmaceutical Research, 24*(6), 1029-1046.

Tripathy, D. B., Mishra, A., Gupta, A., & Yadav, A. (2017). Biodegradability of Laundry Detergent Surfactants. *International Journal of Advanced Research and Innovation, 5*(1), 130-136.

Vangeyte, P., Leyh, B., Auvray, L., Grandjean, J., Misselyn-Bauduin, A.-M., & Jérôme, R. (2004). Mixed self-assembly of poly (ethylene oxide)-b-poly (ε-caprolactone) copolymers and sodium dodecyl sulfate in aqueous solution. *Langmuir, 20*(21), 9019-9028.

Vera, S., & Rodenas, E. (1986). Influence of N-cetyl-N, N, N-trimethylammonium bromide counterions in the basic hydrolysis of negatively charged aromatic esters. *The Journal of Physical Chemistry, 90*(15), 3414-3417.

Vermathen, M., Stiles, P., Bachofer, S., & Simonis, U. (2002). Investigations of monofluoro-substituted benzoates at the tetradecyltrimethylammonium micellar interface. *Langmuir, 18*(4), 1030-1042.

Vincent, B. (2014). McBain and the centenary of the micelle. *Advances In Colloid and Interface Science, 203*, 51-54.

Walker, L. M. (2001). Rheology and structure of worm-like micelles. *Current Opinion in Colloid & Interface Science, 6*(5), 451-456.

Wang, G., Yin, Q., Shen, J., Bai, Y., Ma, X., Du, Z., & Wang, W. (2017). Surface activities and aggregation behaviors of cationic-anionic fluorocarbon-hydrocarbon surfactants in dilute solutions. *Journal of Molecular Liquids, 234*, 142-148.

Wang, M., Han, Y., Qiao, F., & Wang, Y. (2015). Aggregation behavior of a gemini surfactant with a tripeptide spacer. *Soft Matter, 11*(8), 1517-1524.

Wennerström, H., & Lindman, B. (1979). Micelles. Physical chemistry of surfactant association. *Physics Reports, 52*(1), 1-86.

Willcox, M. (2000). *Soap Poucher's Perfumes, Cosmetics and Soaps* (pp. 453-465): Springer.

Xiao, F.-S. (2005). Ordered mesoporous silica-based materials templated from fluorocarbon–hydrocarbon surfactant mixtures and semi-fluorinated surfactants. *Current Opinion in Colloid & Interface Science, 10*(3), 94-101.

Yan, Q., & Zhao, Y. (2015). ATP-triggered biomimetic deformations of bioinspired receptor-containing polymer assemblies. *Chemical Science, 6*(7), 4343-4349.

Yang, J. (2002). Viscoelastic wormlike micelles and their applications. *Current Opinion in Colloid & Interface Science, 7*(5), 276-281.

Yin, H., Lei, S., Zhu, S., Huang, J., & Ye, J. (2006). Micelle‐to‐Vesicle Transition Induced by Organic Additives in Catanionic Surfactant Systems. *Chemistry-A European Journal, 12*(10), 2825-2835.

Yoshida, K., & Dubin, P. L. (1999). Complex formation between polyacrylic acid and cationic/nonionic mixed micelles: effect of pH on electrostatic interaction and hydrogen bonding. *Colloids and Surfaces A: Physicochemical and Engineering Aspects, 147*(1), 161-167.

Yusof, N. S. M., & Khan, M. N. (2010). Determination of an ion exchange constant by the use of a kinetic probe: a new semiempirical kinetic approach involving the effects of 3-F-and 4-F-substituted benzoates on the rate of piperidinolysis of anionic phenyl salicylate in aqueous cationic micelles. *Langmuir, 26*(13), 10627-10635.

Yusof, N. S. M., & Khan, M. N. (2012). Quantitative correlation of counterion (X) affinity to ionic micelles and X-and temperature-induced micellar growth (spherical–wormlike micelles–vesicles) for X= 5-methyl-and 5-methoxysalicylate Ions. *The Journal of Physical Chemistry B, 116*(7), 2065-2074.

Yusof, N. S. M., & Khan, M. N. (2013). Quantitative correlation between counterion-affinity to cationic micelles and counterion-induced micellar growth. *Advances in Colloid and Interface Science, 193*, 12-23.

Yusof, N. S. M., Razak, N. A., & Khan, M. N. (2013). Quantitative Correlation between Counterion (X) Affinity to Cationic Micelles and X-Induced Micellar Growth for X= 2, 4-; 2, 5-; 2, 6-and 3, 4-Dichlorobenzoate Ions. *Journal of Oleo Science, 62*(5), 257-269.

Zakharova, L., Valeeva, F., Zakharov, A., Ibragimova, A., Kudryavtseva, L., & Harlampidi, H. (2003). Micellization and catalytic activity of the cetyltrimethylammonium bromide–Brij 97–water mixed micellar system. *Journal of Colloid and Interface Science, 263*(2), 597-605.

Zhang, J., Ge, Z., Jiang, X., Hassan, P., & Liu, S. (2007). Stopped-flow kinetic studies of sphere-to-rod transitions of sodium alkyl sulfate micelles induced by hydrotropic salt. *Journal of Colloid and Interface Science, 316*(2), 796-802.

Zhang, J., Pellechia, P. J., Hayat, J., Hardy, C. G., & Tang, C. (2013). Quantitative and qualitative counterion exchange in cationic metallocene polyelectrolytes. *Macromolecules, 46*(4), 1618-1624.

Ziserman, L., Abezgauz, L., Ramon, O., Raghavan, S. R., & Danino, D. (2009). Origins of the viscosity peak in wormlike micellar solutions. 1. Mixed catanionic surfactants. A cryo-transmission electron microscopy study. *Langmuir, 25*(18), 10483-10489.

LIST OF PUBLICATIONS AND PAPERS PRESENTED

Journal Articles:

1. **Ibrahim I. Fagge**, K. Khalid, M. Azri Mohd Noh, Nor Saadah M. Yusof, Sharifuddin Md. Zain and M. Niyaz Khan. (2016) Influence of mixed CTABr-$C_{16}E_{20}$ nanoparticles on relative counterion binding constants in solutions of inert salts (2-$HOC_6H_4CO_2Na$ and NaBr): Kinetic and rheometric study. *RSC Adv., 2016, 6, 95504.*
2. **Ibrahim I. Fagge**, K. Khalid, M. Azri Mohd Noh, Nor Saadah M. Yusof, Sharifuddin M. Zain and M. Niyaz Khan. (2018) Study of Cationic and Nonionic Mixed Micelles with NaBr and 3,5-$Cl_2C_6H_3CO_2Na$ by Use of Probe Nucleophilic Reaction of Piperidine with Ionized Phenyl Salicylate. To be published by *Journal of Oleo Science, Vol. 67, No. 1 (2018).* DOI: 10.5650/jos.ess17033

International Conferences:

1. **Ibrahim I. Fagge** and Mohammad Niyaz Khan, Role of non-ionic surfactants on the rate of piperidinolysis of ionized phenyl salicylate with the influence of 4-chlorosodium benzoate. *4th International Congress on Nanoscience and Technology (ICNT),* 28th & 29th January, 2016. Kuala Lumpur, Malaysia (Oral Presentation).
2. **Ibrahim I. Fagge**, Nor Saadah M. Yusof, Sharifuddin Md Zain and M. Niyaz Khan, Effect of halo-substituted aromatic salts on counterion binding constants for cationic nanoparticle catalyzed kinetic reactions of piperidine and phenyl salicylate. *3rd Advanced Materials Conference (AMC),* 28th & 29th November, 2016. Langkawi, Kedah, Malaysia (Oral Presentation).